ROYAUME DU MAROC
Université Mohammed V - RABAT -
جامعة محمد الخامس – الرباط –
Faculté des sciences
كلية العلوم
CENTRE D'ETUDES DOCTORALES - SCIENCES ET TECHNOLOGIES

N° d'ordre : 3551

THESE

En vue de l'obtention du : ***DOCTORAT***

Structure de Recherche *: Equipe des sciences de la matière et du rayonnement*
Discipline *: Physique*
Spécialité *: Thermodynamique quantique*

Présentée et soutenue le 25/11/2021 par :

Kenza HAMMAM

The role of quantum coherence in the performance of quantum thermal machines

JURY

Yahya TAYALATI	PES, Faculté des Sciences, Université Mohammed V, Rabat	Président
Khalid BOUZIANE	PES, Université Internationale de Rabat	Rapporteur/ Examinateur
Morad EL BAZ	PES, Faculté des Sciences, Université Mohammed V, Rabat	Rapporteur/ Examinateur
Adil BELHAJ	PH, Faculté des Sciences, Université Mohammed V, Rabat	Rapporteur/ Examinateur
Rosario FAZIO	PES, ICTP- Trieste, Université de Naples, Frédéric II, Italie	Examinateur
Gonzalo MANZANO	Docteur, Institute for Cross-Disciplinary Physics and Complex Systems, Université IFISC, Majorque, Espagne	Invité
Abderrahim EL ALLATI	PH, Faculté des Sciences et Techniques d'Al-Hoceima Université Abdelmalek Essaâdi de Tétouan	Co-directeur de thèse
Yassine HASSOUNI	PES, Faculté des Sciences, Université Mohammed V, Rabat	Directeur de thèse

Année universitaire : 2020/2021

Acknowledgments

This thesis was achieved in the laboratory of Matter and Radiations Sciences Team (ESMaR) at the Faculty of Sciences of Rabat under the supervision of Professor Yassine HASSOUNI.

First and foremost, I would like to take this opportunity to express my sincere gratitude towards my supervisor Professor Yassine HASSOUNI, full professor at the Faculty of Sciences of Rabat, who accepted me to conduct my PhD research under his auspices. I hope I have lived up to your expectations. Thank you for your invaluable advice, encouragement and patience during the course of my PhD degree. I appreciate how you have always been so friendly and supportive of all of my efforts and struggles. This thesis would not have been completed or written without your aid.

I thank my co-supervisor Mr. Abderrahim El ALLATI, PH professor at the Faculty of Sciences and Technique of Al Hoceima, for the interesting and insightful discussions and providing useful comments on my progress during my PhD.

I express my deep gratitude to Mr. Yahya TAYALATI, full professor at the Faculty of Sciences of Rabat, for accepting to be the president of the Jury. Thank you for your enlightening comments and encouraging words during my defense.

Profuse thanks goes equally to Mr. Khalid BOUZIANE, full professor at International University of Rabat, for accepting to be reporter and examiner of this thesis. Thank you for your encouraging reviews and insightful comments that undoubtedly helped in improving the quality of this thesis.

I would like to show my gratitude to Mr. Morad EL BAZ, full professor at the Faculty of Sciences of Rabat, for accepting to be reporter and examiner of this thesis. Thank you also for your constructive comments and encouraging reviews.

I am deeply thankful to Mr. Adil BELHAJ, PH professor at the Faculty of Sciences of Rabat for accepting to be reporter and examiner of this thesis. I appreciate your helpful and comments and insightful remarks on my thesis.

My acknowledgment goes also to Mr. Rosario FAZIO, full professor at the Abdus Salam International Centre for Theoretical Physics (ICTP) and at Università di Napoli Federico II, for accepting to be an examiner of my thesis and for the highly-competent guidance and support that pushed me forward. I am extremely thankful for welcoming me to ICTP and offering me the opportunity to work under your guidance. Thank you for your time, illuminating instructions and help during my several visits to ICTP.

A special thanks to Mr. Gonzalo MANZANO, doctor and researcher at the Institute for Cross-Disciplinary Physics and Complex Systems, IFISC, for accepting the invitation to be an examiner of my thesis. I am forever grateful for the incredible amount of support with both Physics and academia in general. You are an exemplary physicist and role model that I look up to. Thank you again for always making sure to review my progress, helping me to refine my ideas and opening your office door to have insightful discussions whenever I had a question about my research.

The support from the Abdus Salam centre for Theoretical Physics (ICTP) in Trieste (Italy) and the ICTP/IAEA Sandwich Training Educational programme (STEP) is gratefully acknowledged. I am greatly indebted to all the members and staff of ICTP that helped me to have a comfortable and enjoyable experience to do research and enjoy the beauty of Trieste. I thank Professor Joseph NIEMELA, Professor Nadia BINGELLI, Professor Humberto CABRERA, and Professor Antonello SCARDICCIO for the kind welcome and constant support since I came to ICTP for the first time. My visits would not have been as fun and productive if it was not for all the great secretary of the STEP program: Francesca PRELAZZI and Sandra ALI-

MANOVIC who always assisted me during my stay.

I also extend my thanks to all the members and colleagues of the Condensed Matter and Statistical Physics section particularly my good friend Dr. Silvia PAPPALARDI who has been supportive and caring. For never allowing a day at the office to be boring, thank you to all of my ICTP office mates and friends: Nair, Reyhanneh, Paola, Tommaso, Mattia, Rajat and Vittorio.

A special thanks to Professor Gabriele DE CHIARA and Professor Tapio ALA-NISSILA for the fruitful discussions and endless encouragements during my PhD.

I would like to thank my closest colleagues and friends at the Faculty of Sciences of Rabat: Yousra BOUASRIA, Abdessamad BELFAKIR and Souad BATLAMOUS for all the love, support and help that they provided throughout my PhD. I will never forget the wonderful memories we had all together.

Last but not least, I am thankful to my beloved parents and my brother, who always have nursed me with their continuous support and their dedicated partnership for success in my life. I dedicate this milestone to them, especially to my father and my wonderful mother.

This thesis is a dedication to my deceased grandparents who believed in me until the end. To my uncle Youssef and aunt Amina, I thank you for being my guardians who gave me their full support and encouraged me to go on every adventure especially this one.

My wholehearted thanks to my cousin and sister Meriem for her support, cheerful spirit, and all the memories we have shared together. You are the sister that life forgot to give me.

I would be remiss not save my greatest thanks for all the rest of my family, for anyone who loves me and for all the people that I love!

Abstract

The discovery of heat engines had a huge influence on our society. Their introduction opened the door for the industrial revolution and the development of ground-breaking new technologies. Currently, engineering smaller devices is becoming more popular before, thus requiring smaller sources of energy, particularly at the nanoscale.

In reality, quantum systems can't be entirely isolated in nature, they are always coupled to an environment. Understanding their dynamical and thermodynamic interaction with their respective environments is the ultimate goal of quantum thermodynamics. In this thesis, we study the role of quantum coherence on the transport phenomena and steady-state operation of two thermal machines which can act either as a heat engine or as a refrigerator. Both settings employ a collisional model framework which relies on repeated interactions between a system and the environmental ancillas. In the first model, our findings show that coherence in the state of the ancillas of the cold reservoir results in an efficiency that goes beyond the Carnot limit. In the second model, we express and discuss both the advantages and drawbacks of using coherence as a resource in the case of an autonomous virtual qubit machine.

Keywords (6) : Quantum coherence, quantum thermal machines, collisional models, non-equilibrium thermodynamics, steady-states dynamics, autonomous thermal machines.

Résumé

La découverte des moteurs thermiques a eu un impact considérable sur notre société notamment à travers le déclenchement de la révolution industrielle et le développement de nouvelles technologies. De nos jours, la miniaturisation des appareils est davantage répandue, nécessitant des sources d'énergie microscopiques, bien précisément quantiques.

Dans les faits, les systèmes quantiques ne peuvent pas être entièrement isolés dans la nature, ils sont toujours couplés à un environnement. Comprendre leur interaction dynamique et thermodynamique avec leurs environnements respectifs est le but ultime de la thermodynamique quantique. À travers le travail de cette thèse, nous étudions le rôle de la cohérence quantique sur la performance en régime stationnaire de deux machines thermiques. Ces dernières sont sujets du formalisme des modèles collisionnels qui repose sur des interactions répétées entre un système et les ancillas de l'environnement. Au sein du premier modèle, nos résultats montrent que la cohérence dans l'état des ancillas du réservoir froid génère un meilleur rendement que celle de Carnot dans le cas du moteur thermique et du réfrigérateur. Tant dis que pour le deuxième modèle, nous exprimons à la fois les avantages et les inconvénients de l'utilisation de la cohérence comme ressource dans une machine à qubits virtuels autonome.

Mots-clés (6) : La cohérence quantique, les machines thermiques quantiques, les modèles collisionnels, la thermodynamique hors équilibre, la dynamique des états stationnaires, les machines thermiques autonomes.

Résumé étendu

Les lois thermodynamiques ont une grande influence sur notre vie quotidienne que presque toutes les autres lois physiques. Elles contrôlent l'échange de chaleur et la production de travail en décrivant la conservation de l'énergie et son passage d'une forme à une autre. La météo, les systèmes de climatisation et de chauffage de nos maisons et les moyens de transport sont tous des exemples de l'impact évident de la thermodynamique sur notre société.

Avec le progrès rapide de la nanotechnologie, la capacité de concevoir et de produire des dispositifs à l'échelle microscopique est très demandée. Par conséquent, il est crucial de disposer d'une analyse thermodynamique des processus se produisant à l'échelle nanométrique. En se basant sur les principes de la mécanique statistique, une interprétation des lois de la thermodynamique conduit à la miniaturisation du comportement thermodynamique des systèmes macroscopiques jusqu'au niveau d'une seule particule. Éventuellement, cela établit un lien entre la description microscopique des systèmes quantiques et la thermodynamique.

La conception du maser à trois niveaux par Scovil et Schultz-Dubois à la fin des années cinquante a ouvert la voie à un grand nombre de travaux sur l'étude du comportement des lois de la thermodynamique sur les petits systèmes quantiques en considérant diverses perspectives et approches. Les machines thermiques quantiques représentent la main d'œuvre de la thermodynamique quantique dont le but ultime est de comprendre l'interaction dynamique et thermodynamique des systèmes quantiques avec leurs environnements respectifs. Par conséquent, l'amélioration de nos connaissances sur les lois de la thermodynamique à l'échelle quantique permet d'exercer une meilleure caractérisation et un meilleur contrôle des effets quantiques sur

les performances des machines thermiques quantiques. Étant donné que les propriétés quantiques telles que les corrélations et la cohérence quantique se sont avérées apporter un avantage quantique par rapport aux algorithmes classiques, il est donc naturel de se demander si l'utilisation de la cohérence quantique pourrait produire des résultats similaires affectant la performance des machines thermiques.

Dans notre présent travail, nous nous concentrons principalement sur l'impact de la cohérence quantique sur le fonctionnement de ces machines. La cohérence est la représentation des éléments non diagonaux de la matrice densité d'un système quantique par rapport à une base de référence particulière. La question de savoir si les effets de cohérence peuvent augmenter la fonctionnalité des machines thermiques est encore actuellement discutée, cela est dû au fait que ça dépend principalement du modèle étudié. En fait, de nombreuses études ont démontrés que la cohérence peut être à la fois bénéfique ou nuisible.

L'objectif de ce travail de thèse est d'explorer ces effets de cohérence pour différents scénarios en employant un schéma d'interaction répétée, appelé modèles collisionnels, où les cohérences sont présentes dans les ancillas des réservoirs thermiques et également dans une batterie quantique.

Ce mémoire de thèse s'articule autour de 6 chapitres :

Dans le premier chapitre, nous présentons le contexte, la motivation et l'introduction de cette thèse.

Dans le second chapitre, nous présentons les concepts préliminaires et outils de base de la mécanique quantique ainsi que les notations nécessaires pour comprendre le reste de la thèse. Nous fournissons une caractérisation des états quantiques, des corrélations et de l'entropie qui est un ingrédient clé dans la définition de la deuxième loi de la thermodynamique. Ensuite, nous adoptons une perspective théorique des ressources quantiques pour définir la cohérence quantique et discuter les moyens de la mesurer.

Le troisième chapitre est consacré à l'introduction des fondements théoriques des systèmes

quantiques ouverts, puisqu'une approche dynamique est primordiale pour décrire les machines thermiques quantiques, et à la définition de la thermodynamique quantique. La dynamique markovienne est obtenue en s'attaquant aux semi-groupes dynamiques et en effectuant les approximations de Born-Markov et séculaires. Nous distinguons deux formes des équations maîtresses de Lindblad (GKLS), à savoir les équations maîtresses locales et globales. Avant d'introduire la thermodynamique quantique comme l'essence de ce travail de thèse, nous terminons la première section du chapitre avec un exemple de la thermalisation d'un système quantique ouvert couplé à un environnement avec une température T. Le reste du chapitre est un aperçu de la thermodynamique quantique, nous discutons principalement des lois sur lesquelles elle est construite dans les régimes classique et quantique avec un accent particulier sur la première et la deuxième loi. L'échange d'énergie entre un système quantique et un bain thermique peut être divisé en deux apports : la chaleur et le travail. Ce dernier peut être quantifié par l'énergie libre hors équilibre ou l'ergotropie qui sont utilisées pour traiter l'extraction de travail des systèmes quantiques. Bien que les relations de fluctuation ne soient pas au centre de notre travail de thèse, nous les présentons comme un autre sujet de recherche intrigant à considérer lorsqu'il s'agit de traiter les fluctuations de chaleur et de travail dans les modèles collisionnels cohérents présentés dans le dernier chapitre comme une perspective future.

Dans le quatrième chapitre, nous discutons des caractéristiques quantiques des machines thermiques fonctionnant à l'échelle nanométrique. Nous décrivons le principe de fonctionnement d'un modèle très simple mais intuitif de la première proposition de moteur thermique quantique. Les machines thermiques peuvent fonctionner en cycles avec des courses discrètes et grâce à un couplage continu avec les réservoirs thermiques, nous donnons des exemples fondamentaux des cycles Otto et Carnot qui illustrent des machines cycliques et alternatives ainsi qu'un simple protocole de réfrigération où nous appliquons une transformation unitaire pour refroidir un qubit. L'utilisation de stimulations externes pour réaliser des opérations thermodynamiques peut être évitée en s'appuyant sur des configurations autonomes. La dernière section traite les machines thermiques autonomes qui fonctionnent exclusivement grâce aux interac-

tions incohérentes avec des réservoirs thermiques à différentes températures. Nous présentons le réfrigérateur d'absorption à trois qubits illustrant la simplicité de mise en œuvre des machines thermiques autonomes. Celui-ci peut être analysé différemment en employant le concept de qubits virtuels qui est une approche simple pour prédire le comportement de la machine.

Finalement le cinquième chapitre a pour but de fournir la dérivation du comportement thermodynamique de deux modèles collisionnels soumis à des conditions du régime stationnaire et d'explorer l'influence de la cohérence quantique sur leurs performances. Le premier modèle consiste en un seul qubit interagissant séquentiellement avec les ancillas de deux réservoirs à des températures différentes. Nos résultats démontrent que la cohérence dans l'état des ancillas froids se traduit par l'apparition d'un réfrigérateur hybride qui produit du travail. Cependant ce dispositif ne fonctionne jamais dans le même régime lorsque les cohérences sont présentes dans les ancillas chauds mais on obtient un meilleur rendement que la valeur de Carnot et Curzon-Ahlborn dans le cas du régime du moteur thermique. Tandis qu'au sein du deuxième modèle, nous exprimons à la fois les avantages et les inconvénients de l'utilisation de la cohérence comme ressource dans les machines thermiques quantiques et la nécessité d'être prudent lors de son utilisation dans ces processus. Nous présentons une machine à qubits virtuels autonome qui interagit par résonance avec les qubits dans une bande où ces derniers sont initialement préparées avec de la cohérence. Nous montrons que la cohérence peut améliorer les performances de la machine et lui permet de fonctionner sous des régimes normalement interdits, de facto un meilleur rendement est permis grâce à l'amélioration de la puissance de la machine. En outre, nos résultats indiquent également, que, pour des températures modérées du réservoir froid, la cohérence peut également être nuisible. De ce fait, l'optimisation de modèles particuliers devient une tâche cruciale pour bénéficier des améliorations induites par la cohérence.

Contents

List of Figures

List of Tables

Chapter 1

Introduction

1.1 Background and Motivations

Thermodynamic laws have a greater influence on our daily lives than nearly any other physical laws. They control the exchange of heat and the production of work by describing the conservation of energy and its transition from one form to another. The daily weather, cooling and heating systems in our homes and means of transportation are all examples of how they have an evident impact on our everyday perception.

Sadi Carnot's pioneering study of the performance of a hypothetical heat engine over two centuries ago established thermodynamics as a physical theory [1]. It consists of a set of universal laws that dictate the interplay among the properties of macroscopic systems such as the temperature, entropy and energy. With the rapid advancement in nanotechnology, the ability to design and produce next-generation small scale devices is highly demanded. Therefore, having a thermodynamic analysis of processes occuring at the nanoscale is crucial. A statistical mechanics interpretation of the principles of thermodynamics leads to the miniaturization of the thermodynamic behavior of macroscopic systems to the level of a single particle. Eventually, this establishes a connection between the microscopic description of quantum systems and thermodynamics.

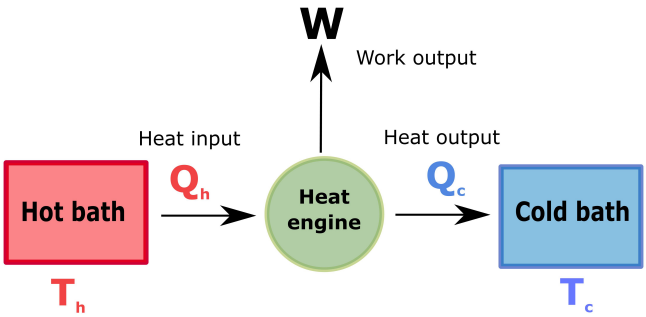

Figure 1.1: A traditional set up of a heat engine. A hot thermal bath provides an input heat Q_h which is partially turned into useful work W and the rest Q_c is deposited into the cold thermal bath.

The rise of quantum theory at the beginning of the 20th century is one of the most intriguing events which have moulded our modern understanding of physics. Planck's work on the thermodynamics of black body radiation [2] inspired Einstein to quantize the electromagnetic field in 1905 [3]. From this point, quantum mechanics thrived individually from thermodynamics, founding its own postulates and experiments [4]. Although both theories were developed independently, one can still wonder to which extent thermodynamics laws can be applied in the quantum regime and if quantum effects such as entanglement and coherence have a noteworthy impact on thermodynamic processes. Addressing these questions led to a novel framework that unifies both theories, and that is quantum thermodynamics, which is the main area of this work, where we indeed put a special emphasis on quantum thermal machines operating outside thermal equilibrium.

In 1959, Scovil and Schultz-Dubois took the credit for realizing the first Gedanken quantum thermal machine [187] during the early days of solid state lasers. Their seminal paper demonstrates that a three-level maser coupled to two thermal baths at different temperatures is capable of acting as a heat engine whose efficiency is upper-bounded by the Carnot efficiency. Their study relied on the equilibrium Boltzmann distribution to analyze the operation of the machine but on the other hand, a dynamical interpretation was missing. Thus, a methodology or approach that describes the evolution in time of open quantum systems is needed.

In the theory of open quantum systems [97] , our interest resides in providing a consistent de-

scription of only a chunk of a larger system. In other words, we perform the partial trace over the environmental degrees of freedom to obtain the dynamics of the open quantum system only. In this thesis, the relevant description of open quantum systems is given by the Lindblad master equations which were developed by Gorini, Kossakowski, Sudarshan [99] and Lindblad [100]. This formalism corresponds to the dynamical semigroups that ensure a Markovian description of the reduced system's time evolution and preserves positivity of the density matrix. Using the Lindblad approach paved the way for a dynamical investigation of quantum thermal machines by considering open quantum systems as the working substance of the machine [219].

In both classical and quantum thermodynamics, heat engines, refrigerators and heat pumps are essential objects of research. For instance, a heat engine uses the energy provided in the form of heat from the hot bath to perform work and then the rest is given off as a waste heat to the cold bath (see Fig. 1.1). Due to the nanotechnological progress and the increasing interest in quantum systems, heat engines can no longer be only seen as machines whose size is as large as steam engines from the industrial revolution. There are numerous realizations of micro-sized thermal machines in laboratories by using solid state nuclear magnetic resonance for algorithmic cooling [5], trapped ions [153, 167], superconducting qubits [6] and single spins [155] as the machine's working medium.

The study of quantum thermal machines is not only driven by the genuine understanding of the principles of quantum thermodynamics but also by the development of efficient thermal devices for technological progress. In quantum information processing and quantum computing, coherence and quantum correlations are vital ingredients that offer an exponential speed up over any known classical algorithms [28, 211]. A similar analysis was adopted to investigate the effectiveness of quantum properties on the enhancement of the performance of thermal machines at the nanoscale. In our present work, we focus mainly on the impact of quantum coherence on the operation of these machines. Coherence is the representation of the non-diagonal elements of quantum system's density matrix with respect to a particular reference basis [56]. The question whether coherence effects can boost the functionality of thermal machines is still currently

discussed, this is due to the fact that it is mostly model dependent. In fact, it has been found that coherence can be both beneficial [129, 175, 187, 244] or detrimental [245, 246, 248, 249]. The aim of this thesis is to explore these coherence effects for different scenarios by employing a repeated interaction scheme, called collision models [241], where the coherences are present in the ancillas of the baths and also in a battery system.

1.2 Contributions

In this thesis, we study the characterization and control of quantum effects, mainly quantum coherence, on the performance of thermodynamic tasks for small thermal machines operating in at the nanoscale by employing a collisional model framework. We start by considering a single qubit system that interacts sequentially with two thermal baths that contain identically prepared ancillas with a small amount of coherence in their state. In the second case, we introduce an autonomous thermal machine consisting of two-level qubits in thermal contact with two baths at different temperatures that form a virtual qubit machine. It operates through the collisions with a serie of qubits in a tape which are initially prepared with energetic coherence. By investigating these models, some intriguing results were found:

- A derivation of thermodynamic quantities for the case of coherent ancillas of the baths was made in the steady state regime. In the situation of one bath with coherence, the expressions of the heat currents and work depend on the strength of coherence but not on its phase. On the other hand, when coherence is present in both baths, only their relative phase would appear in the expressions.

- In the absence of coherence, the efficiency of the heat engine and the refrigerator's coefficient of performance (COP) are less or equal than the Carnot efficiency and the reversible COP. However, in the case of coherence is injected in the cold bath, the refrigerator and heat engine survive in the classical forbidden regime such that their COP and efficiency surpass the Carnot limit for some regions of parameters respectively, which shows that

their value at maximum power is larger in the coherent case. Coherence allows also the machine to go from acting as an accelerator to a refrigerator that produces work (hybrid refrigerator).

- In contrast to the previous situation, the device never operates as a hybrid refrigerator when the hot ancillas contain coherence. In terms of the efficiency at maximum power, the machine's power reaches zero when the maximum achievable efficiency is the Carnot value. Because of the coherent contributions, the efficiency goes beyond the Carnot and the Curzon-Ahlborn value.
- The operation of an autonomous quantum thermal machine powered by energetic coherence is explored. The machine is built by using the notion of virtual qubits which interacts with coherent qubits through energy preserving collisions. These qubits were used to obtain a useful output free energy and also as a fuel to power thermodynamic tasks.
- Coherence is shown to be a powerful resource that can be harnessed to enhance the machine's power and to allow it to function in otherwise forbidden situations.
- The optimization over the machine's design (the tape qubit's initial state) is a crucial element to maximize the free energy and the cooling power. As an alternative work quantifier, ergotropy provides similar results.
- For lower temperatures of the cold bath, coherence enhances both the power and the efficiency of the heat engine contrary to the incoherent case.
- As far as the cooling power is considered, coherence induces detrimental effects on the performance of the machine, which means that coherence enhanced-cooling is not accompanied by an improved efficiency. Thus, there is a trade-off between power and efficiency.

List of Publications

- Kenza Hammam, Yassine Hassouni, Rosario Fazio and Gonzalo Manzano, "Optimizing Autonomous Thermal Machines Powered by Energetic Coherence". New J. Phys. 23

043024,(2021).

- Kenza Hammam, Heather Leitch, Yassine Hassouni and Gabriele De Chiara. “Exploiting coherence for quantum thermodynamic advantage”. (Submitted).
- Abderrahim El Allati, Kenza Hammam, Hicham Amellal and Yassine Hassouni. "Quantum Discord for Information Transmission Using Coherent States". J Russ Laser Res 39, 524–532 (2018).

1.3 Outline of The Thesis

Below, we summarize the content of each chapter of this dissertation.

Chapter 2 settles basic notations and relevant concepts of quantum mechanics with a particular focus on the characterization of quantum states, correlations and quantum coherence as well as means to measure them.

In chapter 3, we review the theory of open quantum systems especially the Markovian approach which is the most common tool used for treating quantum thermal machines. Then we move our attention to the definition of quantum thermodynamics which is the main field of this thesis. We provide an overview of the laws of thermodynamics and define the notion of work extraction for non-equilibrium systems. Although quantum fluctuation theorems are not relevant to our thesis work, we introduce them as another important topic to be considered when one takes into account fluctuations present in quantum systems.

The purpose of chapter 4 is to discuss the fundamental design and working principles of some well-known quantum thermal machines that have been widely explored in the literature. Then we make a distinction between non-autonomous and autonomous thermal machines that use a simple mechanism to function via the notion of virtual qubits at a well chosen virtual temperature.

Chapter 5 is entirely devoted to the study of the impact of quantum coherence on the perfor-

mance of quantum thermal machines. We describe two models where we divide the appearance of coherence. We provide an analysis of the first model in which coherence is present in the ancillary baths, then we pinpoint the role of the initial coherence in the battery system (tape qubits). In both scenarios, we give a detailed description of the different modes of the machine's operation in steady state conditions and perform the optimization of power for different regimes.

Lastly, we conclude the thesis in a final discussion of our results with perspectives for further investigation.

Chapter 2

The Basic Concepts of Quantum Systems, Correlations and Quantum Coherence

"All matter originates and exists only by virtue of a force which brings the particle of an atom to vibration and holds this most minute solar system of the atom together. We must assume behind this force the existence of a conscious and intelligent spirit. This spirit is the matrix of all matter"

Max Planck, 1944.

Quantum mechanics is a counter-intuitive theory that characterizes and makes predictions of the physical world of atoms and subatomic realms more specifically .This mathematical framework introduces a unique study of the phenomenas highlighted empirically of elementary particles which are distinguished by their probabilistic behavior. It encompasses a detailed description of the state of a single and composite quantum systems, the effect of measurement on the system's state, and also the dynamics of open quantum systems in which systems interact with their environments. An interesting amount of experiments have provided results concordant with the predictions of quantum mechanics, in which Newtonian mechanics have failed to explain them [4] [7] [8].

In the ensuing chapter, we recap the basics of quantum mechanics with a particular focus on the characterization of quantum systems, quantum correlations and quantum coherence as well as providing ways to quantify them.

2.1 States in Quantum Mechanics

In Quantum Mechanics, the world is separated into two components, namely the system and the observer. The system is the physical representation of a part of the world. The observer is the rest of the world. One of the many peculiar yet interesting aspects of Quantum Mechanics is the role of the observer. *Quantum measurement* is the process of changing the state of a system as a result of interaction between the observer and the system. Physical quantities such as the momentum, position and energy of a particle can be measured. These properties are defined as *observables*. There will be likely an infinite number of outcomes when measuring one of these observables. Each result is equivalent to a unique physical configuration of the quantum system, referred to as a quantum state. For instance, in the Stern-Gerlach experiment [10], when measuring the spin of a spin $\frac{1}{2}$ particle in a specific direction, two separate and possible outcomes can be obtained:$\pm\frac{\hbar}{2}$ with two corresponding states which are referred to simply as "spin up" and "spin down" along the measured axis. In fact, in quantum mechanics, a system cannot only be limited to one single state at one time but it may exist in a *superposition* of several states simultaneously [12, 13, 18].

Quantum measurement theory emanates from the self-adjoint operators from the theory of self adjoint operators. Notably, to every observable, a linear self-adjoint (Hermitian) operator or matrice $M = M^\dagger$ which acts upon the elements of the Hilbert space is associated. Hermitian matrices have crucial properties such as real eigenvalues and their corresponding eigenvectors are orthogonal, they form a basis for the Hilbert space thus we can express any state as a linear combination of eigenvectors. It is important to mention that throughout this thesis, the operator describing the system's total energy will be used and it is called the system's *Hamiltonian*.

2.1.1 Density Operator

A quantum system is associated with a complex vector space given a scalar product called the *Hilbert space* $\mathcal{H}$. To describe the most general state of a quantum system; we switch from a description in terms of a state vector " $|\psi\rangle$" (Dirac's notation) [9], i.e "ket" in a Hilbert space $\mathcal{H}$ to a description in terms of density operators or density matrices. We define this new object by adopting a physical approach, in terms of a statistical mixture of a set of state vectors since pure states described by a single state vector $|\psi\rangle$ are idealized descriptions which do not occur in nature. We also display its main properties, extend its definition by detaching from the notion of the vector state and reformulate the postulates of quantum mechanics with respect to the density operator.

2 The Basic Concepts of Quantum Systems, Correlations and Quantum Coherence

Density operator for pure states

Introduced by von Neumann [14], density operators also called density matrices are alternate representations of the state vectors that encode all the accessible information about a mechanical quantum system. In order to express the density operator, we suppose that there is a convenient set of orthonormal basis states denoted $\{|U_n\rangle, n = 1, 2, ...\}$. Using the superposition principle, we get the expansion in this basis with respect to the eigenstates of an hermitian operator A, if the system is in the state $|\psi(t)\rangle$ at time t

$$|\psi(t)\rangle = \sum_n C_n(t)|U_n\rangle \qquad \text{with} \qquad A|U_n\rangle = a_n|U_n\rangle. \tag{2.1}$$

The normalization of $|\psi(t)\rangle$ implies that

$$\langle\psi(t)|\psi(t)\rangle = \sum_n \sum_m C_n(t)C_m^*(t)\langle U_m|U_n\rangle = \sum_n |C_n(t)|^2, \tag{2.2}$$

where $|C_n(t)|^2$ measures the eigenvalue a_n such that the coefficients $C_n(t)$ are probability amplitudes. Thanks to superposition they may interfere, a feature which has no equivalent in classical physics.
The expectation value for any operator A with matrix elements is defined as $A_{mn} = \langle U_m|A|U_n\rangle$

$$\begin{aligned} \langle A\rangle_t = \langle\psi(t)|A|\psi(t)\rangle &= \sum_n \sum_m C_n(t)C_m^*(t)A_{mn} \\ &= \sum_{n,m} \rho_{nm}(t)A_{mn} \qquad \text{with} \qquad \rho_{mn}(t) = \langle U_m|\psi(t)\rangle\langle\psi(t)|U_n\rangle. \end{aligned} \tag{2.3}$$

Such that ρ_{mn} are the off-diagonal density operator elements also called *coherences* for $n \neq m$, and ρ_{nn} are the diagonal terms also referred to as *populations*. The decoherence phenomenon generated by the system's interaction with its environment, on the other hand, is equivalent to the decay of coherences over time, as we shall discover later, notably in Chapter 3. Hence, we define the density operator $\rho(t)$ for **pure states** as the outer product of the state $|\psi(t)\rangle$ and its conjugate

$$\rho(t) = |\psi(t)\rangle\langle\psi(t)|. \tag{2.4}$$

We will use ρ instead of $\rho(t)$ every time when the instant t matters less. In the case of pure states, the density operator corresponds simply to the projection operator onto $|\psi\rangle$.

Properties

- ρ is an hermitian operator: $\rho^\dagger = \rho$.

  In fact: $\rho^\dagger = (|\psi\rangle\langle\psi|)^\dagger = |\psi\rangle\langle\psi| = \rho$.

- ρ is a positive operator :$\forall|\phi\rangle \in \mathcal{H}; \langle\phi|\rho|\phi\rangle \geq 0$.

  In fact: $\forall|\phi\rangle \in \mathcal{H}, \langle\phi|\rho|\phi\rangle = \langle\phi|\psi\rangle\langle\psi|\phi\rangle = |\langle\phi|\psi\rangle|^2 \geq 0$.

- $\mathrm{tr}(\rho) = 1$.

  In fact: let's consider that $\{|\phi_i\rangle, i = 1, .., n\}$ an orthonormal basis from $\mathcal{H}$ with dimension n and $|\psi\rangle = \sum_{i=1}^{n} c_i|\phi_i\rangle$ is the decomposition of $|\psi\rangle$ in this basis with $\sum_{i=1}^{n} |c_i|^2 = 1$, we get

$$\mathrm{tr}(\rho) = \sum_{i=1}^{n}\langle\phi_i|\rho|\phi_i\rangle = \sum_{i,j=1}^{n} c_j c_j^* \underbrace{\langle\phi_i|\phi_j\rangle}_{\delta_{ij}}\underbrace{\langle\phi_j|\phi_i\rangle}_{\delta_{ji}} = \sum_{i=1}^{n}|c_i|^2 = 1.$$

- $\langle A\rangle_\psi = \langle\psi|A|\psi\rangle = \mathrm{tr}(\rho A)$.

- $\mathrm{tr}(\rho^2) = 1$.

  In fact, since $\rho^2 = |\psi\rangle\langle\psi|\psi\rangle\langle\psi| = |\psi\rangle\langle\psi| = \rho$, the result comes from Eq.2.1.1.

In the case of pure states, the description of the state of the system in terms of density operators doesn't have any advantages besides the fact that it removes the phase $\mathrm{e}^{i\varphi}$ of a vector state.

Density operator for mixed states

Like in classical physics, many situations exist in quantum physics where it is unrealizable to have a complete knowledge of the state of the prepared system. This lack of information has as a consequence the fact that it is not possible to associate without ambiguity a unique vector state of the physical system to a *mixed state*. However, it is possible if we have a probability distribution that allows us to know with which probability the physical system is likely in a particular state.

Theorem:

We consider the situation of preparing $|\psi_i\rangle(i = 1, .., n)$ pure states with probability p_i. We define the density operator of a mixed ensemble as the summation of projectors $|\psi_i\rangle\langle\psi_i|$, the states $|\psi_i\rangle$ are not necessarily orthogonal:

$$\rho = \sum_{i=1}^{n} p_i|\psi_i\rangle\langle\psi_i| \qquad \text{with} \qquad \sum_{i=1}^{n} p_i = 1 \qquad \text{and} \qquad p_i \geq 0 \quad \forall i. \tag{2.5}$$

A pure state is a special case of a mixed state associated with a non-negative probability which equals to 1.

Properties

We can apply the same properties of the pure state density operator in the case of mixed states. Let be $\rho = \sum_{i=1}^{n} p_i \rho_i$ with $\rho_i = |\psi_i\rangle\langle\psi_i|$, $\sum_{i=1}^{n} p_i = 1$ and $p_i \geq 0$ such that ρ_i represents the density operator associated with the pure state $|\psi_i\rangle$, thus:

- ρ is an hermitian operator: ρ is an hermitian operator: $\rho^\dagger = \rho$.
- ρ is a positive operator : $\forall|\phi\rangle \in \mathcal{H}; \langle\phi|\rho|\phi\rangle \geq 0$.
- $\mathrm{tr}(\rho) = 1$.
- $tr(\rho A) = \sum_{i=1}^{n} p_i \langle\psi_i|A|\psi_i\rangle$ for any operator A.
- $0 \leq tr(\rho^2) \leq 1$.

  In fact, we consider an orthonormal basis from $\mathcal{H}$ of dimension n $\{|i\rangle, i = 1, .., n\}$ composed of eigenvectors $|i\rangle$ of ρ and its respective eigenvalues λ_i. Since the trace is not dependent of the choice of the used basis, we get the following result:

$$tr(\rho^2) = \sum_{i=1}^{n} \langle i|\rho\rho|i\rangle = \sum_{i=1}^{n} \langle i|\lambda_i\lambda_i|i\rangle = \sum_{i=1}^{n} \lambda_i^2 \geq 0 \quad \text{Furthermore: } \sum_{i=1}^{n} \lambda_i^2 \leq \sum_{i=1}^{n} \lambda_i = 1.$$

  Because $\lambda_i \in [0, 1]$, since ρ is a positive operator with a unitary trace, consequently: $0 \leq tr(\rho^2) \leq 1$.

  This property is interesting, because it is a criterion to decide if a state is pure or mixed. We have the maximum possible information about the system when a system is prepared in a pure state. On the other hand, the *degree of purity*, for mixed states, is affiliated with the amount of information we are missing by looking at the system only.

2.1.2 Quantum Mechanics Postulates

Now, we present a review of the fundamental postulates of quantum mechanics in terms of density operator:

Postulate I: State of a quantum system We associate every isolated physical system to a complex vector space with inner product known as the $\mathcal{H}$.A hermitian, unit-trace, positive operator ρ acting on the system's state

space completely represents the system. If a quantum system is in the state ρ_i with probability p_i, then the density operator for the system is $\sum_i p_i \rho_i$.

Postulate II: Dynamics of a quantum system The time evolution of the density operator $\rho(t)$ of an isolated system is defined by the *Liouville-von Neumann* equation as

$$i\hbar \frac{d}{dt}\rho(t) = [H, \rho(t)], \tag{2.6}$$

where $\hbar$ is the $Planck$ constant and H is the hermitian Hamiltonian of the system.

We can also describe the time evolution by applying an unitary operator $U(t, t_0)$ called **propagator**, so that $U(t, t_0) = \mathrm{e}^{-\frac{i}{\hbar}H(t-t_0)}$, we get the effect on the density operator by

$$\rho(t) = U(t, t_0)\rho(t_0)U^{\dagger}(t, t_0). \tag{2.7}$$

Note that this equation look similar to the $Heisenberg$ equation, but it's not the same: in the Heisenberg picture, the equation describes the evolution of the operators in time, whereas here, in the Schrödinger picture, it's the state vectors that are time dependent.

Postulate III: Quantum measurements

Any measurement operation on a physical system is described by a collection of *measurement operators* $\{M_k\}$. The index k refers to the measurement outcomes that might occur in the experiment. These measurement operators satisfy the completeness equation:

$$\sum_k M_k^{\dagger} M_k = \mathbb{1} \qquad \text{where } \mathbb{1} \text{ is the identity operator.} \tag{2.8}$$

If ρ is the state of the system before the measurement, the the probability to obtain "m" results is given by

$$p(m) = \mathrm{tr}(\rho M_m^{\dagger} M_m). \tag{2.9}$$

After the measurement with outcomes "m", the state of the system is represented by the density operator:

$$\rho' = \frac{M_m \rho M_m^{\dagger}}{tr(M_m^{\dagger} M_m \rho)}, \tag{2.10}$$

such that the set of operators $E = M_m^{\dagger} M_m$ is also called a generalized measure or a *positive operator-valued measure* **(POVM)**. The measurement is characterized by a set of positive operators $\{E_m \geq 0\}_{m=1}^{k}$ such $\sum_m E_m =$

$\mathbb{1}$, m labels the outcome of measurement on the state ρ with probability :$p(m) = \mathrm{tr}(E_m\rho)$. Furthermore, the act of measurement disturbs the quantum system in a fundamental way.

The Von Neumann measurement

The projective measurements often referred to as the Von Neumann measurements are a standard and conventional measurements in quantum mechanics. They are also a special case of the generalized measurements described above. They are defined as a collection of projectors that satisfy the following properties:

- $\sum_n P_n = \mathbb{1}$
- $P_i P_j = \delta_{ij} P_i$
- $P_n = P_n^\dagger$.

Given an observable Q, its spectral decomposition is given by a set of projectors

$$Q = \sum_n \lambda_n P_n = \sum_n \lambda_n |\phi_n\rangle\langle\phi_n|, \tag{2.11}$$

where P_n is a projection operator, $|\phi_n\rangle$ are the orthonormal eigenvectors of Q associated with the eigenvalues λ_n. Measuring the observable Q on a state $|\psi\rangle$ yields a result that is labeled with λ_n. The probability of getting λ_n is

$$p(n) = \langle\psi|P_n|\psi\rangle. \tag{2.12}$$

In this case, the state of the system after performing the measurement is

$$Pure \quad states : |\psi\rangle \to |\psi'\rangle = \frac{P_n|\psi\rangle}{\sqrt{\langle\psi|P_n|\psi\rangle}} = \frac{P_n|\psi\rangle}{\sqrt{p(n)}} \tag{2.13}$$

$$Mixed \quad states : \rho \to \tilde{\rho} = \frac{P_n\rho P_n}{\mathrm{tr}(P_n\rho)} = \frac{P_n\rho P_n}{p(n)}. \tag{2.14}$$

The major difference between projective measurement and POVM elements is that the latter do not have to be orthogonal.

Postulate IV: Composite systems The state space $\mathcal{H}$ of a composite physical system is the tensor product of the state spaces of the components of the physical system

$$\mathcal{H} = \mathcal{H}_1 \otimes ... \otimes \mathcal{H}_n. \tag{2.15}$$

Moreover, if the system has been prepared in the states $\rho_i (i = 1, .., n)$, the joint state of the total system is given by

$$\rho = \rho_1 \otimes \rho_2 \otimes ... \otimes \rho_n. \tag{2.16}$$

The reduced density operator:

Sometimes only one of the component systems is interesting and the others are left undetected. This situation is captured by the concept of *the reduced density operator*. Suppose we have a bipartite system composed of the subsystems A and B, whose state is described by the density operator ρ^{AB}. Then we can define the reduced density operator of A as the partial trace tr_B over the subsystem B, described by

$$\rho^A = \mathrm{tr}_B(\rho^{AB}). \tag{2.17}$$

Above the partial trace is

$$\mathrm{tr}_B(|a_1\rangle\langle a_2| \otimes |b_1\rangle\langle b_2|) = |a_1\rangle\langle a_2| \, \mathrm{tr}(|b_1\rangle\langle b_2|), \tag{2.18}$$

where $|a_i\rangle$ and $|b_i\rangle$ are any two vectors in the respective state spaces ($\mathcal{H}_A$ and $\mathcal{H}_B$) and $\mathrm{tr}(|b_1\rangle\langle b_2|) = \langle b_2|b_1\rangle$ is the usual trace operation for system B. It is required that the partial trace must be linear in its input. It turns out that the physical meaning of the partial trace lies in the fact that it is a unique operation which gives rise to the correct description of measurement statistics for the subsystem A.

2.1.3 The Qubit System

A "*quantum bit*" or "*qubit*", as coined by Schumacher [15], is the fundamental unit of information in quantum information theory. As its digital analogue, it describes a two level physical system that can be in its excited or ground state. A qubit is represented by a quantum mechanical system with two elementary orthogonal states denoted by $|0\rangle$ and $|1\rangle$, respectively. In quantum information jargon, the set of states $\{|0\rangle, |1\rangle\}$ is referred to as the computational basis, whereas their orthogonality implies $\langle 0|1\rangle = 0$. Thus, the qubit can be be conceived as a superposition state of the form

$$|\psi\rangle = \alpha|0\rangle + \beta|1\rangle, \tag{2.19}$$

where α and β are two complex coordinates also called the *qubit amplitudes* normalized to unity according to

$$|\alpha|^2 + |\beta|^2 = 1, \tag{2.20}$$

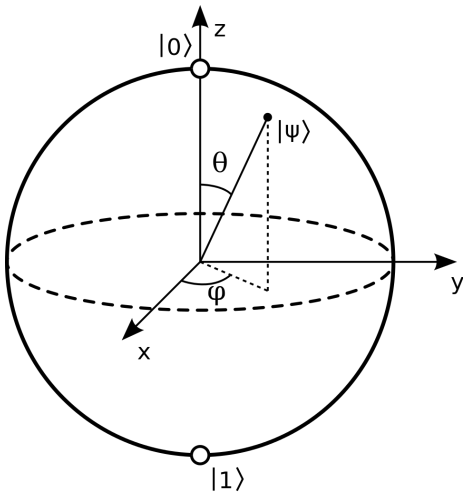

Figure 2.1: Geometrical representation of a single qubit on the Bloch sphere

such that the probability that the qubit measure yields the bit 0 is $|\alpha|^2$ and that of yielding the bit 1 is $|\beta|^2$. The convenient way to visualize the state of a single qubit is through a vector on the on the **Bloch sphere** 2.1. The state $|\psi\rangle$ qubit is represented as a unique point on the surface of the Bloch sphere. In general, the qubit is defined within an unobservable phase vector as

$$|\psi\rangle = \cos(\frac{\theta}{2})|0\rangle + \sin(\frac{\theta}{2})\,\mathrm{e}^{i\varphi}\,|1\rangle \quad \text{With } \theta \in [0,\pi] \text{ and } \varphi \in [0,2\pi]. \tag{2.21}$$

In fact, the variation of these two parameters allows a quantum state to take all values of the Bloch sphere. In the classical case, there exist four possible pairs of classical bits if we have two bits, namely 00, 01, 10 and 11. In parallel, the two qubits system has four corresponding states $|00\rangle$, $|01\rangle$, $|10\rangle$ and $|11\rangle$, and similarly to 2.19 a pair of qubits can exist is any state of the form

$$|\psi\rangle = \alpha_{00}|00\rangle + \alpha_{01}|01\rangle + \alpha_{10}|10\rangle + \alpha_{11}|11\rangle \tag{2.22}$$

$$= \alpha_{00}\begin{pmatrix}1\\0\\0\\0\end{pmatrix} + \alpha_{01}\begin{pmatrix}0\\1\\0\\0\end{pmatrix} + \alpha_{10}\begin{pmatrix}0\\0\\1\\0\end{pmatrix} + \alpha_{11}\begin{pmatrix}0\\0\\0\\1\end{pmatrix}, \tag{2.23}$$

where the complex coefficients α_x ($x = 00, .., 11$) are normalized as $\sum_x |\alpha_x|^2 = 1$.

The Bloch sphere for mixed states:

Each contributing density operator associated with a qubit can be parameterized using the *Pauli operators* is given

as

$$\mathbb{1} = \begin{pmatrix} 1 & 0 \\ 0 & 1 \end{pmatrix}; \quad \sigma_x = \begin{pmatrix} 0 & 1 \\ 1 & 0 \end{pmatrix}; \quad \sigma_y = \begin{pmatrix} 0 & -i \\ i & 0 \end{pmatrix}; \quad \sigma_z = \begin{pmatrix} 1 & 0 \\ 0 & -1 \end{pmatrix}. \tag{2.24}$$

Thus the single qubit density matrix can be written

$$\rho = \frac{1}{2}(\mathbb{1} + r_x\sigma_x + r_y\sigma_y + r_z\sigma_z) = \frac{1}{2}(\mathbb{1} + r.\sigma), \tag{2.25}$$

where $r = (r_x, r_y, r_z)$ is a real vector associated with Bloch coordinates of length $|r| < 1$. In the hand, mixed states reside in the interior of the Bloch sphere and the point $\frac{1}{2}\mathbb{1}$ corresponds to the center of the Bloch sphere, this is the maximally mixed state. On the other hand, pure states lie on the surface of the sphere $|r| = 1$.

2.2 Correlations

Unlike its classical counterpart, the majority of the information held in a generic physical quantum system may be represented as correlations between subsystems that cannot be replicated [16] and is altered as an outcome of a measurement.and are altered as a result of a measurement. Quantum correlations have been studied since the 1960s, when John Bell published his milestone paper [17] in which he discovered that local measurements on an entangled system [18, 19] can create a nonlocal correlation. Studies of quantum correlations have led to intriguing demonstrations of the quantum advantage [20–22]. In this section, we highlight some of the most important entropy-based methods to quantify quantum correlations in a qubit system.

2.2.1 Entropy

Shannon's entropy [23] is a measure of the uncertainty of a classical random variable associated with a classical probability distribution in classical information theory. The *Von Neumann entropy* $S(\rho)$ provides a standard measure of the information contained inside a quantum physical system given by the statistical density operator ρ:

$$S(\rho) = -tr(\rho \log_2 \rho). \tag{2.26}$$

As usual, the logarithm is taken to base 2. If λ_x are the members of the set of eigenvalues of ρ, then the von Neumann entropy can be rewritten as follows

$$S(\rho) = -\sum_x \lambda_x \log_2 \lambda_x. \tag{2.27}$$

Among the features of the von Neumann entropy is that it is non-negative, and since pure states depict full knowledge about a quantum system, $S(\rho)$ is zero. In contrast, for a d-dimensional Hilbert spaces the completely mixed density operator $\frac{\mathbb{1}}{d}$ represents maximal uncertainty with entropy $\log_2 d$.

Properties of $S(\rho)$:

We shall expose some important properties of the von Neumann entropy:

1. $S(\rho)$ is invariant under unitary transformation U: $S(\rho) = S(U\rho U^\dagger)$.
2. For a composite system AB in a pure state: $S(A) = S(B)$.
3. Let p_i be a probability distribution and ρ^i be a family of states that have support on orthogonal subspaces, then we can get
$$S(\sum_i p_i\rho^i) = H(p_i) + \sum_i p_i S(\rho^i), \tag{2.28}$$
such that $\sum_i p_i S(\rho^i)$ is the entropy of residual states and $H(p_i)$ is the classical information gained by measuring the outcomes i with probabilities p_i.
4. $S(\rho)$ is a concave function i.e. if $\lambda_1, ..., \lambda_n \geq 0$ with $\lambda_1 + \lambda_2 + ... + \lambda_n = 1$, then
$$S(\sum_{i=1}^n \lambda_i\rho^i) \geq \sum_{i=1}^n \lambda_i S(\rho^i) \tag{2.29}$$
5. $S(\rho)$ is additive, respectively ρ^A and ρ^B are the states of systems A and B, we get
$$S(\rho^A \otimes \rho^B) = S(\rho^A) + S(\rho^B). \tag{2.30}$$
6. For a bipartite system AB in the state ρ^{AB} with ρ^A and ρ^B are the reduced density operators of the subsystems A and B, the entropy for correlated subsystems is described by
$$S(\rho^{AB}) \leq S(\rho^A) + S(\rho^B). \tag{2.31}$$
This property is known as subadditivity.

Quantum relative entropy

The quantum relative entropy, introduced by Umegaki [24] in the setting of von Neumann's algebras, is seen as a generalisation of the *Kullback Leibler divergence* 2.32 [25]. Given two states ρ and σ belonging to the same quantum system, the quantum relative entropy of ρ with respect to σ is defined by

$$S(\rho||\sigma) = tr(\rho(\log_2 \rho - \log_2 \sigma)) = tr(\rho \log_2 \rho) - tr(\rho \log_2 \sigma). \tag{2.32}$$

This quantity is non-negative and obeys to the *Klein's inequality*

$$S(\rho||\sigma) \geq 0, \tag{2.33}$$

which becomes an equality if $\rho = \sigma$.

It is also a jointly convex function. Let ρ_1, ρ_2, σ_1 and σ_2 be density operators, and p_1 and p_2 are probabilities, then we have

$$S(\rho||\sigma) \leq p_1 S(\rho_1||\sigma_1) + p_2 S(\rho_2||\sigma_2). \tag{2.34}$$

The quantum relative entropy lacks symmetry, technically it is not a metric and it expresses rigorously the distinguishability of states defined in the same Hilbert space.

Quantum joint and conditional entropy:

In analogy with entropies for classical systems, we define quantum joint and conditional entropies for composite quantum systems.

Joint entropy

The joint entropy of the pair of two subsystems A and B is the uncertainty about the entire system

$$S(A, B) = -tr(\rho^{AB} \log_2 \rho^{AB}) = S(\rho^{AB}). \tag{2.35}$$

In quantum information theory, the joint entropy of AB can be smaller than the entropy of one of its subsystems B: $S(A, B) < S(B)$, something which is obviously prohibited in classical information theory.

Conditional entropy

The conditional entropy is the information gained from AB when the subsystem B is known, the joint entropy

$S(A, B)$ is used to express it as follows:

$$S(A|B) = -tr(\rho^{AB} \log_2 \rho^{A|B}) = S(A, B) - S(B). \tag{2.36}$$

The conditional entropy is characterized by its invariance under any unitary transformation of the product form $U_A \otimes U_B$. ($\rho^{A|B} \rightarrow \rho'^{A|B} = (U_A \otimes U_B)\rho^{A|B}(U_A^\dagger \otimes U_B^\dagger)$).
In the case if the quantum system exhibits quantum entanglement, the conditional entropy can be negative which is a feature that doesn't exist in classical systems. Moreover, conditioning does not increase entropy even if the conditioning system is quantum as it is shown in the inequality below

$$S(A) \geq S(A|B). \tag{2.37}$$

2.2.2 Quantum Mutual Information

The quantum mutual information is a generalization of the concept of the mutual information to quantum information theory. It bears the interpretation of total correlations between two subsystems A and B of a bipartite quantum system ρ^{AB}. Since it is regarded as a special case of relative entropy between ρ^{AB} and $\rho^A \otimes \rho^B$ which is non-negative, it is clear that the quantum mutual information is also non-negative. From the relation $log(\rho^A \otimes \rho^B) = \log \rho^A \otimes \mathbb{1}_B + \mathbb{1}_A \otimes \log \rho_B$ we describe this natural quantum extension of the classical mutual information by

$$I(\rho^{AB}) = S(\rho^A) + S(\rho^B) - S(\rho^{AB}). \tag{2.38}$$

Mutual information is also the reduction in uncertainty of a due to the knowledge B, and vice versa it can be written as

$$I(A : B) = S(A, B) - S(A|B) - S(B|A). \tag{2.39}$$

It is equal to zero if the subsystems A and B are independent, and for an ensemble with itself (self information) it is the entropy of one of the subsystems: $I(A : B) = S(A)$.

2.2.3 Quantum Entanglement

Because of the counter-intuitive effects and behavior associated with the correlations it entails, quantum entanglement is of intrinsic conceptual interest that has no classical analogue. It represents the essential physical resource for the description and performance of quantum information processing tasks, like quantum key distribution [20], teleportation [21] and quantum computation [211, 228]. Intriguingly, signatures of non-classical correlations can be detectable even in separable states, but their nature is tremendously different from entanglement. As a matter of fact, while entanglement can be regarded as a result of the superposition principle, more general and genuine forms of quantum correlations emerge actually from the non-commutativity of quantum observables. Separable states are often recognized as fundamentally classical as far as composite systems are concerned. Nevertheless, the quantum content of correlations may be hidden behind the classical correlations in mixed separable states. This has fuelled an active stream of research especially after the discovery of some quantum computational models that perform certain tasks with exponential speed up bigger and more important than of any classical algorithm without necessarily requiring the usage of entanglement as a quantum resource (such as the DCQ1 model [28]). In fact, this has led to define a class of quantum correlations which are more fundamental and general than entanglement. This type of non-classical correlations beyond entanglement is called quantum discord [83, 84].

Quantum Entanglement for Bipartite Pure States

Schmidt decomposition

Before delving into defining entanglement for bipartite pure states, we introduce a powerful tool that is regarded as a special basis representation of bipartite states which the quantification of pure states entanglement relies on, that is the Schmidt decomposition.

Theorem *Let $\{|\varphi_i\rangle\}$ and $\{|\phi_i\rangle\}$ be a set of orthonormal local bases in the Hilbert spaces $\mathcal{H}_A$ and $\mathcal{H}_B$. Any pure state $|\psi_{AB}\rangle \in \mathcal{H}_A \otimes \mathcal{H}_B$ can be expressed in an appropriately chosen basis as*

$$|\psi_{AB}\rangle = \sum_i \sqrt{p_i}|\varphi_i\rangle \otimes |\phi_i\rangle \tag{2.40}$$

$$= \sum_i \lambda_i|\varphi_i\rangle \otimes |\phi_i\rangle. \tag{2.41}$$

Where $p_i = \lambda_i^2$ are non-negative real numbers satisfying $\sum_i p_i = 1$, known as the Schmidt coefficients.

The Schmidt coefficients contain all the information on the entanglement of the state $|\psi_{AB}\rangle$, any measure of entanglement is a function of the Schmidt coefficients. Thus, $|\psi_{AB}\rangle$ is entangled if and only if the decomposition has more than one Schmidt coefficient. Conversely, when there is only one Schmidt coefficient, $|\psi_{AB}\rangle$ is expressed as a product of states (*separable*). However, if the absolute values for all non-zero Schmidt coefficient are equal then the system is said to be *maximally entangled*. Furthermore, the squares of the Schmidt coefficients of a bipartite pure state are the eigenvalues of either the reduced density operators $\rho_A = \mathrm{tr}_B(\rho_{AB})$ and $\rho_B = \mathrm{tr}_A(\rho_{AB})$. For pure states, the Schmidt decomposition is a very important separability criterion that enables us to distinguish entangled states.

Definition: Let $\mathcal{H}_A$ and $\mathcal{H}_B$ be Hilbert spaces of the subsystems A and B and let $|\psi\rangle \in \mathcal{H}_A \otimes \mathcal{H}_B$ be a pure state. The state $|\psi\rangle$ is said to be entangled if and only if $|\psi\rangle$ cannot be factorized into pure states of their individual components. Thereof we have

$$\forall |\phi^A\rangle \in \mathcal{H}_A, \forall |\phi^B\rangle \in \mathcal{H}_B : \quad |\psi\rangle \neq |\phi^A\rangle \otimes |\phi^B\rangle. \tag{2.42}$$

Otherwise, it is called separable.

Example: Bell states A perfect example of an entangled pure state of two qubits is

$$|\psi^+\rangle = \frac{1}{\sqrt{2}}(|0\rangle_A \otimes |1\rangle_B + |1\rangle_A \otimes |0\rangle_B). \tag{2.43}$$

Suppose that Alice and Bob represent the subsystems A and B respectively. They both make measurements on their part of the entangled state $|\psi^+\rangle$. They will both get the outcome 0 or 1 with equal probability $\frac{1}{2}$ which means that neither the subsystems is in a precise state. Although on the other hand, whenever Alice measures 1, then Bob will measure 0 with certainty and vice versa. $|\psi^+\rangle$ is one of the four Bell states

$$|\psi^\pm\rangle = \frac{1}{\sqrt{2}}(|01\rangle_{AB} \pm |10\rangle_{AB}) \qquad |\phi^\pm\rangle = \frac{1}{\sqrt{2}}(|00\rangle_{AB} \pm |11\rangle_{AB}). \tag{2.44}$$

These states are maximally entangled and form a convenient basis of bipartite quantum states of two dimensional Hilbert spaces.

Quantum Entanglement for Bipartite Mixed States

Unlike pure states, the situation for mixed states describes more complicated matters. In fact, both classical and quantum correlations may be present in mixed states. It is the concept of separability that accentuates the distinction between those two kinds of correlations. In order to define entangled and separable states, the following preparation process of a bipartite state between Alice and Bob is considered. Suppose that there exist states $\rho_A \in \mathcal{H}_A$ for Alice and $\rho_B \in \mathcal{H}_B$ for Bob. Then, the combined state is a probabilistic mixture of product states ρ_A and ρ_B and is given by

$$\rho = \rho_A \otimes \rho_B. \tag{2.45}$$

The next step focuses on the communication between Alice and Bob over a classical channel (a telephone line for instance). Subsequently, Alice prepares the state $\rho_A^{(i)}(i = 1, 2, .., n)$ with probability p_i, she transfers that to Bob, and equivalently Bob prepares his system in the state $\rho_B^{(i)}(i = 1, 2, .., n)$ with $\sum_{i=1}^{n} p_i = 1$. The state prepared then is

$$\rho_{AB} = \sum_{i=1}^{n} p_i \rho_A^{(i)} \otimes \rho_B^{(i)}. \tag{2.46}$$

The substantial point to note here is that a state of the form 2.46 is the most general state prepared by Alice and Bob using local operations and classical communication [31, 32].

Definition: In technical terms, a state ρ_{AB} is said to be separable or classically correlated if it can be produced locally in separable labs and which can be expressed as a convex combination of tensor product of states as stated in 2.46. However, if there are no local states $\rho_A^{(i)}$, $\rho_B^{(i)}$ and non-negative probability p_i, such that ρ_{AB} can be cast into the form

$$\nexists \rho_A^{(i)}, \rho_B^{(i)}; p_i \geq 0 \qquad : \qquad \rho_{AB} = \sum_{i=1}^{n} p_i \rho_A^{(i)} \otimes \rho_B^{(i)}. \tag{2.47}$$

Then the mixed state ρ_{AB} is entangled. Therefore, entangled states imply that it is not possible to prepare them locally by two systems even after communicating over a classical channel.

Quantifying Entanglement

After being able to identify entangled states, it is a natural task to quantify the contained amount of entanglement. An entanglement measure is a mathematical function that captures the crucial features associated with entanglement, it is conventionally denoted by $E(\rho)$, where ρ is the density opertor of the system on which we perform measurements.

A good and a useful entanglement measure is expected to fulfill at least the first two following conditions:

1. A bipartite entanglement measure should vanish when ρ is separable: $E(\rho) = 0$.

2. Since entanglement cannot be created under LOCC (*local operations and classical communication*) [31], the $E(\rho)$ does not increase under LOCC operations. Therefore, for any LOCC operation Λ_{LOCC} we have

$$E(\Lambda(\rho)) \leq E(\rho). \tag{2.48}$$

   In other words, if the quantum state ρ can be transformed into another state $\Lambda(\rho)$ via LOCC, then ρ is at least as entangled as $\Lambda(\rho)$.

3. For any entanglement measure $E(\rho)$, it is required that $0 \leq E(\rho) \leq 1$ with $E(\rho) = 0$ if and only if the state ρ is disentangled (separable), and $E(\rho) = 1$ if at least ρ is the density operator of a maximally entangled state.

4. *Convexity*: $E(\rho)$ cannot increase under mixing of two or more states

$$E(\sum_i p_i \rho_i) \leq \sum_i p_i E(\rho_i). \tag{2.49}$$

5. $E(\rho)$ is invariant under local unitary transformations. Any change of basis caused by local unitary operations doesn't affect the quantum correlations between two subsystems [33]

$$E(\rho) = E((U_A \otimes U_B)\rho(U_A^\dagger \otimes U_B^\dagger)). \tag{2.50}$$

6. *Additivity*: The entanglement of divers copies of a state aggregates to n times the entanglement of a single copy

$$E(\rho^{\otimes n}) = nE(\rho). \tag{2.51}$$

7. *Subadditivity*: The sum of the entanglement of individual states is larger than the entanglement of both states

$$E(\rho_1) + E(\rho_2) \geq E(\rho_1 \otimes \rho_2). \tag{2.52}$$

After defining the conditions for measuring entanglement, we will discuss some of the most important entanglement quantifiers.

Entropy of Entanglement: As we have seen previously, the Schmidt decomposition helps distinguishing entanglement in pure bipartite states, but it can also yield to a perfect measure for evaluating pure entangled states, called *entropy of entanglement*. According to this measure, for a bipartite pure state $|\psi_{AB}\rangle$, tracing out one of the subsystems A guides to the same value of entanglement as tracing out the other subsystem B:

$$E(\rho^{AB}) = E(|\psi_{AB}\rangle\langle\psi_{AB}|) \qquad \text{where } \rho^A = \mathrm{tr}_B(\rho^{AB}) \tag{2.53}$$

$$= S(\rho^A) = S(\rho^B) \geqslant 0. \tag{2.54}$$

The relative entropy of entanglement: The relative entropy of entanglement is seen as a useful distance measure generated by the quantum relative entropy. To understand the motive for its definition is by taking into account the total correlations which are measured by the quantum mutual information

$$I(\rho^{AB}) = S(\rho^A) + S(\rho^B) - S(\rho^{AB}). \tag{2.55}$$

Since the mutual information is defined also as the relative entropy between ρ^{AB} and a completely uncorrelated (i.e disentangled) state $\rho^A \otimes \rho^B$, we may rewrite the quantum mutual information as

$$I(\rho^{AB}) = S(\rho^{AB}||\rho^A \otimes \rho^B). \tag{2.56}$$

This approach leads to the rise of the general definition of the relative entropy of entanglement with respect to the set of all disentangled states D [34]

$$E_{RE}^D(\rho) = \min_{\sigma \in D} S(\rho||\sigma), \tag{2.57}$$

where $S(\rho||\sigma) := \mathrm{tr}\{\rho \log \rho - \rho \log \sigma\}$

Entanglement of formation: One possibility to characterize the entanglement of statistical mixture is to define the *entanglement of formation* (EOF) [31]. It has been shown that EOF is a mathematically chiseled measure that corresponds to the necessary minimal quantity of entanglement for Alice and Bob in order to create a single copy of the quantum state ρ. Thus, it is defined as the minimum value of convex sum of pure states entanglement (the von Neumann entropy) over all decompositions $\{p_k, |\psi_k\rangle\}$ for the quantum state ρ of the form: $\rho = \sum_k p_k |\psi_k\rangle\langle\psi_k|$ with $p_k \geq 0$ and $\sum_k p_k = 1$, it is expressed as

$$E_f(\rho) = \min_{p_k, |\psi_k\rangle} \sum_k p_k E(|\psi_k\rangle). \tag{2.58}$$

The EOF satisfies the convexity and the invariance under local unitary transformations conditions. Moreover, if ρ is a pure state i.e $\rho = |\psi\rangle\langle\psi|$ it is easy to see that the EOF is equal to the entropy of entanglement and it is equal to zero if and only if ρ is a separable state.

2.3 Quantum Coherence

One of, if not the most essential, features that mark the departure of quantum physics from the classical realm is *quantum coherence*. It arises from quantum superposition describing the capability of a quantum state to exhibit quantum interference phenomena. The coherence effect of a state is usually attributed to the non-diagonal elements of its density matrix with respect to a certain reference basis which is established according to the physical problem under consideration. Due to the fact that it plays a pivotal role in quantum mechanics, it became a physical resource and an essential ingredient in a wide variety of research fields such as quantum information processing [72], quantum optics [40–42], quantum metrology [43] and quantum thermodynamics [44, 45, 75, 76]. Research on the practical role of coherence in biological systems has also attracted a considerable amount of interest [47, 48, 86]. The development of quantum information over the last three decades has led to the revaluation of quantum phenomena as resources that may be used to accomplish tasks that are otherwise impossible within the classical physics realm. This resource-driven perspective has prompted the development of a quantitative theory that captures the resource aspect of coherence in a mathematically rigorous way. Thus, establishing a full fledged resource theory of coherence and putting forward different measures to quantify it. In this section, We will examine the coherence theoretic framework established in [60] and explore potential metrics of coherence, with an emphasis on the relative entropy of coherence.

2.3.1 Coherence as a Resource

Quantum resource theories (QRT) [49–51] provide a rigorous and general framework to study various and different quantum phenomena in Quantum Mechanics. From Quantum information to thermodynamics, resource theories are used for the identification, characterization and the interpretation of different quantum effects including entanglement [33, 52, 53, 228], discord [38, 83, 84], magic in stabilizer computation [54, 55], quantum coherence and superposition [56–60]. They are usually generated from constraints which might arise from either conservation rules or practical limitations coming from the difficulty of performing quantum operations. For example, in a situation where a quantum state cannot be sent by Alice to Bob, quantum entanglement can be employed as a resource to overcome this restriction by sharing it between both parties together with classical communication, thus Alice is able to achieve her purpose via teleportation [21]. Generally speaking, a generic quantum resource theory is determined by two key components (some examples are illustrated in figure 2.2:

- A class of *free states*: states that do not possess any resource, and which can be obtained by using allowed operations
- A class of *free operations*: Transformations that cannot produce resources from free states, they can be implemented at zero cost.

As a matter of fact, in the resource theory of entanglement, local operations and classical communication (LOCC) [31] are associated with the free operations that generate for free a set of separable states 2.46. Moreover, in thermodynamics [61–65], a resource theory approach was adopted to model a quantum system in a thermal contact with a reservoir characterized by an arbitrary Hamiltonian H_R through thermal operations (TO) which are described by partial traces and energy-preserving unitaries. In this case, the resulting free states are thermal states or Gibbs states

$$\tau_R = e^{-\beta H_R}/Z_R, \tag{2.59}$$

where $Z_R = \mathrm{tr}(e^{-\beta H_R})$ is the partition function and $\beta = (T_R)^{-1}$. Given an arbitrary state ρ of the system, the previous transformation can be combined (system+reservoir) to get the following set of non-equilibrium states with TO described by the completely-positive trace-preserving (CPTP) map (see chapter 2 for more details),

$$\mathcal{T} : \rho \to \mathrm{tr}_R[U(\rho \otimes \tau_R)U^\dagger] \qquad , \qquad [U, H_S + H_R] = 0. \tag{2.60}$$

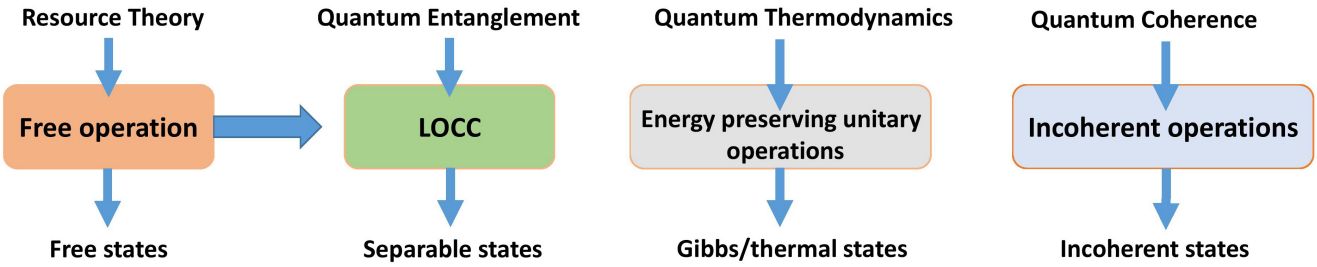

Figure 2.2: Main examples of quantum resource theory

By using the energy conservation of U, one can prove that TO preserve the Gibbs state

$$\begin{aligned} \mathcal{T}(\tau_S) &= \mathrm{tr}_R[U(\tau_R \otimes \tau_R)U^\dagger] = \mathrm{tr}_R[\frac{Ue^{-\beta(H_S+H_R)}U^\dagger}{Z_S Z_R}] \\ &= \frac{e^{-\beta H_S}}{Z_S} = \tau_S. \end{aligned} \tag{2.61}$$

It means that τ_S is a fixed point of every thermal operation $\mathcal{T}$.

Just like entanglement and thermodynamics, a resource theoretic outlook was applied to analyze the operational applicability of the superposition and the off diagonal elements of the density matrix, namely the QRT of coherence. In the following we briefly review the resource theory of coherence introduced in [56, 58, 60]. For the QRT of coherence, the key elements are the *incoherent states* as the free states and the *incoherent operations* as the allowed (free) operations. In this approach, quantum states with non-zero coherence can be regarded as useful resources. Therefore, every state with a finite amount of coherence is referred to as a *coherent state*.

Incoherent states

Quantum coherence is intrinsically basis dependant. The physical problem under consideration determines the reference basis on which coherence is identified and measured. For instance, the energy eigenbasis would be a genuine choice of basis in transport phenomena or in quantum metrology [66] as the generator's eigenbasis of an unknown phase shift. Given a finite n-dimensional Hilbert space H, an arbitrary reference basis $\{|i\rangle\}_{i=1}^{n-1}$ to be called the incoherent basis is fixed. The set of incoherent states denoted as $\mathcal{I}_n \subset S(\mathcal{H})$ can be expressed as

$$\mathcal{I}_n := \{\rho \in S(\mathcal{H}) : \sigma = \sum_{i=1}^{n-1} p_i |i\rangle\langle i|\}, \tag{2.62}$$

with probability p_i. Hence, $\mathcal{I}_n$ represents all the density matrices which are diagonal and have zero coherence in the incoherent basis. When there are more systems involved, the ideal basis for studying coherence will be generated as the tensor product of each subsystem's corresponding local reference basis states. General multipartite incoherent states [57, 67, 68] stem from convex combinations of incoherent pure product states.

Incoherent operations

Incoherent operations are operations that do not create coherence. In contrast to the QRT of thermodynamics, entanglement and asymmetry [69, 70], where free operations are only determined on operational grounds, the QRT of coherence lacks such consensus. It means that there is a variety of choices of free operations that have been brought forward in the literature. Each one of them describes a different resource theory of coherence. Some of the most notable incoherent operations are identified as:

- **Maximally incoherent operations (MIO)** which is the most extensive class of incoherent operations [58] that comprises any CPTP and non-selective map ξ such that:

$$\xi(\mathcal{I}_n) \subseteq \mathcal{I}_n. \tag{2.63}$$

  By providing an ancillary environment in a state σ_R and a global unitary operation U between the ancilla and the system of interest and tracing out the environmental degrees of freedom, any quantum operation can be created by the Stinespring dilation

$$\xi(\rho) = \mathrm{tr}_R[U(\rho \otimes \sigma_R)U^\dagger]. \tag{2.64}$$

  If the set of free states is described by an incoherent state σ_R in 2.64, then the operation involved has a free dilation. Despite the fact that MIO can't produce coherence, it has been demonstrated that such operations do not have in general free dilation [59, 71].

- **Incoherent operations (IO)** [60] are the subset of MIOs which are represented by the *Kraus decomposition* [72] with operators K_m satisfying $\xi(\rho) = \sum_m K_m \rho K_m^\dagger$ and $\sum_m K_m^\dagger K_m = \infty$, and for all n and $\rho \in \mathcal{I}_n$:

$$\frac{K_m \rho K_m^\dagger}{\mathrm{tr}[K_m \rho K_m^\dagger]} \in \mathcal{I}_n. \tag{2.65}$$

  IOs guarantee that no coherence can be created from an incoherent input state.

- as we have seen previously, coherence cannot emerge from MIO and IO. **Strictly incoherent operations(SIO)** are slightly different as they rely on the condition that the allowed operations are not able to use the coherence existing in the quantum system. SIO [57] are expressed by the dephasing operation δ:

$$\delta(\rho) = \tilde{\rho} = \sum_i |i\rangle\langle i|\rho|i\rangle\langle i|, \tag{2.66}$$

where $\tilde{\rho}$ is the dephased state with the same diagonal elements as ρ and zero non-diagonal ones on the *n*-dimensional reference basis of the Hilbert space. Moreover, SIO can be also decomposed in terms of Kraus operators $\{K_m\}$ such that the results of a measurement in the reference basis do not depend on the input coherence in the quantum state which cannot either be created or detected by these operations

$$\langle i|K_m \rho K_m^\dagger|i\rangle = \langle i|K_m \delta(\rho) K_m^\dagger|i\rangle. \tag{2.67}$$

In general, SIOs do not have free dilation either.

It is worth mentioning that under this context of incoherent states and operations, the *n*-dimensional states that contain a maximum amount of coherence are characterized as useful resources. The canonical illustration of a maximally coherent state is given by [60]

$$|\varphi_n\rangle = \frac{1}{\sqrt{n}} \sum_{i=0}^{n-1} |i\rangle \tag{2.68}$$

These states play a role similar to that of Bell states 2.44 in entanglement theory. Besides the fact that coherent states are resourceful, it is necessary to quantify their coherence. In the next section, we discuss the proposed measures of coherence.

2.3.2 Coherence Measures

Building upon the works of Baumgratz *et al.* [60] and following the axiomatic quantification of entanglement 2.2.3, a parallel framework has been developed to quantify coherence. A measure of coherence $\mathcal{C}(\rho)$ for a density operator ρ must fulfill the following postulates:

1. *Non-Negativity*: $\mathcal{C}(\rho) \geq 0$. When the equality holds , it means that coherence must vanish if ρ is an incoherent state.

2. *Monotonicity*: Due to the fact that coherence cannot be formed through incoherent operations, it cannot be increased either:

$$\mathcal{C}(\rho) \geq \mathcal{C}(\xi(\rho)). \tag{2.69}$$

In fact, to speak of a coherence measure, the first two requirements must be met. It is good to satisfy the following ones, which are axiomatically requested, but they are not thoroughly required.

3. *Strong monotonicity*: Before any measurement, $\mathcal{C}$ should be greater than the average coherence of possible outcomes:

$$\mathcal{C}(\rho) \geq \sum_i p_i \mathcal{C}(\sigma_i), \tag{2.70}$$

where $p_i = \mathrm{tr}(K_i \rho K_i^\dagger) \geq 0$ are the probabilities with $\sum_i p_i = 1$, $\sigma_i = \frac{K_i \rho K_i^\dagger}{p_i}$ are the possible results of the measurement. This property shows that coherence is not increasing under incoherent measurements.

4. *Convexity*: $\mathcal{C}$ decreases under mixing, for $\rho = \sum_i q_i \rho_i$ such that $\{q_i\}$ is a probability distribution, we have

$$\sum_i q_i \mathcal{C}(\rho_i) \geq \mathcal{C}(\sum_i q_i \rho_i). \tag{2.71}$$

It's worth noting at this point that combining properties 3 and 4 ensures monotonicity. Any quantity $\mathcal{C}$ that fulfills property 1 and one of properties 2 or 3 is called a coherence monotone. To build a Bona fide coherence quantifier, one needs to add more conditions along with condition 1-4 [56]:

5. *Uniqueness* for pure states: $\mathcal{C}$ should fulfill for any pure state $|\varphi\rangle$

$$\mathcal{C}(|\varphi\rangle) = S(\delta(|\varphi\rangle\langle\varphi|)), \tag{2.72}$$

with $S(\rho) = -\mathrm{tr}(\rho \log \rho)$ is the Von Neumann entropy.

6. *Additivity*: $\mathcal{C}$ is additive under the tensor product of quantum states

$$\mathcal{C}(\rho \otimes \sigma) = \mathcal{C}(\rho) + \mathcal{C}(\sigma). \tag{2.73}$$

Following the standard notions of entanglement, two important coherence quantifiers that satisfy the property 1-6 can be distinguished: distillable coherence which has been proven to be quantified by the relative entropy of

coherence in the asymptotic limit [57] and coherence cost which happens to be equal to the coherence of formation.

Relative entropy of coherence

Although there exist several ways to quantify coherence, *relative entropy of coherence* (REC) is the one that most closely associated with the thermodynamic formalism. REC is distance based and which measures the minimum distance between the state of interest and the set of incoherent states. Thus REC of a state ρ with respect to a Hilbert space basis $\mathcal{P}$, conventionally one of the eigenbases of the Hamiltonian H, is defined as follows

$$\begin{aligned} \mathcal{C}(\rho) &= \min_{\sigma \in \mathcal{I}_n} S(\rho||\sigma) \\ &= S(\rho||\tilde{\rho}) = S(\tilde{\rho}) - S(\rho), \end{aligned} \tag{2.74}$$

where $\tilde{\rho}$ is the dephased state Eq.2.66 and $S(\rho||\sigma)$ is the quantum relative entropy Eq.2.32. The definition above Eq.2.75 is monotonic under incoherent operations, and can be viewed as the distillable coherence in the state ρ. Aditionally, it is worthwile mentioning that there are other slightly different approaches which are proposed to study coherence in the context of reference frames [73]. These approaches describe coherence as asymmetry relative to time translation or to phase shifts [69, 71, 74, 75]. They were investigated in the context of quantum thermodynamics [76] where only energy preserving unitaries are free. Asymmetry can be viewed as coherence relative to the eigenbasis of a given observable when the symmetry group is the set of translations induced by this observable. In this case, asymmetry is characterized by a measure based on relative entropy called, *relative entropy of asymmetry* (REA) which is obtained with respect to the Hamiltonian H and not the basis [70, 71, 178]

$$\mathcal{A}(\rho) \equiv S(\rho||\overline{\rho}) = S(\overline{\rho}) - S(\rho), \tag{2.75}$$

such that $\overline{\rho}$ is the partially dephased state which depends on the projectors $\mathcal{M}_i$ of the spectral decomposition of H

$$\overline{\rho} = \sum_i \mathcal{M}_i \rho \mathcal{M}_i. \tag{2.76}$$

We can clearly compare the two expressions of the dephased state in the case of REC Eq.2.75 and Eq.2.76. REC and REA coincide $\tilde{\rho} = \overline{\rho}$ when the Hamiltonian is non-degenerate. On the contrary, when H is degenerate the partially dephased state maintains the off-diagonal components in the degenerate eigenspaces. This is because, unlike REC, which quantifies the overall amount of coherence, REA is only sensitive to coherence between non-

degenerate energy levels. As a consequence, REC is always larger than REA:

$$\mathcal{C}(\rho) - \mathcal{A}(\rho) \equiv \mathcal{C}(\tilde{\rho}) \geq 0. \tag{2.77}$$

Another important property of REA is that it doesn't increase under translationally invariant operations ε [69,70,77] defined by H such that

$$\mathrm{e}^{-iHt}\,\varepsilon(\rho)\,\mathrm{e}^{iHt} = \varepsilon(\mathrm{e}^{-iHt}\,\rho\,\mathrm{e}^{iHt}). \tag{2.78}$$

These operations play a crucial role in the resource theory of asymmetry and quantum thermodynamics, they have a free dilation [71] if a postselection is permitted with an incoherent measurement on the environmental ancillas.

Besides the relative entropy of coherence, there exists a plethora of proper measures of coherence such as l_1-norm of coherence which is also a measure based distance that quantifies coherence by the absolute value of the non-diagonal elements of the quantum state [60, 78–80]. For instance, It was shown in the context of frozen coherence (i.e coherence which is unaffected by quantum noise) [68] that for a one qubit system there is no nontrivial condition under which the relative entropy coherence and the l_1-norm can be frozen simultaneously in any quantum channel , and that all coherence measures in a strictly incoherent channel can be frozen in an initial state if and only if the REC is frozen for a high dimensional quantum system. Robustness of coherence is another tool to characterize coherence as the minimum amount of noise needed to add it to a state to turn it into an incoherent state [81]. Other proposals include also geometric [82] and trace distance measures of coherence [83,84] and its quantification with concurrence [85].

Chapter 3

Open Quantum System Dynamics and Thermodynamics

"Yesterday is history. Tomorrow is a mystery. Today is a gift. That's why it is called the present."

Alice Morse Earle, 1851-1911.

The time evolution of a system is depicted, in quantum theory, by the deterministic and linear Schrödinger equation. Contrariwise, when the system interacts with the external environment, the quantum system displays irreversible demeanor not predicted by the standard theory. This irreversibility emanates when considering another formalism different than the Schrödinger equation based closed systems which is offered and described by the *theory of open quantum systems* [97]. The latter has piqued the curiosity of plethora of researchers and physicists over the years. It can be of great use in many applications of quantum physics: For instance, in quantum optics [96], it is encountered as well in quantum chemistry and biology [86] and in condensed matter physics [87] to name a few. The primary interest of the study of open quantum systems is to investigate the dynamical behavior of quantum mechanical systems interacting with their surroundings. The influence of the environment on the system's dynamics threatens the quantumness of its state. This can result in dissipation [88] and decoherence, which is expressed by the damping and decay of the off-diagonal elements of the density matrix (coherences). This emergence of classicality from quantum theory was initially discussed in the works of Zeh [89] and Zurek [90] [91]. Due to the fact that open quantum systems are generally arduous to tackle, a series of approximations should be performed so that the equations of motion for the state of the system can be derived and solved, and therefore apprehend the dynamics of the studied system. The first description of open quantum systems amounts to assuming the weak system-environment

coupling and involves the theory of dynamical semigroups which is represented by the **Markovian** memoryless dynamics. The second one concerns the presence of systems strongly interacting with their reservoirs and creating massive correlations with them and which is identified as the **Non-Markovian** dynamics.

Since the field of open quantum systems is undergoing a fast phase of development due to the appearance of new devices based on quantum features such as coherence and entanglement, it is necessary to understand the thermodynamic behavior of small quantum systems. The emerging framework of quantum thermodynamics [117] seeks to comprehend the operation of classical thermodynamics concepts at the quantum level and its impact on other areas like quantum information [62] as well as the related fluctuations that link the thermodynamic quantities such as free energy and work of the quantum system.

The purpose of this chapter is to go through fundamental properties of open quantum system theory, with a focus on the derivation of the Lindblad master equation, which is required to describe the dynamics of quantum thermal machines. The second half of the chapter covers an overview of the thermodynamic principles, as well as establishing the concepts of work extraction and thermal fluctuations, which govern the dynamics of small systems.

3.1 Introduction To Open Quantum Systems

3.1.1 Closed Systems

As we have already seen in chapter 2 and more precisely in subsection 2.1.2, closed systems display a unitary evolution, they do not interchange any information with their surrounding environment. According to [92], the time evolution of a closed system in a pure state $|\psi(t)\rangle$ with a Hamiltonian H is described by the *Schrödinger* equation

$$i\hbar\frac{d}{dt}|\psi(t)\rangle = H|\psi(t)\rangle, \tag{3.1}$$

its formal solution is determined by:

$$|\psi(t)\rangle = \mathcal{U}(t,t_0)|\psi(t_0)\rangle, \tag{3.2}$$

where $\mathcal{U}(t,t_0)$ is known as the unitary time-evolution operator satisfying the condition

$$\mathcal{U}^\dagger(t,t_0)\mathcal{U}(t,t_0) = \mathcal{U}(t,t_0)\mathcal{U}^\dagger(t,t_0). \tag{3.3}$$

Substituting 3.2 into 3.1, the propagator or the unitary time-evolution operator $\mathcal{U}(t,t_0)$ takes the following form

$$i\frac{\partial}{\partial t}\mathcal{U}(t,t_0) = H\mathcal{U}(t,t_0). \tag{3.4}$$

In this thesis, we will set $\hbar = 1$, and we have the initial condition given by

$$\mathcal{U}(t,t_0) = \mathbb{1}. \tag{3.5}$$

For a time independent Hamiltonian, the time evolution operator reads as

$$\mathcal{U}(t,t_0) = e^{-iH(t-t_0)}. \tag{3.6}$$

Changing H in time, however, the time evolution operator is defined by the time-ordered exponential

$$\mathcal{U}(t,t_0) = \mathcal{T}exp[-i\int_{t_0}^{t} dt' H(t')], \tag{3.7}$$

$\mathcal{T}$ is the chronological time-ordering operator which guarantees that all the operators in the sum are ordered by increasing time values.

In the case of a mixed state ρ, the time evolution of a closed system with a time independent Hamiltonian is governed by the *Liouville-Von Neumann* equation

$$\frac{d}{dt}\rho(t) = -i[H,\rho(t)], \tag{3.8}$$

where $[A,B] = AB - BA$ is the canonical commutation relation. The solution can be also expressed in terms of the time evolution operator

$$\rho(t) = \mathcal{U}(t,t_0)\rho(t_0)\mathcal{U}^\dagger(t,t_0). \tag{3.9}$$

The equation 3.8 represents the quantum analogue of the classical Liouville equation which is given by

$$\frac{d}{dt}\rho(t) = \mathcal{L}\rho(t), \tag{3.10}$$

where $\mathcal{L}$ is the Liouville superoperator. The corresponding solution of this equation reads as

$$\rho(t) = \mathcal{T}exp[\int_{t_0}^{t} dt' \mathcal{L}(t')]\rho(t_0). \tag{3.11}$$

For a time independent Hamiltonian, 3.11 takes the form

$$\rho(t) = e^{[\mathcal{L}(t-t_0)]}\rho(t_0). \tag{3.12}$$

Although closed systems dynamics can be of great importance, they limit the thermodynamical possibilities because there is no interaction with the surrounding environment, thus there will be no heat flows or energy exchange in and out of the system. We look at open quantum systems to broaden our perspectives.

3.1.2 Open Quantum Systems and Dynamical Maps

Since realistic quantum systems cannot be totally isolated in nature, they are usually regarded as components of a bigger system in which they are coupled to a larger environment despite how weak or strong is the interaction between them. Thus, the situation drastically changes and the dynamics get more convoluted.

In fact, as shown in figure 3.1, an open system is defined by a quantum system S which is coupled to an environment E which is commonly but not exclusively seen as a thermal bath or reservoir, and has a notable impact on the quantum system which must be considered when identifying its dynamical evolution and features. Even though, we assume that the combined system is closed and so follows the unitary Hamiltonian dynamics, the time evolution of the open system S is not generally unitary. Due to the interaction between S and E, certain correlations are formed between them, so that the dynamics of S can no longer be modeled by a unitary evolution operator acting on S alone. We refer to the dynamics S as the reduced system dynamics which are described by a quantum master equation that will be derived in the next subsections.

The Hilbert space of the combined total system $S + E$ is given by a tensor product $\mathcal{H} = \mathcal{H}_{SE} = \mathcal{H}_S \otimes \mathcal{H}_E$, where $\mathcal{H}_S$ and $\mathcal{H}_E$ denote the Hilbert spaces of the system S and the environment E respectively. The total system is

governed by the total Hamiltonian that can be taken of the form

$$H = H_S \otimes \mathbb{1}_E + \mathbb{1}_S \otimes H_E + H_I, \tag{3.13}$$

H_S and H_E represent the time-independent Hamiltonians of the system and its environment, respectively. Explicitly, we take $H_0 = H_S + H_E$ and the interaction Hamiltonian H_I is assumed to be the only part involving both the system and the environment degrees of freedom. The environment can be characterized by a heath bath or a reservoir that has many degrees of freedom which causes the irreversibility of the behavior of the open quantum system. In this case, it is more convenient to stay in the reduced system space to avoid the problem of having to solve an infinite number of equations of motion.
We put our interest in observables which are associated with the system S that take the form $A \otimes \mathbb{1}_E$, such that A is the operator acting on the Hilbert space $\mathcal{H}_S$ and $\mathbb{1}_E$ is the identity matrix of $\mathcal{H}_E$. The reduced dynamics of the system S is then given by taking a partial trace over the environment degrees of freedom on the total system

$$\rho_S(t) = \mathrm{tr}_E\, \rho(t), \tag{3.14}$$

$\rho(t) = U(t, t_0)\rho(t_0)U^\dagger(t, t_0)$ stands for the state of the combined system which is governed by the time-evolution operator $U(t, t_0)$.

The dynamics of the reduced density matrix are obtained from the Liouville-Von Neumann equation Eq.3.8 and by using the partial trace in Eq.3.14

$$\frac{d}{dt}\rho_S(t) = \frac{d}{dt}\,\mathrm{tr}_E\, \rho(t) = -i\,\mathrm{tr}_E[H(t), \rho(t)]. \tag{3.15}$$

In the following subsections, we will present instruments and approaches to describe the dynamical evolution of open quantum systems, mainly *quantum dynamical maps* and some important approximations that will lead us to the equations of motion often called *master equations* which comprise only the object of our primary interest that is the reduced density state ρ_S.

Quantum dynamical maps and semigroups

The dynamics of a finite closed system is represented conventionally by unitary transformations in the Hilbert space. This formalism does not stand when one deals with irreversible processes involving the influence of external environments on the evolution of the open quantum system. In this situation, we rely on quantum dynamical

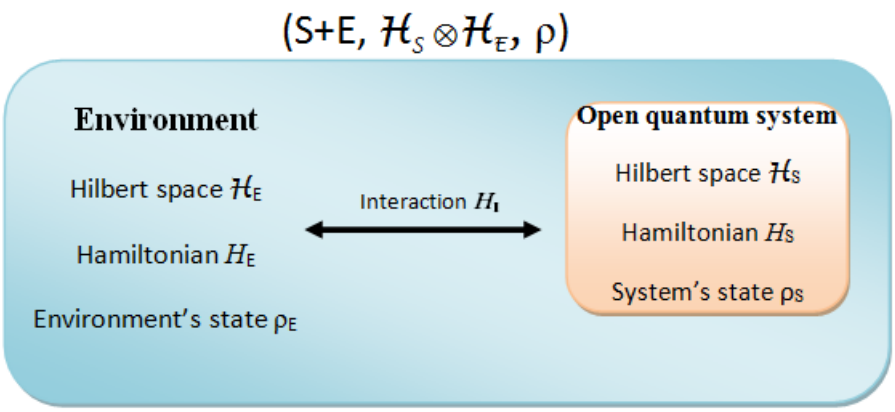

Figure 3.1: Sketch of an open quantum system S coupled to an environment E

semigroups which are central in the description of open quantum systems under the conditions of weak system-reservoir coupling, short environmental correlation times and the neglect of memory effects.

To explain the concept of quantum dynamical semigroups, we first have to prepare the state of the total system $S + E$ at the initial time $t = 0$, and we assume that it is an uncorrelated product state

$$\rho(0) = \rho_S(0) \otimes \rho_E(0), \tag{3.16}$$

which means that the initial state of the system is prepared independently of the environment, and where the reference state ρ_E is fixed. Now the state transformation from a reduced system at time $t = 0$ to a reduced system at time $t > 0$ can be written in the form

$$\Lambda(t): \qquad \mathcal{M}(\mathcal{H}_S) \to \mathcal{M}(\mathcal{H}_S) \tag{3.17}$$

$$\rho_S(0) \to \rho_S(t) = \Lambda(t)\rho_S(0) = \mathrm{tr}_E\{U(t,0)\rho_S(0) \otimes \rho_E(0)U^\dagger(t,0)\}, \tag{3.18}$$

$\mathcal{M}(\mathcal{H}_S)$ denotes the open system's state space. In Eq. 3.18 the initial state is connected with the final state. For a fixed time t, the map Λ is referred to as a *quantum dynamical map* [93] or a quantum operation. It should satisfy the following conditions:

1 The quantum map must be **trace preserving** such that $\mathrm{tr}(\Lambda(t)(\rho)) = \mathrm{tr}(\rho) = 1$.

2 It is required to be **convex-linear** on the set of density matrices, that is for probabilities $\{p_i\}$

$$\Lambda(t)(\sum_i p_i\rho_i) = \sum_i p_i\Lambda(t)\rho_i. \tag{3.19}$$

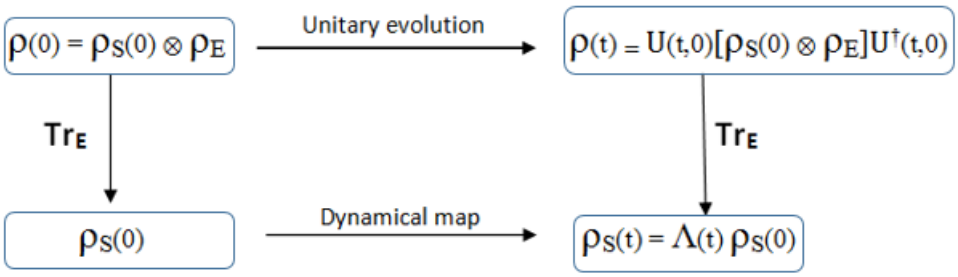

Figure 3.2: Commutative diagram displaying the action of the dynamical map $\Lambda(t)$.

3 $\Lambda(t)$ must be **completely-positive** implies in particular that $\Lambda(t)$ maps positive operators onto positive operators.

Thus, we conclude that a dynamical map $\Lambda(t)$ represents a convex-linear, completely positive and trace-preserving (CPTP) quantum operation, also called *quantum channel* that belongs to a *quantum dynamical semigroup*.

Definition Quantum dynamical semigroups are irreversible continuous *one-parameter* family of dynamical maps $\Lambda_t : \mathcal{M} \to \mathcal{M}$ on a finite Banach space [1] satisfying the following properties:

- Λ_t is a positive linear map for every $t \in \mathbb{R}^+$.
- $\Lambda_{t=0} = \mathbb{1}$.
- $\Lambda_s \Lambda_t = \Lambda_{s+t}$ for $s, t \in \mathbb{R}^+$.

The action of the dynamical map $\Lambda = \Lambda_t$ is illustrated in figure 3.2. As a matter of fact, the trace preservation condition assures the normalization of the state and the convex linearity is given by

$$\Lambda_t(\lambda\rho + (1-\lambda)\rho') \leq \lambda\Lambda_t(\rho) + (1-\lambda)\Lambda_t(\rho') \quad \text{for} \quad 0 \leq \lambda \leq 1. \tag{3.20}$$

Both criterias guarantee that density operators are mapped to density operators. The last requirement of complete positivity is stronger than mere positivity which maps positive into positive. It also signifies that all tensor product extensions of Λ_t to spaces of higher dimension, characterized by the identity map $\mathbb{1}_{ext}$, are positive such that

$$\Lambda_t \otimes \mathbb{1}_{ext} > 0. \tag{3.21}$$

[1] Banach space: Let $\mathbb{K}$ be one of the fields $\mathbb{R}$ or $\mathbb{C}$. A Banach space over $\mathbb{K}$ is a normed $\mathbb{K}$- vector $(\mathcal{X}, ||.||)$, which is complete with respect to the metric: $d(x,y) = ||x-y||$, $x, y \in \mathcal{X}$

In this way, the image under this extended map must be a positive density operator.

After we have presented the quantum dynamical semigroups, their maps and their corresponding properties, we show how to construct such maps using an explicit standard form of quantum operations, that is the *Kraus representation*.

3.1.3 Kraus Representation

Any dynamical map can be constructed with the help of operators on the underlying Hilbert space $\mathcal{H}_S$ of the open system which are the **Kraus operators**. To obtain them, we use firstly the spectral decomposition of the environment density matrix

$$\rho_E = \rho_E(0) = \sum_\alpha \lambda_\alpha |\nu_\alpha\rangle\langle\nu_\alpha|. \tag{3.22}$$

Here, $\{|\nu_\alpha\rangle\}$ form an orthonormal basis in $\mathcal{H}_E$ and λ_α are positive real coefficients satisfying $\sum_\alpha \lambda_\alpha = 1$. By using 3.22, 3.16 and **??**, 3.18 may be rewritten as

$$\rho_S(t) = \Lambda(t)\rho_S(0) = \sum_{\alpha,\beta} \lambda_\alpha \langle\nu_\beta|U\rho_S(0)|\nu_\alpha\rangle\langle\nu_\alpha|U^\dagger|\nu_\beta\rangle \tag{3.23}$$

$$= \sum_{\alpha,\beta} \lambda_\alpha \langle\nu_\beta|U|\nu_\alpha\rangle\rho_S(0)\langle\nu_\alpha|U^\dagger|\nu_\beta\rangle \tag{3.24}$$

$$= \sum_{\alpha,\beta} E_{\alpha,\beta}(t)\rho_S(0)E^\dagger_{\alpha,\beta}(t), \tag{3.25}$$

which is known as *operator-sum representation* or *Kraus representation* [94] [72]. The Kraus operators are $E_{\alpha,\beta}(t) = \sqrt{\lambda_\alpha}\langle\nu_\beta|U|\nu_\alpha\rangle$. Since the quantum map Λ is trace preserving, the Kraus operators must satisfy the completeness relation

$$\sum_{\alpha,\beta} E^\dagger_{\alpha,\beta}(t)E_{\alpha,\beta}(t) = \mathbb{1}. \tag{3.26}$$

3.1.4 Markovian Dynamics of Open Quantum Systems

The other approach that allows to look at the open quantum system dynamics is the derivation of an equation of motion of the reduced state dynamics, known as the *master equation* [95–98]. The simplest prototype to achieve that is provided by a Markovian process for which the dynamics is stationary in time and all memory effects are

disregarded, that means that the environment disremembers its interactions in the past with the system because of the correlations dispersion into the many environmental degrees of freedom. For the family of dynamical maps $\{\Lambda_t\}_{t\geq 0}$, this statement may be formulated using the semigroup property that represents the time-homogeneous Markovian case

$$\Lambda(t_1 + t_2) = \Lambda(t_1)\Lambda(t_2) \qquad \forall t_1, t_2 \geq 0. \tag{3.27}$$

Thanks to the dynamical semigroups approach and the two main ponderous approximations which are the **Markov** and the **Born** approximations, we now are going to derive the Lindblad master equation that provides a full depiction of the Markovian dynamics.

The Markovian Lindblad Master equation

The Lindblad theorem is a milestone theorem in the theory of open quantum systems [99, 100]. It gives a well defined mathematical structure to the master equation and is called the *Lindblad form*. For a given dynamical semigroup associated with the Lindblad form, there exists a generator, i.e, a superoperator $\mathcal{L}$ satisfying

$$\Lambda(t) = exp(\mathcal{L}t). \tag{3.28}$$

With the help of the linear map $\mathcal{L}$, a first order differential equation for the reduced density operator of the open system is yielded, known as the **Markovian quantum master equation**

$$\frac{d}{dt}\rho_S(t) = \mathcal{L}\rho_S(t). \tag{3.29}$$

Since our CPTP map can be expressed as in 3.28, the following step is to calculate the explicit and most general form of $\mathcal{L}$, given the above requirements. To this end, we choose an orthonormal basis of the bounded space of operators $\mathcal{B}(\mathcal{H}_S)$ that form a d^2-dimensional complex vector space represented by $\{C_i, 1 \leq i \leq d^2\}$ that satisfies

$$\langle\langle C_i, C_j\rangle\rangle \equiv \mathrm{tr}(C_i^\dagger C_j) = \delta_{ij}. \tag{3.30}$$

Conveniently, one of the basis operators is selected to be proportional to the identity operator

$$C_{d^2} = \frac{1}{\sqrt{d}}\mathbb{1}_S. \tag{3.31}$$

It is trivial to show that the norm of this element is 1. We can easily see from 3.31 that the other basis operators are traceless

$$\mathrm{tr}_S(C_i) = 0 \qquad \text{for} \qquad \forall i = 1, 2, ..., d^2 - 1. \tag{3.32}$$

Operators in this space can be expanded as

$$W_{\alpha,\beta}(t) = \sum_{i=1}^{d^2} \langle\langle C_i | W_{\alpha,\beta}(t)\rangle\rangle |C_i\rangle\rangle. \tag{3.33}$$

By using the Kraus representation 3.25 and 3.33, the action of the dynamical map Λ_t is provided as follows

$$\begin{aligned} \Lambda_t \rho_S &= \sum_{\alpha,\beta} [\sum_{i}^{d^2} \langle\langle C_i | W_{\alpha,\beta}(t)\rangle\rangle C_i \rho \sum_{j=1}^{d^2} C_j^\dagger \langle\langle W_{\alpha,\beta}(t) | C_j\rangle\rangle] \\ &= \sum_{i,j=1}^{d^2} k_{i,j}(t) C_i \rho C_j^\dagger, \end{aligned} \tag{3.34}$$

where $k_{i,j}$ is a time dependent, positive and hermitian coefficient matrix such that

$$k_{i,j} = \sum_{\alpha,\beta} \langle\langle C_i | W_{\alpha,\beta}(t)\rangle\rangle \langle\langle W_{\alpha,\beta}(t)) | C_j\rangle\rangle. \tag{3.35}$$

The semigroup generator can be formulated in terms of the differential quotient created by the map 3.34:

$$\begin{aligned} \mathcal{L}\rho_S &= \lim_{\mu\to 0} \frac{1}{\mu} \{\Lambda_\mu \rho_S - \rho_S\} \\ &= \underbrace{\frac{1}{d} \lim_{\mu\to 0} \frac{k_{d^2 d^2}(\mu) - d}{\mu}}_{k_0} \rho_S + \underbrace{\frac{1}{\sqrt{d}} \lim_{\mu\to 0} \sum_{i=1}^{d^2-1} \frac{k_{i d^2}(\mu) C_i}{\mu}}_{F} \rho_S \\ &+ \rho_S \underbrace{\lim_{\mu\to 0} \frac{k_{d^2 i}(\mu) C_i^\dagger}{\sqrt{d}\mu}}_{F^\dagger} + \sum_{i,j=1}^{d^2-1} \underbrace{\lim_{\mu\to 0} \frac{k_{ij}(\mu)}{\mu}}_{\nu_{ij}} C_i \rho_S C_j^\dagger \end{aligned} \tag{3.36}$$

$$= k_0 \rho_S + F \rho_S + \rho_S F^\dagger + \sum_{i,j=1}^{d^2-1} \nu_{ij} C_i \rho_S C_j^\dagger \tag{3.37}$$

$$\implies \mathcal{L}\rho_S = -i[H, \rho_S] + \{G, \rho_S\} + \sum_{i,j=1}^{d^2-1} \nu_{ij} C_i \rho_S C_j^\dagger. \tag{3.38}$$

We have introduced two new hermitian operators

$$H = \frac{1}{2i}(F - F^\dagger) \tag{3.39}$$

$$G = \frac{1}{2}(F + F^\dagger + k_0)\mathbb{1}. \tag{3.40}$$

Since that the preservation of the trace implies $\mathrm{tr}(\mathbb{L}\rho_S) = 0$, we can relate the operator G to the matrix $\mu = (\mu_{ij})$ such that

$$0 = \mathrm{tr}(\mathbb{L}\rho_S) = 0 + \mathrm{tr}[(2G + \sum_{i,j=1}^{d^2-1} \nu_{ij} C_j^\dagger C_i)\rho_S]. \tag{3.41}$$

Thus, we deduce the relation between the operator G and ν_{ij}:

$$G = -\frac{1}{2}\sum_{i,j=1}^{d^2-1} \nu_{ij} C_j^\dagger C_i. \tag{3.42}$$

Therefore, substituting Eq.3.42 into Eq.3.38 one the first standard form of the generator of a dynamical semigroup

$$\mathcal{L}\rho_S = -i[H_S, \rho_S] + \sum_{i,j=1}^{d^2-1} \nu_{ij}[C_i \rho_S C_j^\dagger - \frac{1}{2} C_j^\dagger C_i \rho_S - \frac{1}{2}\rho_S C_j^\dagger C_i]. \tag{3.43}$$

The complex coefficients ν_{ij} constitute a positive matrix called the *Kossakowski* matrix. To obtain the Lindblad form or the second standard form, the matrix ν should be diagonalized by using a unitary transformation u satisfying

$$u\nu u^\dagger = diag(\gamma_1, ..., \gamma_d^2 - 1), \tag{3.44}$$

where γ_i are non-negative eigenvalues. And this allows us to introduce a new set of operators A_k named the Lindblad operators [100]:

$$A_k = \sum_{i=1}^{d^2-1} C_i u_{ik}^\dagger \tag{3.45}$$

$$C_i = \sum_{k=1}^{d^2-1} u_{ki} A_k. \tag{3.46}$$

Therefore, according to the *Gorini-Kossakowski- Sudarshan- Lindblad* theorem [99, 100] we get the most general form for the generator $\mathcal{L}$ associated to a dynamical semigroup which represents the *Lindblad* or GKSL master

equation

$$\mathcal{L}\rho_S = -i[H_S, \rho_S] - \frac{1}{2}\sum_{k=1}^{d^2-1} \gamma_k (A_k^\dagger A_k \rho_S + \rho_S A_k^\dagger A_k - 2A_k \rho_S A_k^\dagger). \tag{3.47}$$

In the equation above, we see that the first term corresponds to the unitary part of the evolution generated by the Hamiltonian of the system H_S. The second term denotes the **dissipator** which depicts the influence of the environment on the system such that

$$\mathcal{D}(\rho_S) = \frac{1}{2}\sum_{k=1}^{d^2-1} \gamma_k (2A_k \rho_S A_k^\dagger - A_k^\dagger A_k \rho_S - \rho_S A_k^\dagger A_k), \tag{3.48}$$

where the operators appearing in the dissipator are called *jump operators* or *Lindblad operators*. We note that γ_k are constant, positive decay rates that have the dimension of the inverse of time, they play the role of relaxation rates for different channels of the open system. The summation is limited by the dimension $dim\{\mathcal{H}_S\} = d$ of the Hilbert space of the system.

Now we are able to write the master equation in its simplest form

$$\frac{d}{dt}\rho_S(t) = -i[H, \rho_S] + \mathcal{D}(\rho_S). \tag{3.49}$$

Properties of the GKSL master equation

At this point, it is worth mentioning some interesting properties of the Lindblad equation which are:

- The generator is invariant under the unitary transformations of the set of jump operators:

$$\sqrt{\gamma_i} A_i \to \sqrt{\gamma_i'} A_i' = \sum_j u_{i,j} \sqrt{\gamma_j} A_j, \tag{3.50}$$

  u_{ij} is a unitary matrix. It is invariant under Inhomogeneous transformations as well

$$\begin{aligned} A &\to A_i' = A_i + a_i \\ H &\to H' = H + \frac{1}{2i}\sum_j \gamma_j (a_j^* A_j - a_j A_j^\dagger) + b, \end{aligned} \tag{3.51}$$

  where the a_i are complex numbers and b is real. Because of these properties it is possible to choose traceless Lindblad operators without loss of generality.

- Under a Lindblad dynamics, the purity of a system fulfils $\frac{d}{dt}(\mathrm{tr}(\rho^2)) \leq 0$ when all the jump operators are Hermitian.

The microscopic derivation of the Markovian master equation in the weak coupling limit

In the following, we get to derive the Markovian master equation using possible approaches and approximation schemes. We have seen that Eq.3.13 describes the Hamiltonian of the total system, where we assume that the interaction Hamiltonian is the only part that involves both the system S and the environment E degrees of freedom, such that $\tilde{H}_I(t) = \mathrm{e}^{i(H_S+H_E)t}\, H_I\, \mathrm{e}^{-i(H_S+H_E)t}$ is acting in $\mathcal{H}_S \otimes \mathcal{H}_E$. It is more useful to work in the interaction picture for a better representation of the system's dynamics ([101] includes a more detailed explanation on the Schrödinger, Heisenberg, and interaction pictures). Therefore, our focus is directed towards the Von Neumann equation in the interaction picture where the density matrix evolves with time due to the interaction Hamiltonian, while the operators evolve with the system and environment Hamiltonian

$$\frac{d}{dt}\tilde{\rho}(t) = -i[\tilde{H}_I(t), \tilde{\rho}(t)]. \tag{3.52}$$

The associated formal integral solution is given by

$$\tilde{\rho}(t) = \rho(0) - i\int_0^t ds[\tilde{H}_I(s), \tilde{\rho}(s)]. \tag{3.53}$$

Taking the partial trace over the environment and inserting the integral form into Eq.3.52, we get

$$\frac{d}{dt}\tilde{\rho_S}(t) = -\int_0^t ds\, \mathrm{tr}_E[\tilde{H}_I(t), [\tilde{H}_I(s), \tilde{\rho}(s)]], \tag{3.54}$$

where $\mathrm{tr}_E[\tilde{H}_I(t), \rho(0)] = 0$, is disregarded.

So far, no approximations have been performed yet. The aim of the microscopic derivation is to determine the constraints and approximations that lead to the Markovian equation given in 3.47. The crucial approximations shall be summarized and further derivation details can be found in e.g. [97].

- The first approximation is the **Born approximation** which implies that the system-environment coupling is sufficiently weak that the impact of the system of interest on the reservoir during evolution is absent, and thus the total system can be factorized for $t > 0$ as: $\rho(t) \approx \rho_S(t) \otimes \rho_E(0)$, with the state of the reservoir ρ_E remaining constant over the course of time.

- The second approximation called the **Markov approximation** relies on the fact that the memory effects of the reservoir are negligible in the long run, which means that the dynamics at time t do not depend on the past states $\rho_S(s)$ ($s < t$), such that $\rho_S(s)$ is replaced in the integrant with $\rho_S(t)$ at the present time.

Then the obtained equation of motion which is now in the local time form is called the **Redfield equation**

$$\frac{d}{dt}\tilde{\rho_S}(t) = -\int_0^t ds\, \mathrm{tr}_E[\tilde{H_I}(t), [\tilde{H_I}(s), \tilde{\rho_S}(t) \otimes \rho_E(0)]]. \tag{3.55}$$

The equation above is not truly a Markovian master equation as it contains a reference to the initial preparation time $t = 0$ in the lower limit of integration. However, in order to satisfy the dynamical semigroup property, we substitute s by $t - s$ and we extend the limit of the integration to infinity. Then, we can rewrite Eq.3.55 as

$$\frac{d}{dt}\tilde{\rho_S}(t) = -\int_0^\infty ds\, \mathrm{tr}_E[\tilde{H_I}(t), [\tilde{H_I}(t-s), \tilde{\rho_S}(t) \otimes \rho_E]]. \tag{3.56}$$

This is acceptable provided the integrand Eq.3.56 disappears quickly for $s \gg \tau_E$ if we have $\tau_R \gg \tau_E$, such that τ_E is the time scale over which the environment correlation functions decay and τ_R is the time scale over which the system relaxes to a steady state.

In fact, the Born-Markov approximations do not guarantee getting the master equation in the form Eq.3.47. To solve this issue, one should consider decomposing the interaction Hamiltonian into

$$\tilde{H}_I(t) = \sum_\alpha \tilde{A}_\alpha(t) \otimes \tilde{R}_\alpha(t). \tag{3.57}$$

$\tilde{R}_\alpha$ and $\tilde{A}_\alpha$ are both Hermitian operator such that the latter acts on the subspace of the system. The first method or assumption is the *secular approximation* in which we perform an averaging over rapidly oscillating terms in the master equation [97] A. The second assumption considers applying the Markov approximation to the Hamiltonian operators

$$\tilde{A}_\alpha(t-s) \simeq \tilde{A}_\alpha(t) \tag{3.58}$$

$$\tilde{R}_\alpha(t-s) \simeq \tilde{R}_\alpha(t). \tag{3.59}$$

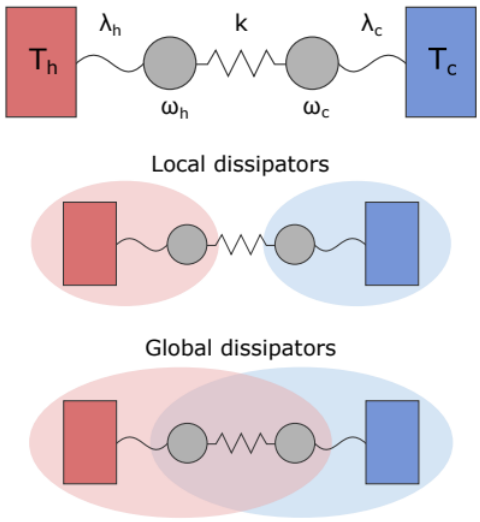

Figure 3.3: Illustration of an open quantum system described in the local and global picture: two coupled resonators of frequencies ω_h and ω_c weakly interacting with two thermal baths at temperatures T_h and T_c respectively. The shaded area that reflects the scope of the hot and cold dissipators represent the local and global master equations. Figure taken from [108].

Substituting Eq.3.59 into Eq.3.56, we get

$$\begin{aligned}\frac{d}{dt}\tilde{\rho_S}(t) &= -\int_0^\infty ds \sum_\alpha \mathrm{tr}_E[\tilde{R}_\alpha(t)\tilde{R}_\alpha^\dagger(t-s)\rho_E](\tilde{A}_\alpha(t)\tilde{\rho_S}_\alpha(t)\tilde{A}_\alpha^\dagger(t-s) \\ &+ \tilde{A}_\alpha(t-s)\tilde{\rho_S}_\alpha(t)\tilde{A}_\alpha^\dagger(t) - \{\tilde{A}_\alpha^\dagger(t-s)\tilde{A}_\alpha(t), \tilde{\rho_S}(t)\} \\ &= \sum_\alpha \tilde{\Gamma}(t)(2\tilde{A}_\alpha(t)\tilde{\rho_S}(t)\tilde{A}_\alpha^\dagger(t) - \{\tilde{A}_\alpha^\dagger(t)\tilde{A}_\alpha(t), \tilde{\rho_S}(t)\}).\end{aligned} \tag{3.60}$$

with $\tilde{\Gamma}(t) = \mathrm{tr}_E(\tilde{R}_\alpha(t)\tilde{R}_\alpha^\dagger(t)\rho_E)$. Then we can return to the Schrödinger picture

$$\dot{\rho}_S = -i[H_S, \rho_S] + \sum_\alpha \Gamma(2A_\alpha\rho_S A_\alpha^\dagger - \{A_\alpha^\dagger A_\alpha, \rho_S\}). \tag{3.61}$$

3.1.5 Global Versus Local GKLS Approach

The two master equations derived in Eq.3.61 and Eq.A.17 have the GKLS form but at the same time they are remarkably different from each other. As a matter of fact, the jump operators in Eq.3.61 depend on the choice of the interaction Hamiltonian while in Eq.A.17 they are associated with the eigenstates of the Hamiltonian of the system. Both equations adopt respectively the *local* and *global* approaches. When considering a composite system, this distinction becomes even more evident. The local master equation (LME) arises when neglecting the interactions

between the subsystems while in the global master equation (GME), the environment is coupled to the delocalized eigenstates of the system's Hamiltonian (figure 3.3). For instance, this can be shown in the equilibrium situation, for the LME where the subsystems are expected to equilibrate individually to the environment's temperature T which results in a steady state (SS) (i.e. state that the system reaches in the long time limit such that it implies $\dot{\rho_S} = 0$). In this case, the resulting steady state is a product of Gibbs states with respect to the subsystems Hamiltonian [102]

$$\rho_{SS} = \frac{\otimes_j e^{-\beta H_j}}{\mathrm{tr}(\otimes_j e^{-\beta H_j})}, \tag{3.62}$$

where H_j is the j^{th} subsystem's Hamiltonian and $\beta = 1/T$. On the other hand, the GME emanates from the desired steady state which is represented by the Gibbs state with respect to the full system's Hamiltonian

$$\rho_{th} = \frac{e^{-\beta H_S}}{\mathrm{tr}(e^{-\beta H_S})}. \tag{3.63}$$

The validity of the local and global approaches has been investigated in several works [103, 104, 107, 108, 110] which demonstrated that the proper master equation to use depends on the strengh of the interaction between the subsystems. For example in [104], the authors showed that an accurate application of the secular approximation always leads to a correct Markovian ME. The global approach is often regarded superior than the local approach for strong interaction between the subsystems. On the other hand, even in the limit of relatively weak system-environment interactions, LME fail to lead the system's to thermal equilibrium, unlike GME [105, 106]. On the other hand, when the system is driven out-of-equilibrium, the situation changes radically. In this case, if there is no interaction between the subsystems and they eventually thermalize with their respective baths, the local approach does prove to be more convenient to describe the transport dynamics [107]. In [108], the authors are comparing to the exact dynamics in a simple system and also agree that when it comes to dynamics, the GME fails at capturing the correct dynamics because the secular approximation destroys key dynamical properties even when the local and global approach agree in the steady state thermodynamic predictions for some cases (they are usually not identical [107, 109]). It is interesting to mention that in [110], LMEs show consistencies with thermodynamics when considering a microscopic model based on a collisional framework and the breaking of the global detailed balance.

Despite the fact that the GKLS master equation is a powerful tool to investigate open quantum systems, it is limited by the Born-Markov approximation used in the derivation. It means that the environment is large and memoryless. While this can be suitable for some physical configurations, such as optical cavities [102] and Josephson

junctions [111], there are others in which the system's memory effects build up and cause Non-Markovian features [112].

3.1.6 Example of Thermalization in Open Quantum Systems

According to thermodynamics principles, a system put in a thermal bath at a temperature T ($\beta = 1/T$) will eventually attain equilibrium with the bath. This principle also applies to open quantum systems. We can use as an example a single qubit that is exposed to an external magnetic field $\mathcal{B}$ and with a Hamiltonian $H_S = \mathcal{B}\sigma_z$. Either an absorption of excitation from the bath or an emission of excitation into the bath defines the interaction between the system and the bath. The master equation that describes this is as follows

$$\frac{d}{dt}\rho_S(t) = -i[H_S, \rho_S(t)] + \gamma(\overline{n})\mathcal{L}[\sigma_+] + (\overline{n}+1)\mathcal{L}[\sigma_-]), \tag{3.64}$$

where one has

$$\begin{aligned} \mathcal{L}[\sigma_+] &= 2\sigma_+\rho_S(t)\sigma_- - \frac{1}{2}\{\sigma_-\sigma_+, \rho_S(t)\} \\ \mathcal{L}[\sigma_-] &= 2\sigma_-\rho_S(t)\sigma_+ - \frac{1}{2}\{\sigma_+\sigma_-, \rho_S(t)\}. \end{aligned} \tag{3.65}$$

It is denoted that $\sigma_+ = |0\rangle\langle 1|$ and $\sigma_- = |1\rangle\langle 0|$ are the raising and lowering operators. $\overline{n}$ is the average thermal occupation of the bath

$$\overline{n} = \frac{1}{e^{2\beta\mathcal{B}-1}.} \tag{3.66}$$

Since the state of the qubit can be described by $\{\sigma_x, \sigma_y, \sigma_z\}$, the time evolution can be found by calculating the averages $\{\langle\dot{\sigma}_x\rangle, \langle\dot{\sigma}_y\rangle, \langle\dot{\sigma}_z\rangle\}$. Substituting them in Eq.3.64, we get the solutions

$$\begin{aligned} \langle\sigma_{x,y}\rangle_t &= \langle\sigma_{x,y}\rangle_0 e^{\gamma(1+2\overline{n})t} \\ \langle\sigma_z\rangle_t &= \frac{-1}{1+2\overline{n}} + (\langle\sigma_z\rangle_0 + \frac{1}{1+2\overline{n}})e^{-2\gamma(1+2\overline{n})t}. \end{aligned} \tag{3.67}$$

Substituting Eq.3.68 into the Bloch sphere representation of the single qubit in Eq.2.25, we obtain the thermal

steady state at equilibrium at the limit of $t \to \infty$

$$\rho_{th} = \frac{1}{1+2\overline{n}} \begin{pmatrix} \overline{n} & 0 \\ 0 & 1+\overline{n} \end{pmatrix}. \tag{3.68}$$

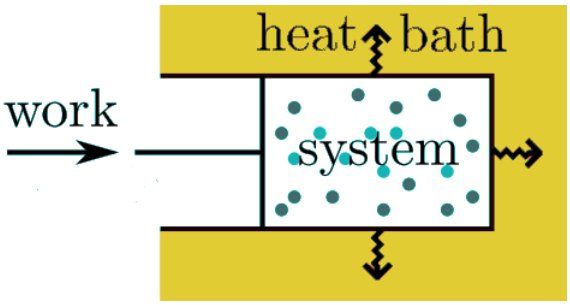

Figure 3.4: Schematic figure of a system as a gas in a contained. The thermodynamic functions (P,T,V) can be varied in a controlled way by pushing a piston. Besides the gas is simultaneously in contact with the heat bath through the walls of the contained. This energy transfer is assisted with an exchange of entropy.

3.2 Quantum Thermodynamics

3.2.1 The Laws of Thermodynamics

Thermodynamics is a phenomenological theory that is reputed to deal with the behavior of energy exchange in the form of heat and work. It provides a description of transformations and relations between equilibrium states of a small number of macroscopic variables or observables such as pressure "P", temperature "T" and volume "V". It relies entirely on statistical principles and makes no assumptions about the microscopic dynamics that underpin them. Despite the unrivaled success and universality of thermodynamics, it cannot characterize states beyond equilibrium, and in particular, it can only cover infinitely slow quasi-static processes. The macroscopic systems which are described by (P,T,V) can exchange heat $\mathcal{Q}$ with their environment and mechanical work $\mathcal{W}$ is used as a supply. A classical example of a basic thermodynamical set up divided into a system, heat and work reservoirs is illustrated in figure 3.4. Thermodynamics is an axiomatic theory, it is built upon four famous axioms often known as the *laws of thermodynamics*:

- **The zeroth law of thermodynamics** states that if two systems are in thermodynamic equilibrium with a third system, the two original systems are in thermal equilibrium with each other [113]. Essentially, they will not exchange any heat and will have the same the same temperature.
- **The first law of thermodynamics** is the application of the conservation of energy principle to heat and thermodynamic processes [114]. It states that the change in internal energy of a system ΔU is balanced by the heat $\mathcal{Q}$ added to the system and the work $\mathcal{W}$ done by the system

$$\cdot\mathcal{U} = \mathcal{Q} - \mathcal{W}. \tag{3.69}$$

The first law makes use of the fundamental concepts of internal energy, heat and work. It is a consequence of energy conservation applied to the system, the heat and the work reservoirs. It is extensively used in the discussion of thermal machines as we will see in the next chapters. On the other hand, the essential contrast between heat and work becomes clear when the second law is considered.

- **The second law of thermodynamics** in its most general form, states that the entropy of the universe , as an isolated system, will always increase in time [115]

$$\Delta S_{universe} \geq 0, \tag{3.70}$$

such that $S_{universe}$ stands for the entropy of the universe which should be distinguished from any information theoretic definition of entropy at this point.The *entropy production* of a process is defined as the change in entropy of the universe [114]

$$\Sigma = \Delta S_{universe}. \tag{3.71}$$

This relation gives rise to the distinction of two important types of processes:

1. **Reversible process**: When the entropy of the universe remains constant and unchanged, a process is said to be reversible $\Sigma = 0$. Because each reversible process passes through a series of equilibrium states, the concept of reversibility is closely linked to the concept of equilibrium. By going backwards along the process's path, the system and its surroundings can be restored precisely to their original state. The quasi-static criterion is therefore a prerequisite for a reversible process.
2. **Irreversible process**: In this process, the entropy of the universe increases such that the final entropy must be greater than the initial entropy. In other words, a system and its surrounding cannot be restored to their initial states. Irreversibility is considered as a real phenomenon that occurs in nature.

Using the system-bath configuration in figure 3.4 as an example, the entropy of the universe is additively split into the system's and environment's entropies

$$S_{universe} = S_s + S_{env}. \tag{3.72}$$

Thus, the second law reads

$$\Sigma = \Delta S_s + \Delta S_{env} \geq 0. \tag{3.73}$$

Besides, the environment is assumed to be described by an equilibrium state with a temperature T such that $\Delta S_{env} = -\int \frac{\delta \mathcal{Q}}{T}$ with $\delta \mathcal{Q}$ being an infinitesimal heat flox into the system. Then, the second law reduces to the *Clausius inequality*

$$\Sigma = \Delta S_s - \int \frac{\delta \mathcal{Q}}{T} \geq 0. \tag{3.74}$$

Eventually, when the environment gets slightly perturbed from its initial temperature, indicated by T_0, Eq.3.74 becomes

$$\Sigma = \Delta S_s - \frac{\mathcal{Q}}{T_0} \geq 0, \tag{3.75}$$

such that $\mathcal{Q} = \delta \mathcal{Q}$ is the overall heat flow from the environment. The Clausius statement of the second law is as follows: *No process is possible whose sole result is the transfer of heat from a body of lower temperature to a body of a higher temperature*. This means that heat flows spontaneously only from a higher to lower temperature bodies but never spontaneously in the opposite direction. On the other hand, the reverse heat transfer may occur only when the system receives an input work, and that is exactly what a refrigerator does.

- **The third law of thermodynamics**, also called the Nernst theorem [114, 116], paraphrases that the entropy of an equilibrium system tends to zero as the temperature approaches the absolute zero ($S_s \rightarrow 0$ with $T \rightarrow 0$).

For a better understanding of thermodynamics of small quantum systems, a new theoretical framework supplemented by statistical and quantum mechanical considerations was established, called *quantum thermodynamics* [117]. In this thesis, we will focus primarly on two central axioms: the first and the second law of thermodynamics in the quantum regime.

For a quantum system in a state ρ with a Hamiltonian H at a given time and weakly interacting with a thermal bath, the first law can be stated by defining the system's internal or average energy with the expectation value of the system's Hamiltonian

$$U = \mathrm{tr}(\rho(t)H(t)) \qquad t \in [0, \tau]. \tag{3.76}$$

This energy varies in time as the system exchanges energy, and can be divided into two contributions:

- **Work-like energy**: This type of energetic resources corresponds to the time variation of H that can be

controlled. It is identified as a fully controllable and useful kind of energy transfer

$$W = -\int_0^\tau dt\, \mathrm{tr}(\rho(t)\frac{dH(t)}{dt}). \tag{3.77}$$

- **Heat-like energy**: It represents the uncontrolled energy transfer between the system and its environment

$$\mathcal{Q} = \int_0^\tau dt\, \mathrm{tr}(\frac{d\rho(t)}{dt}H(t)). \tag{3.78}$$

Conventionally, here we'll assume that work is extracted from the system and heat is absorbed. Together, these expressions imply that the first law holds

$$\Delta U = \mathcal{Q} - W, \tag{3.79}$$

which describes the conservation of energy. It is worth mentioning that work and heat are process dependent, they depend on the system's time evolution from $(\rho(0), H(0))$ to $(\rho(t), H(t))$. As a consequence, work and heat at the infinitesimal level are not full differentials which are denoted by δW and $\delta\mathcal{Q}$. Compared to the average energy with differential dU, they do not correspond to observables [118]. We can have a better grasp of the definition above by considering a simple example of a thermally isolated system. In this situation, the variation of energy stems from the time dependency of the Hamiltonian $H(t)$

$$H(t) = H + A(t). \tag{3.80}$$

The evolution of ρ is expressed as

$$\frac{d\rho(t)}{dt} = -i[H(t), \rho(t)]. \tag{3.81}$$

From Eq.3.78 and by using the cyclic property of the trace, we get

$$\mathcal{Q} = -i\int_0^\tau dt\, \mathrm{tr}([H(t), \rho(t)]H(t)) = 0. \tag{3.82}$$

Thus the obtained work is

$$W = \mathrm{tr}(H(0)\rho(0)) - \mathrm{tr}(H(\tau)\rho(\tau)). \tag{3.83}$$

To sum up, there is no heat transfer when the system is thermally isolated, and work corresponds just to the change of internal energy in this case. The decomposition of the energy change into two kinds of energy transfer is essential to formulate the second law of thermodynamics. A crucial physical law whose origins can be traced back to Sadi Carnot's pioneering study of heat engines in 1828 [1], it defines the concept of irreversibility and sets restrictions on work extraction. In 1865, Clausius found that thermodynamic entropy of the system is useful to investigate the exchange of heat to the system when it is immersed in a thermal reservoir at a temperature T [119]. It is introduced through its change in a reversible process

$$\Delta S_{th} \equiv \int_{rev} \frac{\delta \mathcal{Q}}{T}, \tag{3.84}$$

$\delta \mathcal{Q}$ is the absorbed heat by the system and T is the temperature associated with the heat transfer. This led Clausius to propose a formulated version of the second law of thermodynamics Eq.3.74. If we determine the free energy of a system with a Hamiltonian H as

$$F(\rho) \equiv U(\rho) - T\Delta S_{th}(\rho), \tag{3.85}$$

with $U(\rho) = \mathrm{tr}(H\rho)$. The Clausius inequality becomes a statement of the upper bound on the extractable work from a system. An equivalent formulation of the second law can be obtained from the first law and Eq.3.74

$$W = \mathcal{Q} - \Delta U \leq -\Delta U + T\Delta S_{th} = \Delta F. \tag{3.86}$$

For equilibrium states, the thermodynamic entropy is identified through the Von Neumann entropy Eq.2.26

$$S_{th}(\tau_E) = k_B S(\tau_E), \tag{3.87}$$

where τ_E is the Gibbs state and k_B denotes the Boltzmann constant that we will take to be equal to 1 from now on. In non-equilibrium processes, the definition of the thermodynamic entropy remains a difficult and complex issue that is still debated. A simple and standard way is to keep Eq.3.87 and identify the non-equilibrium entropy of a state ρ as its Von Neumann entropy. In this case, the non-equilibrium free energy is given by

$$F(\rho) \equiv \mathrm{tr}(H\rho) - TS(\rho). \tag{3.88}$$

Next, we will discuss further the notion of work for systems out of equilibrium.

3.2.2 The Concept of Work Extraction in Non-Equilibrium Quantum Thermodynamics

Work extraction and ergotropy

Let us first look at the problem of work extraction from quantum systems in more detail. Our study focuses on processes in which the system is thermally isolated, which means that it is not in touch with any thermal reservoir and no heat is transmitted at any point throughout the process. In this case, work is extracted from the system S by performing a cyclic process in which the Hamiltonian characterized by its initial state remains the same at the start and at the end of the process. Cyclic Hamiltonian processes can be obtained by any time-dependent interaction $K(t)$ applied to the system for a time $t \in [0, \tau]$ [120] and accounts for work transfer with $K(0) = K(\tau) = 0$. At $t = 0$, the isolated system S at initial state $\rho(0)$ is unitarily driven by the Hamiltonian

$$H(t) = H_0 + K(t). \tag{3.89}$$

For a time evolution τ and the condition of $\{t \leq 0, t > \tau, K(t) = 0\}$, the dynamics are described by

$$i\frac{d}{dt}\rho(t) = [H(t), \rho(t)]. \tag{3.90}$$

The corresponding driving generates a unitary evolution operator

$$\mathcal{U}(\tau) = \mathcal{T}e^{-i\int_0^\tau dt(H_0+K(t))}, \tag{3.91}$$

such that the final state is $\rho(\tau) = \mathcal{U}\rho(0)\mathcal{U}^\dagger$. As a result of unitarity and within the framework of unitary cyclic processes such that $:= \rho(0) \rightarrow \rho^{'} := \rho(\tau)$, any change in average energy of the system must be regarded as the extracted work

$$\mathcal{W} = \mathrm{tr}(\rho^{'}H) - \mathrm{tr}(\rho H) \equiv E_f - E_i. \tag{3.92}$$

This expression yields a criteria for whether a state is *passive* with respect to a given reference Hamiltonian.

Passive states

Passive states are defined as states that do not allow the reduction of their average energy by a cyclic unitary process and that no work can be extracted from them. Given a system S at a state σ and a reference time independent Hamiltonian H such that

$$H = \sum_i e_i |i\rangle\langle i| \qquad \text{with} \qquad e_{i+1} \geq e_i \forall \tag{3.93}$$

$$\sigma = \sum_i r_i |i\rangle\langle i| \qquad \text{with} \qquad r_{i+1} \leq r_i \forall. \tag{3.94}$$

σ is a passive state with respect to H if σ is diagonal in the same energy eigenbasis as the Hamiltonian $[\sigma, H] = 0$ and do not possess population inversion. We can prove this result by considering a unitary operation $\mathcal{U}$ and a passive state σ such that:

$$\mathrm{tr}(H\mathcal{U}\sigma\mathcal{U}^\dagger) = \sum_k r_k e_k |\langle k|\mathcal{U}|k\rangle|^2 \geq \sum_k r_k e_k = \mathrm{tr}(H\sigma). \tag{3.95}$$

$|\langle k|\mathcal{U}|k\rangle|^2$ is a probability distribution and the eigenvalues $\{r_k\}$ are of decreasing order, which means that any unitary operation acting on σ can only boost its energy, thus it is impossible to extract work from it. In fact, thermal Gibbs states Eq.3.63 are the only example of *completely passive* state. No matter how many copies one can consider, they remain passive unlike other passive states that can become non-passive or active by processing several copies of them $\rho = \bigotimes^n \sigma$. This scheme of system combination is often refered to as *activation*.

Ergotropy work extraction

Building upon the work of [121], Allahverdyan et al. [122, 123] explored the following question: *"What is the maximum extracted amount of work from a system S through an external source of work acting cyclically in a thermally isolated process?"* As we have seen before, the fact that the process is thermally isolated implies that it is unitary. Following the expression of the state ρ in its decreasing eigendecomposition and its reference Hamiltonian in its increasing spectral decomposition Eq.3.98, we can define the maximum amount of work that can be extracted from an active state ρ with respect to H by means of a cyclic unitary process [122] as the energy difference between

ρ and the passive state σ

$$\mathcal{W} = \mathrm{tr}((\rho-\sigma)) = \mathrm{tr}(\rho H) - \min(\mathcal{U}\rho\mathcal{U}^{\dagger}H) \tag{3.96}$$

$$= \sum_j \sum_k r_j e_k (|\langle e_k|r_j\rangle|^2 - \delta_{kj}), \tag{3.97}$$

with

$$\rho = \sum_k r_k |r_k\rangle\langle r_k| \qquad ,H = \sum_k e_k |e_k\rangle\langle e_k|. \tag{3.98}$$

This quantity is called the *ergotropy*, it is also found by performing minimization of the internal energy of the final state Eq.3.96. $\mathcal{W}$ is non-negative, $\mathcal{W} = 0$ if only if ρ is a passive state. By construction, ergotropy is upper bounded by the free energy $F(\rho) \geq \mathcal{W} \geq 0$ [197]. In the emerging field of quantum thermodynamics, ergotropy has been established as an essential and significant quantity. It was recently evaluated in two experiments that investigate work deposition to external loads coupled to microscopic thermal engines [124, 125]. Ergotropy was also analyzed for a heat pumped three-level maser as a simple example of an autonomous quantum heat engine [126], it has also been used to recover the first and second law for an open system thermodynamic description of finite quantum systems [127]. An identification of a coherent contribution to the ergotropy was shown [128] by dividing the optimal transformation into an incoherent operation and a coherent extraction cycle for bosonic Gaussian states and finite dimentional systems as examples.

In the next chapters, we will demonstrate that coherence plays a significant role in the enhancement of the performance of autonomous thermal machines [129].

Work extraction and free energy

Suppose that we have, in the context of classical thermodynamics, a system S from which we want to perform work extraction. We are able to notice through experimental observation that there is an omnipresent existence of systems in thermal states around us. Therefore, we assume that extracting work can be carried out with free access to a thermal bath at temperature T which should be large compared to the system S, so that its state remains unchanged during the entire process and particularly its temperature stays constant. The free energy is a crucial thermodynamic potential behind this problem. For a system with internal energy U and thermodynamic entropy S_{th}, the free energy with respect to a reservoir at temperature T is defined as

$$F \equiv U - k_B T S_{th}, \tag{3.99}$$

where k_B is the Boltzmann constant. As we have already seen before in Eq.3.86, the second law imposes that work can be extracted from S

$$W \leq -(F_f - F_i). \tag{3.100}$$

F_i and F_f are respectively the initial and final free energies of S. The maximum amount of work is achieved when the final state of S is thermal, since the free energy is minimized for thermal states.

Extracting work from quantum systems

Now we address work extraction in the quantum regime: Given a system S with coherence at a state ρ, how much work can we extract from coherence? We will explore this question by considering a particular model of coherent work extraction which was proposed in [130]. The authors demonstrated that the extracted work from ρ is defined as the free energy difference if the use of average energy preserving operations are allowed. The protocol that employed to attain this consists of two stages. First, work is extracted from coherence and partially from populations. Second, work is extracted from incoherent states. Given a system described by the state $\rho = \sum_i p_i |\varphi_i\rangle\langle\varphi_i|$ such that $p_{i+1} \leq p_i$ with a Hamiltonian $H = \sum_i E_i |E_i\rangle\langle E_i|$ and a weight, where both are initially uncorrelated $\rho \otimes \rho_w$. In the coherent work extraction protocol, the system interacts with the weight via a unitary transformation

$$\mathcal{U} = \sum_i |E_i\rangle\langle\varphi_i| \otimes \Gamma_{\varepsilon_i}, \tag{3.101}$$

where the energy of the weight is shifted by Γ_{ε_i} the shift operator by energy $\varepsilon_i = \langle\varphi_i|H|\varphi_i\rangle - E_i$. The system reaches the final state $\rho^{'} = \sum_i p_i |E_i\rangle\langle E_i|$ and the average change of the system $\Delta U = \mathrm{tr}(\rho H) - \mathrm{tr}(\rho^{'} H)$. Since $\rho^{'}$ is diagonal thus incoherent in the energy eigenbasis, an average amount of work equal to the change of the free energy can be extracred from it

$$\langle W\rangle(\rho^{'}) \equiv \Delta F(\rho^{'}) := F(\rho^{'}) - F(\tau_{th}), \tag{3.102}$$

$F(.)$ 3.88 is the quantum non-equilibrium free energy and τ_{th} is the thermal Gibbs state. The total extractable amount of work is

$$\begin{aligned} \Delta F &= \mathrm{tr}(\rho H) - \mathrm{tr}(\rho^{'}) + F(\rho^{'}) - F(\tau_{th}) && (3.103)\\ &= F(\rho) - F(\tau_{th}), && (3.104) \end{aligned}$$

$\mathcal{U}$ doesn't strictly preserve energy since it is not a free operation [131]. Then one wonders if it can be attained by using an energy preserving unitary $V(\mathcal{U})$ on a bigger system that makes use of an ancillary system ρ_a

$$\begin{aligned} \Omega(\rho) &= \mathrm{tr}(V(\mathcal{U})(\rho \otimes \rho_a)V(\mathcal{U})^{\dagger}) && (3.105)\\ &= \mathcal{U}\rho\mathcal{U}^{\dagger}, && (3.106) \end{aligned}$$

such that the ancillary system is carrying some quantum coherence. A time-translation symmetric map would be recovered in the left hand side of Eq.3.105 if ρ_a doesn't contain coherence which is not the case for the right hand side.

In fact, the topic of work extraction can be approached depending on the nature of the employed protocol. For instance, in [132] the authors consider almost deterministic work extraction from the *single shot* perspective [133, 134]. Meaning that once focuses on single instances of the work extraction scheme rather than average quantities that we have discussed previously. In this situation, the deterministic extractable work is provided by

$$W = F_{min}(\rho) - F_{min}(\tau_{th}). \tag{3.107}$$

$F_{min}(\rho) = k_B T \sum_E h(w, E) e^{-\beta E}$, with w is the dephased state in the energy eigenbasis and $h(w, E) = 0$ if the energy level E is not populated and is equal to 1 otherwise.

3.2.3 Fluctuations Relations

After defining the free energy, work and its extraction protocols, we will introduce the fluctuation relations related to them. *Thermal fluctuations* govern the dynamics of small systems, hence, thermodynamic quantities like work and heat fluctuate. Suprisingly, single fluctuations can contradict the second law's macroscopic statements. For example, the work done can be less than the free energy difference or the change of entropy can be negative. The probability distribution for the thermodynamic observables does, however, satisfy a symmetry relation that goes

by the name of fluctuation theorem. Fluctuation theorems connect the probability of finding a negative entropy production with the probability of finding a positive value in its most generic form:

$$\frac{P(\Sigma = -A)}{P(\Sigma = A)} = e^{-A}. \tag{3.108}$$

We can recover the Clausius inequality by using Jensen's inequality for exponentials $e^{-\langle x \rangle} \geq \langle e^{-x} \rangle$ such that 3.108 implies

$$\langle \Sigma \rangle \geq 0. \tag{3.109}$$

For non-equilibrium systems, Eq. 3.108 may be thought of as an extension of the second law. Gallavotti et al. gave the first thorough proof of the fluctuation theorem [135], which was later extended to generic Markov processes [136] and to Langevin dynamics [137]. Fluctuation theorems have established basically a new branch of thermodynamics known as stochastic thermodynamics. It focuses on the thermodynamic behavior of non-equilibrium small systems and whose dynamics are described by fluctuations rather than focusing on characterizing macroscopic systems in thermal equilibrium. Because quantum systems clearly fall into this category, we will outline briefly, the most prominent fluctuation theorems, namely the Jarzynski equality and the Crooks theorem in the classical and the quantum regimes.

The Jarzynski equality

Now, let's assign a single particle to a point $x = (q, p)$ which is called a microstate in a many-dimensional phase space spanned by the position and momentum coordinates of the particle system. The Hamiltonian of the particle is denoted $H(x, \lambda)$ such that λ is an external controlled force parameter that can vary with time. We consider the Liouville equation

$$\frac{\partial}{\partial t} P(x, t) = -\{P(x, t), H(x, \lambda)\}, \tag{3.110}$$

$\{., .\}$ denotes the Poisson Brackets. Next, we suppose that the system was initially prepared in a Gibbs thermal state

$$p_{\lambda}^{eq}(x) = \frac{1}{Z_{\lambda}} e^{-\beta H(x,\lambda)}, \tag{3.111}$$

such that

$$Z_\lambda = \int dx e^{-\beta H(x,\lambda)} \qquad \text{and} \qquad \beta F_\lambda = -\log Z_\lambda. \tag{3.112}$$

Z_λ and F_λ denote the partition function and the Helmoltz free energy respectively. We can identify the work done during a single realization with the change in the Hamiltonian because the system is isolated during the thermodynamic process

$$W^{closed}_{\tau,x_t} = H(x_\tau(x_0), \lambda_\tau) - H(x_0, \lambda_0), \tag{3.113}$$

where $x_\tau(x_0)$ is a time-evolved point in phase space given the system was initially in x_0. Deriving the Jarzynski equality is not an arduous task to achieve. To this end, we consider

$$\begin{aligned} \langle e^{-\beta W} \rangle &= \int dx_0 p^{eq}_{\lambda_0}(x_0) e^{-\beta W(x_0)} \\ &= \frac{1}{Z_{\lambda_0}} \int dx_0 e^{-\beta H(x_\tau(x_0),\lambda_\tau)} \\ &= \frac{1}{Z_{\lambda_0}} \int dx_\tau |\frac{\partial x_\tau}{\partial x_0}|^{-1} e^{-\beta H(x_\tau,\lambda_\tau)}. \end{aligned} \tag{3.114}$$

By using Liouville's theorem which guarantees the conservation of the phase space volume, i.e $|\frac{\partial x_\tau}{\partial x_0}|^{-1} = 1$ and changing variables. The Jarzynski equality reads as

$$\begin{aligned} \langle e^{-\beta W} \rangle &= \frac{1}{Z_{\lambda_0}} \int dx_\tau e^{-\beta H(x_\tau,\lambda_\tau)} = \frac{Z_{\lambda_\tau}}{Z_{\lambda_0}} \\ &= e^{-\beta \Delta F}. \end{aligned} \tag{3.115}$$

The Jarzynski equality is of great importance in modern thermodynamics. Despite we provided here a simple derivation for the isolated case, the Jarzysnki equality have been proved to hold for a large class of open classical systems including, for instance, those with rapid and slow dynamics, with weak and strong coupling, with Markovian and Non-Markovian noises [138].

The Crooks fluctuation theorem

The second most well known fluctuation theorem is the work relation by Crooks [139, 140]. It is described for a system in contact with a thermal bath at inverse temperature β for which the detailed balance is valid by

$$\frac{P_f(W)}{P_b(W)} = e^{\beta(W-\Delta F)}. \tag{3.116}$$

A backward process is considered for this equation. That means that the change of the parameter λ from λ_τ to λ_0 is done under the same but time reversed protocol. This results in a distribution of work which is denoted with $P_b(W)$ just like in the forward process $P_f(W)$. There are several formulations of this theorem depending on the system and the non-equilibrium process. For example, a relation for the entropy production rate or a formulation that connects the forward and backward trajectories [139]. The interested reader can be referred to explore detailed derivations in the literature [139–142].

Equation 3.116 holds true for every process, regardless of how far the system is driven out of equilibrium or if it is coupled to a heat reservoir or not. The only thing that matters is that both the backward and forward process start in equilibrium at inverse temperature β and we have the free energy difference $\Delta F = F(\tau) - F(0)$ which refers to the two thermal distributions with respect to the initial $H(x, \lambda_0)$ and final $H(x, \lambda_\tau)$ Hamiltonian in the forward protocol. The derivation of the fluctuation theorems has significantly enhanced our understanding of non-equilibrium thermodynamics. They have been testbeds for different laboratory and numerical experiments where both the Jarzynski and Crooks theorems have been verified [143, 144]. They were applied for single molecule experiments [145] where they were employed to estimate the free energy difference [146].

The two-time measurement of energy

The two-time measurement [147] procedure is the operational illustration of the measure of work along a single path $\lambda_0 \to \lambda_\tau$,which we have seen previously in the classical regime, is a special instance of all possible trajectories derived from the initial thermal state. This description can be instantly transferred to the quantum realm where quantum fluctuations will be added to the classical ones thanks to the measurement procedure. Let us follow the steps of the two-time measurement process:

- The system is prepared in a Gibbs state just like in the classical case

$$\rho^{\lambda_0} = \frac{1}{Z_{\lambda_0}} \sum_n e^{-\beta E_n^{\lambda_0}} \Pi_n^{\lambda_0}. \tag{3.117}$$

- At $t = 0$, the energy of the system is measured, the corresponding eigenvalues for some n is $E_n^{\lambda_0}$. The state of the system becomes

$$\rho_n = \frac{\Pi_n^{\lambda_0} \rho^{\lambda_0} \Pi_n^{\lambda_0}}{p_n^{\lambda_0}}. \tag{3.118}$$

with $p_n^{\lambda_0} = \mathrm{tr}(\rho^{\lambda_0} \Pi_n^{\lambda_0}$ is the probability of getting $E_n^{\lambda_0}$ as an outcome.

- The system evolves in time τ and becomes

$$\rho_n(\tau) = \mathcal{U}_{\tau,0} \rho_n \mathcal{U}_{\tau,0}^{\dagger}. \tag{3.119}$$

- Finally, a second energy measurement occurs at $t = \tau$ and the obtained state is

$$\rho_{m,n} = \frac{\Pi_m^{\lambda_\tau} \mathcal{U}_{\tau,0} \rho_n \mathcal{U}_{\tau,0}^{\dagger} \Pi_m^{\lambda_\tau}}{p_{m|n}}, \tag{3.120}$$

where $p_{m|n} = \mathrm{tr}(\Pi_m^{\lambda_\tau} \rho_n(\tau))$ is the probability of getting the result $E_m^{\lambda_\tau}$. To sum up, the total work performed on the system in this specific instance is given by the difference of the final and initial measurement results

$$W = E_m^{\lambda_\tau} - E_m^{\lambda_0} \tag{3.121}$$

, whose probability is

$$\begin{aligned} p_{m,n} &= p_{m|n} p_n^{\lambda_0} \\ &= \mathrm{tr}(\mathcal{U}_{\tau,0}^{\dagger} \Pi_m^{\lambda_\tau} \mathcal{U}_{\tau,0} \Pi_n^{\lambda_0} \rho^{\lambda_0} \Pi_n^{\lambda_0}). \end{aligned} \tag{3.122}$$

From Eq.3.117, it follows

$$\Pi_n^{\lambda_0} \rho^{\lambda_0} \Pi_n^{\lambda_0} = \frac{1}{Z_{\lambda_0}} e^{-\beta E_n^{\lambda_0}} \Pi_n^{\lambda_0}. \tag{3.123}$$

So that the probability of obtaining ($E_n^{\lambda_0}$,$E_m^{\lambda_\tau}$) is

$$p_{m,n} = \frac{e^{-\beta E_n^{\lambda_0}}}{Z_{\lambda_0}} \mathrm{tr}(\mathcal{U}_{\tau,0}^{\dagger} \Pi_m^{\lambda_\tau} \mathcal{U}_{\tau,0} \Pi_n^{\lambda_0}). \tag{3.124}$$

Now we compute the average exponentiated work done on the system over all possible outcomes

$$\begin{aligned} \langle e^{-\beta W} \rangle_\lambda &= \sum_{m,n} p_{m,n} e^{-\beta(E_m^{\lambda_\tau} - E_n^{\lambda_0})} \\ &= \frac{1}{Z_{\lambda_0}} \mathrm{tr}(e^{-\beta H(\lambda_\tau)}) = \frac{Z_{\lambda_\tau}}{Z_{\lambda_0}} = e^{\beta \Delta F}. \end{aligned} \tag{3.125}$$

Therefore, we get the Jarzynski equality for an isolated quantum system. This equality encompasses both thermal fluctuations due to the initial Gibbs state as in the classical regime as well as the quantum fluctuations in the two-time energy measurement process.

Chapter 4

Quantum Thermal Machines

"Nature, in providing us with combustibles on all sides, has given us the power to produce, at all times and in all places, heat and the impelling power which is the result of it. To develop this power, to appropriate it to our uses, is the object of heat-engines."

Nicolas Léonard Sadi Carnot , 1824.

In 1824, the development of ideal reversible thermal machines by the French military engineer and physicist Sadi Carnot in his single publication [1], led to the origin of thermodynamics. More than a century later, the investigation of quantum mechanics outside of its original context caused its union with thermodynamics. The conception of the three-level maser by Scovil and Schultz-Dubois in the late fifties [148] paved the way for an explosion of works on the study of how thermodynamics laws rise from small quantum systems by considering various perspectives and approaches. Quantum thermal machines are the workforce of quantum thermodynamics. As a matter of fact, a profusion of research works that focus on the effect of quantum features such as coherence and entanglement on the performance of thermal machines have been proposed [129, 175, 187, 203, 233]. Because of their importance in this thesis, quantum thermal machines are going to be the core axis of our study.

This chapter aims to provide an essential review of the fundamental design and the working principles of some of the large classes of quantum thermal machines that have been extensively explored in the literature. In the first section, we will discuss the quantumness of thermal machines and present the two major figures of merit that define their performance, namely, the efficiency and the coefficient of performance. Then in the following sections, we will distinguish between non-autonomous and autonomous thermal machines and we will mainly analyze the concept of virtual qubits [161] that are the central elements of the design of one of the coherent thermal machines

discussed in the next chapter 5, mainly in sec.5.1.

4.1 Quantumness of Thermal Machines and Their Efficiency

Until now, we have discussed the fundamental concepts to study the thermodynamics of open quantum systems. Thermodynamics was mainly conceived in the XIX century to describe and eventually improve thermal machines, namely steam engines [1, 198]. Thermal machines are defined as a large category of devices whose functioning is linked to the transfer/exchange and conversion of heat and work energy. They consist of two or more heat thermal reservoirs and a working medium that helps facilitating the intended process. Classical heat engines and refrigerators are well-known examples, as they are the cornerstone of mostly all industrial and mechanical devices that employ thermal energy, ranging from freezers and air conditioners to the fuel based automobiles and nuclear thermal propulsion engines for spacecraft technologies. In fact, the monumental technological advancement in nanofabrication led to the miniaturization of thermal machines. The limits of such reduction of the size of these machines have been pushed to the nanoscale, where quantum properties become important and dominate the dynamics of physical systems. Similar to the merits of the research on classical thermal machines, the study of quantum thermal machines (QTM) has basically two sides. The first one is motivated by the desire to comprehend the functioning principles of these devices at the fundamental level and the other one is driven by technological developments.

The description and analysis of QTMs which operate far from equilibrium require a small quantum system coupled to two or more different thermal reservoirs or some external driving system that helps achieving a thermodynamic task such as work extraction in the case of heat engines and cooling for refrigerators. There are two major categories of quantum thermal machines: reciprocating thermal machines that operate in a cycle which consists of discrete strokes, for example, the four stroke engines that use the Otto and Carnot cycles [199], and continuous machines which are identified by their perpetual coupling with heat reservoirs and through the working medium, reaching a steady-state operation [149, 200]. The three-level maser, being the first operating prototype of a quantum heat engine which was analyzed by Scovil and Schultz-Dubois in 1959 [148], can be defined as the simplest example of continuous thermal machines. In their pioneering work, they demonstrated that the efficiency of the three-level maser engine is bounded by the Carnot efficiency.

Exploring how quantum phenomena such as entanglement and coherence can be best leveraged to improve and optimize the performance of quantum machines is one of the principal goals of quantum thermodynamics. The two crucial figures of merits which characterize the performance of QTMs and which we will come across several

times in the next sections and chapter, are the efficiency (η) and the coefficient of performance (COP).

The efficiency of any heat engine is given by the ratio of the heat supplied from the hot reservoir to the engine that appears as work

$$\eta = \frac{\langle W \rangle}{\langle Q_{in} \rangle}. \tag{4.1}$$

The second law of thermodynamics sets also the bound on the performance of thermal machines, it can be restated in terms of the Carnot cycle which is possibly the most efficient cyclical process. Any heat engine operating under reversibility conditions and utilizing the Carnot cycle is called a Carnot engine. The efficiency of a Carnot engine depends only on the temperatures of the hot T_h and cold T_c baths

$$\eta_c = 1 - \frac{T_c}{T_h}. \tag{4.2}$$

Since no realistic engine is reversible or undergoes infinitely slow cycles, its efficiency is upper bounded by the Carnot efficiency

$$\eta \leq \eta_c. \tag{4.3}$$

This statement is equivalent to the fact that the total entropy cannot decrease (2^{nd} law Eq.3.70). From finite-time thermodynamics, it is well-known that thermal machines operating with quasi-static transformation of the system with $\Delta S_{tot} = 0$, have zero output power. Hence, the issue of efficiency at finite power of engines was addressed in the seminal paper by Curzon and Ahlborn [201]. By considering a classical Carnot engine functioning between the cold and hot temperatures of two reservoirs, they observed that power reaches a maximum and that its associated efficiency is given by the Curzon-Ahlborn efficiency

$$\eta_{CA} = 1 - \sqrt{\frac{T_c}{T_h}}. \tag{4.4}$$

When the machine is acting as a refrigerator, its performance is quantified by the COP which is the ratio of extracted heat from the cold bath to the work performed on the working medium, the maximum attainable COP for a reversible cycle is defined by the reversible COP

$$COP_c = \frac{T_c}{(T_h - T_c)}. \tag{4.5}$$

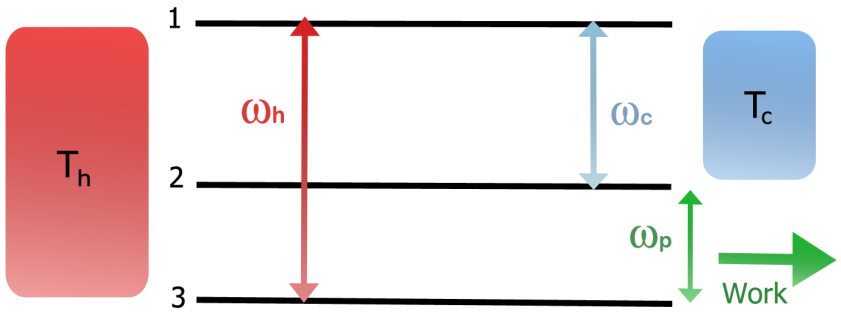

Figure 4.1: Schematic representation of the three-level maser which can act as a heat engine. The working medium is defined by a three level system operating between two thermal baths at different temperatures T_c and T_h with $T_h \geq T_c$ and work extraction is done by an external radiation field with frequency ω_p.

At the quantum level, Linden et al. investigated whether or not, there is a fundamental limit to the size of quantum thermal machines [160] and if there exists a complementarity between size and efficiency [202]. They found that there are no fundamental difficulties in constructing autonomous, small refrigerators. The size of the machine does not impose any constraints on its performance, thus there is no trade-off between size and efficiency and that the Carnot limit can be reached by the smallest possible refrigerators.

The analysis of quantum heat engines has developed one of the primordial toolboxes of methods and concepts for understanding how quantum phenomena change a system's thermodynamic behavior. A non-exhaustive list of literature that investigates the performance of quantum heat engines includes works studying the role of genuine quantum features, namely quantum correlations [203] and coherence [129, 175, 187], shortcuts to adiabaticity [204–206], endoreversible cycles [207, 208], relativistic effects [209, 210] and the distinction between classical and quantum machines [151, 211]. There are proposals of their implementation in a wide range of systems that include atomic clouds [212], harmonically confined single ions [213], optomechanical systems [214], magnetic systems [215] and quantum dots [163, 216]. Nanobeam oscillators [217] and two-level ions [218] have been experimentally used to implement a quantum thermal machine.

4.1.1 Example of a Preliminary Model: The Three-Level Maser

We outline the working of a very simple yet intuitive model of a quantum thermal machine which is the earliest proposal of a quantum heat engine, the three-level maser engine whose steady state operation is similar to that of a heat engine or refrigerator [187]. The working medium is represented by a three-level system with three energy levels ($E_1 \geq E_2 \geq E_3$) and a population p_1,p_2 and p_3. In figure 4.1, the levels 1 and 3 of the system are coupled to a hot bath with temperature T_h through a frequency filter that can generate transitions between E_1 and E_3 with

frequency ω_h in the system. Analogously, the excitations between E_2 and E_1 with a frequency ω_c can be induced by a cold bath with temperature T_c. Besides, a radiation field with a frequency ω_p is also coupled resonantly with the system. Once the latter reaches equilibrium, we obtain the ratios of the populations of the energy levels

$$\frac{p_1}{p_3} = e^{-\frac{\omega_h}{T_h}} \qquad ; \qquad \frac{p_1}{p_2} = e^{-\frac{\omega_c}{T_c}}. \tag{4.6}$$

The system loses energy to the cold bath and to the radiation field for each quanta of transition with frequency ω_h generated by the hot bath, keeping the population stable. The energy exchanged with the baths is referred to as heat, whereas the energy provided to the radiation field is referred to as work extracted from the system which satisfies the first law

$$\omega_h = \omega_c + \omega_p. \tag{4.7}$$

When one considers the efficiency, the most striking result appears. The operation of a heat engine is feasible when population inversion occurs between levels 2 and 3 ($p_2 \geq p_3$), leading to the following condition

$$\begin{aligned} \frac{p_2}{p_3} &= \frac{p_2 p_1}{p_1 p_3} = exp(\frac{\omega_c}{T_c} - \frac{\omega_h}{T_h}) \geq 1 \\ \Rightarrow \frac{\omega_c}{\omega_h} &\geq \frac{T_c}{T_h}. \end{aligned} \tag{4.8}$$

By using Eq.4.7 and Eq.4.9, we can express this condition in terms of the efficiency η and the Carnot efficiency η_c

$$\eta = \frac{\omega_p}{\omega_h} = 1 - \frac{\omega_c}{\omega_h} \leq 1 - \frac{T_c}{T_h}. \tag{4.9}$$

To get a refrigerator-like operation, we can reverse the above discussed heat engine regime because all instants of time are assumed to obey a dynamical equilibrium, meaning that the maser system undergoes reversibility conditions. In this situation, the radiation field induces a quanta of excitation with frequency ω_p that extracts a quanta of energy with frequency ω_c from the cold bath and simultaneously loses an energy quanta to the hot bath. We can deduce the coefficient of performance

$$COP = \frac{\omega_c}{\omega_p} = \frac{\omega_c}{\omega_h - \omega_c} \leq \frac{T_c}{T_h - T_c}. \tag{4.10}$$

The above results appear to be similar to those of the classical Carnot cycle. This remarkable observation proves

that the second law sets also the bounds on the performance of thermal machines based on quantum systems. The implementation of open quantum systems, which was done about twenty years later by Alicki [219] and Kosloff [220], paved the way for a deluge of studies on the influence of quantum characteristics on the operation of thermal machines and made them apparent and significant to the study of quantum thermodynamics.

4.2 Non-Autonomous Thermal Machines

Previously, we mentioned that quantum thermal machines can operate continuously or in cycles. In fact, they can also be classified into autonomous and non-autonomous thermal machines. In the present section, we will devote a particular focus on the analysis of non-autonomous thermal machines. These types of machines rely on external driving or time-dependent fields to perform or extract work, their components can be usually designed explicitly by using time-dependent Hamiltonians. Reciprocating thermal machines represent this class of machines. There are proposals of quantum analogues of classical Carnot engines [221, 222], as well as Otto cycles [223–225], on atoms [153] or trapped ions [213], they might be useful in biological processes [227], metrology [66], quantum state preparation [43] and for the applications of quantum computing [72, 228]. Following that, we will discuss two well-known non-autonomous reciprocating engines, namely the Carnot and Otto quantum engines, before presenting the working principle of a continuous model of a two-qubit refrigerator that employs an external source of work and precise unitary transformations to perform thermodynamic tasks.

4.2.1 Quantum Carnot Engine

Classically, the Carnot engine can be implemented as a four-stroke cycle engine which consists of two isothermal strokes and two adiabatic strokes. The working substance of the quantum counterpart of a Carnot engine can be represented by qubits [221], multilevel atoms [151], particle in a box [229] or harmonic oscillators [220, 230]. We take into consideration the model proposed in [221] which is composed of many non-interacting spin $1/2$ systems. The Carnot cycle for this model Fig.4.2 is described by

- **A hot isothermal expansion** which is realized by coupling the spin system to a hot heat bath at inverse temperature β_h ($\beta_h \leq \beta_c$). This leads to the generation of work and the absorption of Q_h.
- **A cold isothermal compression** when the spin is coupled to a cold heat bath at inverse temperature β_c. This generates work to be done on the system where it transfers heat from the machine to the cold bath.

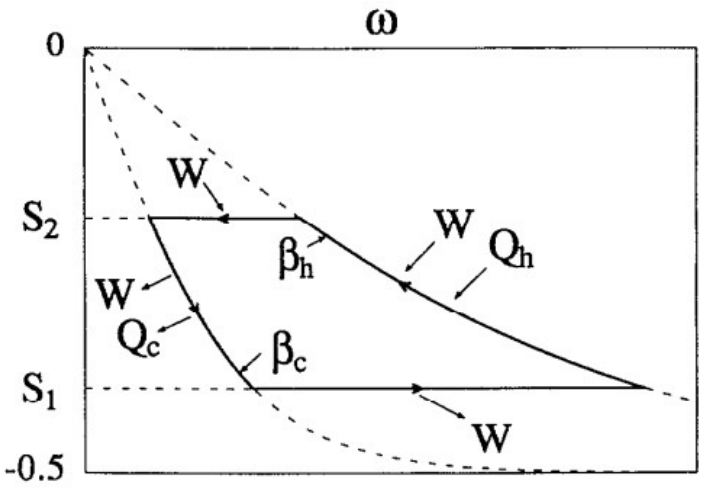

Figure 4.2: Diagram depicting the four strokes of the Carnot cycle in the field ω and polarization S plane. The cycle operates with two isothermal processes associated with the temperatures of the hot and cold bath ($\beta_c \geq \beta_h$) and two adiabatic processes in which the working substance is detached from the baths whilst the magnetization field is switched between two different values $S_1 < S_2 < 0$. (Figure taken from [221]).

- **A hot adiabatic expansion** which is achieved by decoupling the system from the hot bath and having it evolve unitarily for a time τ as a closed system during which work is performed by the spin and its Von Neumann entropy remains constant.
- **Adiabatic compression** where the system is decoupled from all heat baths while work is being done on the system, then the cycle is closed.

The dynamics of the system are described by a time-dependent Hamiltonian given by

$$H(t) = \omega_t S_z = \omega_t \frac{\sigma_z}{2}, \tag{4.11}$$

with a time-dependent driving parameter that can be represented by an external magnetic field. The inverse temperature of the system $\beta^{'}$ is established for a given (S,ω) by the magnetisation relation $S = -\frac{1}{2}\tanh(\beta^{'}\omega/2)$. The operation of the machine can be followed through the Heisenberg picture with the change in the observables of the system and is written in terms of the Lindbladian dissipative term $\mathcal{L}_D(\sigma_z)$

$$\dot{\sigma}_z = i[H, \sigma_z] + \frac{\partial \sigma_z}{\partial t} + \mathcal{L}_D(\sigma_z). \tag{4.12}$$

This relation can be utilized to obtain the rate of change of energy which is expressed by the expectation value of the Hamiltonian

$$\begin{aligned} \frac{d}{dt}\langle H(t)\rangle &= \frac{1}{2}(\frac{d\omega}{dt}\langle\sigma_z\rangle + \omega\langle\mathcal{L}_D(\sigma_z)\rangle) \\ &= \frac{1}{2}(\frac{d\omega}{dt}\langle\sigma_z\rangle + \omega\frac{d\langle\sigma_z\rangle}{dt}). \end{aligned} \tag{4.13}$$

Therefore, this result represents the time derivative of the first law. Eventually, we identify the thermodynamic quantities: the power as $P = \langle\frac{\partial H}{\partial t}\rangle = \frac{1}{2}\frac{d\omega}{dt}\langle\sigma_z\rangle$ and the instantaneous heat flow : $\dot{Q} = \langle\mathcal{L}_D(H)\rangle = \frac{\omega}{2}\frac{d}{dt}\langle\sigma_z\rangle$. This quantum Carnot engine reaches a maximum efficiency which is identified as the Carnot efficiency Eq.4.2.

4.2.2 Quantum Otto Cycle

The Otto cycle is a practical model that may be used to describe a wide range of technical motor applications, such as gasoline vehicle engines [116]. As a result, it's only logical that its quantum equivalent fulfills the same function, bridging the gap between the microscopic world of quantum physics and the macroscopic world of classical machines. The Otto engine is a prime example of four-strokes machines just like the Carnot engine. It has received most attention by doing an extensive and a meticulous study on its quantum counterpart in the last few decades [152,203,204,207,209,210,223–225] , it was also studied in the presence of squeezed baths [226] and was experimentally implemented in the lab [153]. This is due to the simplicity of its analysis because work and heat exchanges are clearly separated between its four strokes unlike any other arbitrary driven open quantum system for which it is in general difficult to distinguish heat and work. In the following, we will discuss the working principle of the harmonic oscillator implementation of quantum Otto engines [152]. The working substance is a quantum harmonic oscillator (QHO) whose frequency is time dependent and controlled externally, its Hamiltonian is given by

$$\begin{aligned} H(t) &= \frac{\hat{x}^2}{2m} + \frac{1}{2}m\omega^2(t)\hat{x}^2 \\ &= \omega(t)(a^\dagger a + 1/2), \end{aligned} \tag{4.14}$$

$(\hat{x}, \hat{p})$ and a are the position, momentum and annihilation operators, respectively. Now, let us consider the coupling of the QHO with two thermal baths at different temperatures T_h and T_c ($T_h > T_c$). The cycle starts when the QHO is in thermal equilibrium with initial frequency $\omega(t = 0) = \omega_A$ and a Hamiltonian $H(t = 0) = H_A =$

$\omega_A(a^\dagger a + 1/2)$ such that

$$\rho_A = \frac{e^{H_A/T_h}}{Z_A}, \tag{4.15}$$

where $Z_A = \mathrm{tr}(e^{H_A/T_h})$ and the expectation value of the energy is:

$$\langle E_A \rangle = \mathrm{tr}(\rho_A H_A) = \omega_A(\langle n \rangle + 1/2) \tag{4.16}$$

with $\langle n \rangle$ is the mean occupation number. The four strokes of the quantum Otto cycle are performed as follows:

- **Isentropic compression:** The QHO is separated from the hot bath during which its Hamiltonian is changed adiabatically $H_A \to H_B$ with $H_B = \omega_B(a^\dagger a + 1/2)$ and $\omega_B \leq \omega_A$. This operation is governed by a unitary transformation $\mathcal{U}_{A\to B}$ such that the state of the QHO at point B is $\rho_B = \mathcal{U}_{A\to B}\rho_A\mathcal{U}^\dagger_{A\to B}$, this unitary evolution does not have any effect on the entropy, hence, it is defined as an isentropic process. The work done by the external driving is given by

$$\begin{aligned} W_{A\to B} &= \mathrm{tr}(\rho_B H_B) - \mathrm{tr}(\rho_A H_A) \\ &= \frac{\omega_B - \omega_A}{2}\coth(\frac{\omega_A}{2T_h}). \end{aligned} \tag{4.17}$$

- **Cold isochore:** The QHO is coupled with the cold bath until it reaches a thermal equilibrium state $\rho_C = \frac{H_B/T_c}{Z_B}$ with its Hamiltonian remaining unchanged. In this stroke, no work is performed, there is only heat absorption from the bath

$$\begin{aligned} Q_{B\to C} &= \mathrm{tr}((\rho_C - \rho_B)H_B) \\ &= \frac{\omega_B}{2}(\coth(\frac{\omega_B}{ET_c}) - \coth(\frac{\omega_A}{ET_h})). \end{aligned} \tag{4.18}$$

- **Isentropic expansion:** Similar to the compression stroke, the QHO is again detached from the bath and the Hamiltonian is modulated back to its original expression $H_B \to H_A$. The state of the QHO is changed to $\rho_D = \mathcal{U}_{C\to D}\rho_C\mathcal{U}^\dagger_{C\to D}$ and the work done is found to be

$$\begin{aligned} W_{C\to D} &= \mathrm{tr}(\rho_D H_A) - \mathrm{tr}(\rho_C H_B) \\ &= \frac{\omega_A - \omega_B}{2}\coth(\frac{\omega_B}{2T_c}). \end{aligned} \tag{4.19}$$

- **Hot isochore:** In the fourth stroke, the cycle is completed by putting the QHO in contact with the hot bath and to its initial state ρ_A. The exchanged heat during this process is

$$\begin{aligned} Q_{D\to A} &= \mathrm{tr}((\rho_A-\rho_D)H_A) \\ &= \frac{\omega_A}{2}(\coth(\frac{\omega_A}{2T_h})-\coth(\frac{\omega_B}{2T_c})). \end{aligned} \tag{4.20}$$

The total energy is preserved as the system relaxes back to its initial state after each cycle which can be expressed by using the first law

$$W_{A\to B}+Q_{B\to C}+W_{C\to D}+Q_{D\to A}=0. \tag{4.21}$$

We can deduce the total extracted work in the cycle

$$W_{tot}=-(W_{A\to B}+W_{C\to D})=Q_{B\to C}+Q_{D\to A}. \tag{4.22}$$

The efficiency of the machine operating as a heat engine is

$$\begin{aligned} \eta_{otto} &= \frac{W_{tot}}{Q_{D\to A}}=1+\frac{Q_{B\to C}}{Q_{D\to A}} \\ &= 1-\frac{\omega_B}{\omega_A}\leq\eta_C. \end{aligned} \tag{4.23}$$

Similarly to the Carnot cycle, a perfect and ideal Otto engine has a zero output power, and this is due to the fact that an infinite time is required to attain an ideal adiabatic evolution and thermalization. Therefore, it is crucial to look at the efficiency at maximum power to quantify the machine's performance 5. We do the expansion of the expression of total work

$$\begin{aligned} W_{tot} &= -(W_{A\to B}+W_{C\to D}) \\ &= (\frac{\omega_B}{\omega_A}-1)(\frac{T_c}{(\frac{\omega_B}{\omega_A})}-T_h). \end{aligned} \tag{4.24}$$

The power reaches its maximum when $\frac{\omega_B}{\omega_A}=\sqrt{\frac{T_c}{T_h}}$, correspondingly its efficiency is identical to the Curzon-Ahlborn efficiency

$$\eta(P_{max})=1-\sqrt{\frac{T_c}{T_h}}. \tag{4.25}$$

4.2.3 Simple Two-Qubits Refrigerator

Let's consider a very simple refrigeration protocol, discussed in [160], where two qubits are initially in the same reservoir at a room temperature T_r 4.3, but afterwards they are immersed in two separate reservoirs at different temperatures T_c and T_h respectively. The qubit to be cooled is qubit A, whereas qubit B acts as a spiral system that absorbs heat from qubit A and dumps it into the surrounding environment. The two qubits are described by their free Hamiltonian

$$H_0 = H_A + H_B = E_A|1\rangle_A\langle 1| + E_B|1\rangle_B\langle 1| \qquad \text{with} \qquad E_B > E_A. \tag{4.26}$$

Their state at equilibrium is a Gibbs thermal state

$$\tau_i = \frac{e^{-H_i/T_r}}{Z_i} \qquad \text{with} \qquad i = A, B, \tag{4.27}$$

where $Z_i = \mathrm{tr}(e^{-H_i/T_r})$ is the partition function. The qubits are uncorrelated, then it follows that the total thermal state is a thermal product state

$$\rho_{AB} = \tau_A \otimes \tau_B. \tag{4.28}$$

The thermal state 4.27 can be expressed as a function of probabilities p_i and $(1 - p_i)$ to have the qubit found in the eigenstates $|0\rangle$ and $|1\rangle$ respectively

$$\tau_i = p_i|0\rangle_i\langle 0| + (1 - p_i)|1\rangle_i\langle 1|. \tag{4.29}$$

When qubit A reaches the steady state, refrigeration occurs when the steady state temperature is lower than the room temperature ($T_A^{ss} < T_r$) meaning that we have a higher ground state probability ($p_A^{ss} > p_A$). This model is similar to the one used in algorithmic cooling [231] in which the transfer of excitations to qubit B increases p_A^{ss}. Since $E_B > E_A$, the probability of $|10\rangle$ where qubit A is excited is larger than the probability of $|01\rangle$: $(1 - p_A)p_B > (1 - p_B)p_A$. In this case, if we want to cool down qubit A we need to increase its ground state probability and reduce the ground state probability of the other qubit. To achieve this goal, we perform a swap of the states $|01\rangle$ and $|10\rangle$ by applying a unitary transformation $\mathcal{U}$ which is induced by an external work that can be

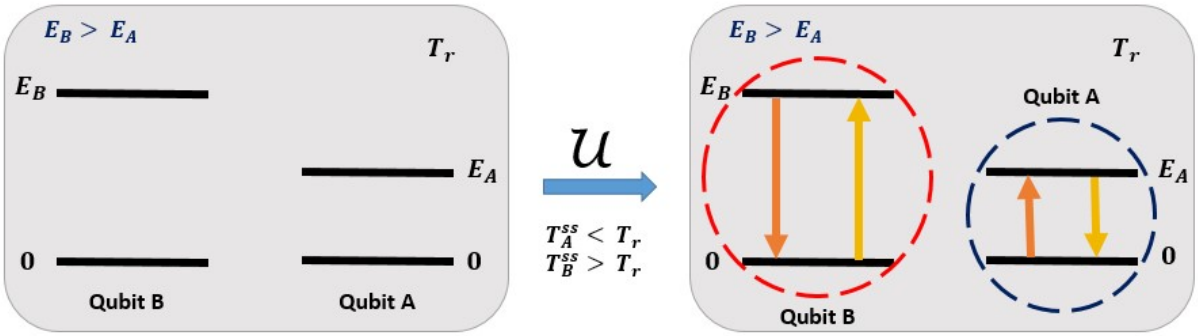

Figure 4.3: Model of two qubits A and B immersed in a reservoir at room temperature T_r in which a non-autonomous refrigeration is realized by applying a unitary transformation $\mathcal{U}$ which performs cooling on the qubit A when $T_A^{ss} < T_r$ and heating on qubit B when $T_B^{ss} > T_r$.

done, for instance, through a sequence of a magnetic field pulses in an NMR experiment

$$|10\rangle \Longleftrightarrow |01\rangle. \tag{4.30}$$

If we keep continuously using $\mathcal{U}$, both qubits will attain steady state temperatures $T_A^{ss} < T_r$ and $T_B^{ss} > T_r$. Elseways, the qubits relax back to the original room temperature. In fact, this procedure can be realized without the need of an external work to achieve refrigeration, and can be done autonomously by adding a third qubit, creating an auntonomous self-contained machine which we will introduce in the following section.

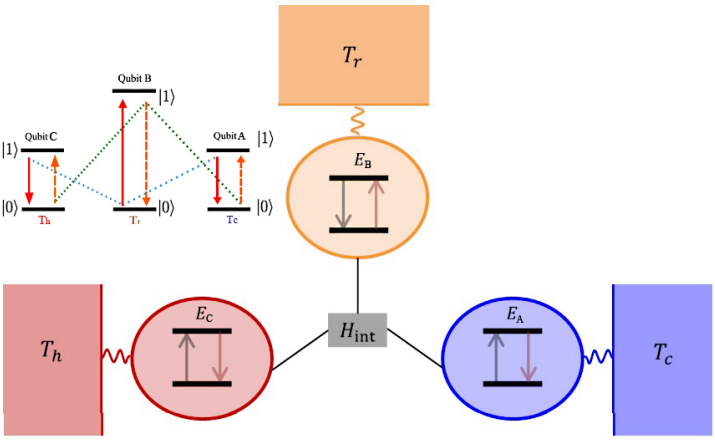

Figure 4.4: Model of a self-contained quantum absorption fridge composed of qubit B and qubit C that plays the role of an engine, which cools qubit A via an interaction Hamiltonian that swaps the eigenstates $|101\rangle$ and $|010\rangle$.

4.3 Autonomous Thermal Machines

Autonomous thermal machines are a class of machines that, instead of being externally driven or controlled, are self-contained and all the machine's degrees of freedom must be taken into account in the dynamics by avoiding time-dependent Hamiltonians because time is seen as an external macroscopic parameter. Such machines function exclusively via incoherent interactions with thermal baths at different temperatures, thus requiring no source of external work or control. They feature the lowest level of control and energetic cost [232] unlike non-autonomous engines, specifically cyclic machines in which the study of quantum phenomena usually involves baths in very unprobable non-thermal states which can take a lot of energy and experimentation to prepare. They represent well-fitted platforms for non-invasive and local applications. Different models of autonomous thermal machines using few quantum levels, qubits or harmonic oscillators have been considered [159–162]. Proposals for their implementation include different platforms, like quantum dots [163, 164], circuit QED architectures [165] or atoms in optical cavities [166]. An autonomous quantum absorption refrigerator has been recently realized in the laboratory with trapped ions [167].

Quantum features like entanglement and quantum coherence [129, 233] as well as common environmental effects [234] were shown to bring some advantage in the performance of these machines . For instance, in [235] Brask et al. discussed a simple set up of two resonant qubits in thermal contact with their respective reservoirs at different temperatures that use a supply of free energy to generate steady state entanglement. This scheme can be implemented with double quantum dots and superconducting flux qubits. Moreover, entanglement was demonstrated to enhance cooling and energy transport [233]. The concept of autonomy of thermal machines was

also used to design autonomous quantum clocks which are driven by only the heat flow between two thermal reservoirs at different temperatures with the goal to measure time [236].

4.3.1 The Smallest Autonomous Refrigerator

Three Qubit Absorption Refrigerator

In 4.2.3, we discussed how to cool a single qubit by using an external source of work provided by a unitary transformation that contributes in increasing the qubit's ground state probability. However, this process can be replaced by considering a quantum absorption refrigerator based on three qubits [239]. All that is required is the addition of another two-level qubit C which plays the role of an engine fig.4.4, it is in thermal contact with a heat reservoir at a larger temperature than the room temperature $T_h > T_r$. Therefore, qubit B and C form the fridge that refrigerates qubit A. The engine's energy level spacing $E_c = E_B - E_A$ allows the swapping of the two degenerate eigenstates $|010\rangle$ and $|101\rangle$ without an input of external work

$$|101\rangle \Longleftrightarrow |010\rangle. \tag{4.31}$$

The transitions between $|010\rangle$ and $|101\rangle$ happen through an interaction Hamiltonian rather than unitary operations

$$H_{int} = g(|010\rangle\langle 101| + |101\rangle\langle 010|, \tag{4.32}$$

such that $g \geq 0$ is the strength of the interaction. In comparison with the free Hamiltonian $H_0 = E_A|1\rangle_A\langle 1| + E_B|1\rangle_B\langle 1| + E_C|1\rangle_C\langle 1|$, this interaction is assumed to be weak, $E_i >> g$. The system would thermalize if the three qubits have the same temperature because the flip Eq.4.31 probability is equal for all of them. Placing qubit C in a hotter reservoir would increase the probability of the forward flip 4.31 while reducing the backward flip's probability. This explains the absorption of heat from qubit A and dumping it into qubit B which results in the creation of a refrigerator.

Steady State Cooling

Deriving the system's dynamics in the weak coupling regime results in obtaining the following master equation

$$\frac{\partial \rho}{\partial t} = \underbrace{-i[H_0 + H_{int}, \rho]}_{\text{closed evolution}} + \underbrace{\sum_{i=A,B,C} D_i(\rho)}_{\text{dissipative evolution}}, \tag{4.33}$$

with $D_i(\rho) = \Gamma(\tau_i^{th} \otimes \mathrm{tr}_i\, \rho - \rho)$. This equation models the system's behaviour in the weak interaction regime as long as $\Gamma, g << E_i$. In fact, to achieve cooling under steady state conditions, 4.33 needs to be solved at the limit $t \to \infty$ such that $\frac{\partial \rho}{\partial t} = 0$ [202]. It's practical to write the master equation in the form of an inhomogeneous linear matrix equation $a\overrightarrow{x} + b = 0$ with $\overrightarrow{x}$ is a vector that represents all the density matrix variables, a and b are respectively the square and the column matrices, they are dependent on the physical parameters of the machine $(E_r, E_c, E_h, T_r, T_c, T_h, \Gamma, g)$. This way, this equation can be solved as $\overrightarrow{x} = -a^{-1}b$. The density matrix is at all times of the form

$$\rho = \begin{pmatrix} \rho_{11} & 0 & 0 & 0 & 0 & 0 & 0 & 0 \\ 0 & \rho_{22} & 0 & 0 & 0 & 0 & 0 & 0 \\ 0 & 0 & \rho_{33} & 0 & 0 & c & 0 & 0 \\ 0 & 0 & 0 & \rho_{44} & 0 & 0 & 0 & 0 \\ 0 & 0 & 0 & 0 & \rho_{55} & 0 & 0 & 0 \\ 0 & 0 & c^* & 0 & 0 & \rho_{66} & 0 & 0 \\ 0 & 0 & 0 & 0 & 0 & 0 & \rho_{77} & 0 \\ 0 & 0 & 0 & 0 & 0 & 0 & 0 & \rho_{88} \end{pmatrix}. \tag{4.34}$$

The explicit expression of the steady state can be written as

$$\rho^{ss} = \tau_A \otimes \tau_B \otimes \tau_C + \Delta\sigma, \tag{4.35}$$

Δ is a dimensionless parameter that depends on all the components of the machine $(E_r, E_c, E_h, T_r, T_c, T_h, \Gamma, g)$, and σ is a matrix where the trace is zero and has one single coherence. The steady state of the individual qubits is obtained by tracing out over the degrees of freedom of the two qubits that are not "i"

$$\rho_i^{ss} = \tau_i + \Delta\, \mathrm{tr}_{\bar{i}}\, \sigma \qquad ; \qquad i = A, B, C, \tag{4.36}$$

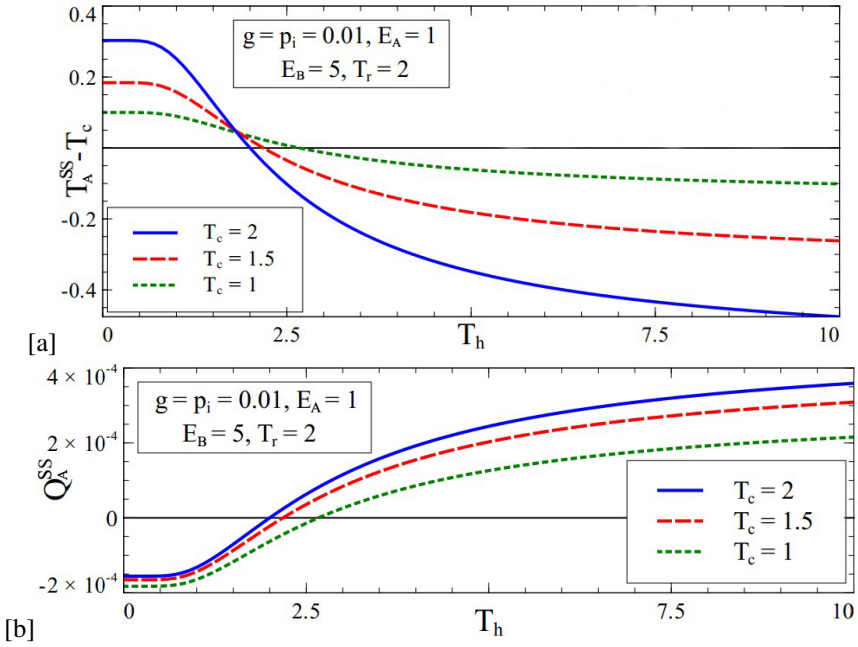

Figure 4.5: (a) The steady state cold qubit temperature difference $T_A^{ss} - T_c$ as a function of the hot reservoir temperature T_h for different values of T_c. (b) Qubit A steady state heat current Q_A^{ss} as a function of the hot temperature T_h. Figure taken from [160].

with $\bar{i}$ denotes the double partial trace. All three reduced states are diagonal and propotional to the Z Pauli matrix. Hence, the steady state of qubit A is

$$\rho_A^{ss} = \tau_A + \frac{\Delta}{\Gamma}\bar{\sigma}_z, \tag{4.37}$$

where $\bar{\sigma}_z$ is the Z Pauli matrix multiplied by a positive constant.

Whenever $\Delta > 0$, the machine is effectively performing cooling of the qubit A if its thermal state is associated to a steady state temperature lower than of the cold bath temperature. The refrigeration procedure can be shown in figure 4.5(a) which describes the temperature difference between the qubit A and its reservoir as a function of the temperature of the hot reservoir T_h. Cooling is achieved $T_A^{ss} < T_r$ when $T_h > T_r$ (blue solid curve), and when the temperature of qubit A is constant and $T_h = T_r$, there is no supply of free energy. Moreover, the green dotted and red dashed curves explain the cooling process $T_A^{ss} < T_c$ when the cold qubit A is in thermal contact with a colder reservoir $T_c < T_r$. As a result, the system operates as a refrigerator in all instances. As a matter of fact, qubit A can be also used to cool other systems, in figure 4.5(b), the steady state heat current $Q_A^{ss} = \mathrm{tr}(H_A D_A(\rho^{ss}))$ of the cold qubit is displayed as a function of the hot temperature. We get similar results as in fig 4.5(a), $Q_A^{ss} > 0$ is equivalent to $T_A^{ss} < T_c$ and that heat can be extracted from the reservoir thus cooling it. In this case, the environment is seen

as the arbitrary system to be cooled. This setting confirms once again that small autonomous refrigerators are not difficult to construct.

4.3.2 Thermodynamic Concept of The Virtual Qubit

The two qubit refrigerator discussed in 4.3.1 can be analyzed in a different way by using the concept of virtual qubits [161]. The smallest quantum thermal machines operate through a simple mechanism because of this notion of virtual qubits that offers a clear insight into the core of thermodynamics, free of complications and unnecessary details. In recent years, virtual qubits became a simplifying approach to predict the relevant machine's behavior in several works: For example, they were used to model a two qubit autonomous engine for which the thermodynamic uncertainty relations (TUR) describing the fluctuations of power were derived [237]. In [238], a set of virtual qubits was considered as a proxy for the complexity of the microscopic structure of clockwork (a system whose purpose is to concentrate the probability of an occuring irreversible event). They also form minimal template and testbed for quantum absorption refrigerators [160, 239]. Moreover, the idea of virtual qubits was employed to construct effective reset master equation for three-level quantum systems and compare it with optical master equations [240].

Now, let's review the notion of virtual qubits with more details. Suppose we have two non-interacting qubits in thermal contact with thermal baths at different temperatures T_c and T_h respectively. We refer to this set of qubits as a pair of two-level qubits machine. If we consider that there is no external system, each qubit will exclusively interact with their own thermal bath until they thermalize at the corresponding temperature of the bath. Therefore, the thermal state of each qubit will be subject to the Boltzmann distribution with the free Hamiltonian of each qubit

$$\tau_i = \frac{e^{-H_i/T_i}}{Z_i}, \tag{4.38}$$

such that $H_i = E_i|1\rangle_i\langle 1|$ is the qubit's free Hamiltonian. Note that this two qubit machine is composed of the energy eigenstates with their corresponding eigenvalues

$$\begin{aligned} e.s &\rightarrow \{|0\rangle_c|0\rangle_h, |1\rangle_c|0\rangle_h, |0\rangle_c|1\rangle_h, |1\rangle_c|1\rangle_h\} \\ e.v &\rightarrow \{0, E_c, E_h, E_c + E_h\}. \end{aligned} \tag{4.39}$$

Here, we focus on the inner transition $\{|1\rangle_c|0\rangle_h, |0\rangle_c|1\rangle_h\}$, it represents the *virtual qubit* with energy spacing $\varepsilon_v = \varepsilon_h - \varepsilon_c = E_h - E_c$ such that $E_h > E_c$. This is because each machine qubit interacts resonantly with the bath's associated qubit with the same energy $\varepsilon_c = E_c$ and $\varepsilon_h = E_h$. This allows the machine to pinpoint an exact

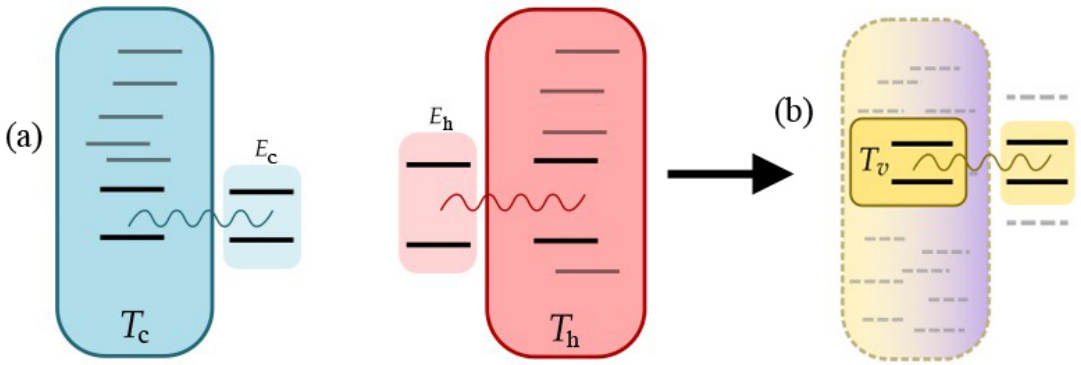

Figure 4.6: Schematic representation of the virtual qubit machine. (a) The machine is composed of two qubits with energy spacings E_c and E_h in thermal contact with two thermal baths at different temperatures T_c and T_h respectively. (b) The virtual qubit machine is described by the two inner energy levels with energy gap $E_v = E_h - E_c$. The individual energy spacings allow the machine to select the appropriate virtual temperature T_v to perform thermodynamic tasks. Figure taken from [161].

virtual temperature T_v, which is calculated by dividing the population of the virtual excited and ground states

$$e^{E_v/T_v} = \frac{P_v^{01}}{P_v^{10}} \quad \text{and} \quad P_v^{01} = p_c^0 p_h^0 e^{E_h/T_h} \tag{4.40}$$

$$P_v^{10} = p_c^0 p_h^0 e^{E_c/T_c}. \tag{4.41}$$

The virtual temperature is written as

$$T_v = \frac{E_h - E_c}{\frac{E_h}{T_h} - \frac{E_c}{T_c}}. \tag{4.42}$$

Note that T_v depends on the energy spacing between the individual levels. Because T_v is not a real temperature, it might be negative, resulting in population inversion. The virtual qubit efficiently reduces the Hilbert space and aids understanding the physical role of the two qubit machine. Basically, the virtual temperature is a versatile parameter that can be tuned for performing different thermodynamics tasks: when $T_v < T_{c,h}$ then the machine is able to cool down another system, $T_v > T_{c,h}$ means that the machine performs heating. On the other hand, work extraction occurs when $T_v < 0$. Since we have all the equipments to analyze autonomous thermal machines. All that remains is to bring an external or target system into contact with the machine's virtual qubit. Let us add another physical qubit with energy spacing $E_k = E_h - E_c$ and resonantly couple it with the two qubit machine fig. 4.6. In this situation, the interaction Hamiltonian 4.32 that induces the transitions between $|0\rangle_v|1\rangle_k \leftrightarrow |1\rangle_v|0\rangle_k$ can be written in terms of the virtual qubit

$$H_{int} = g(|0\rangle_v|1\rangle_k\langle 1|_v\langle 0|_k + |1\rangle_v|0\rangle_k\langle 0|_v\langle 1|_k). \tag{4.43}$$

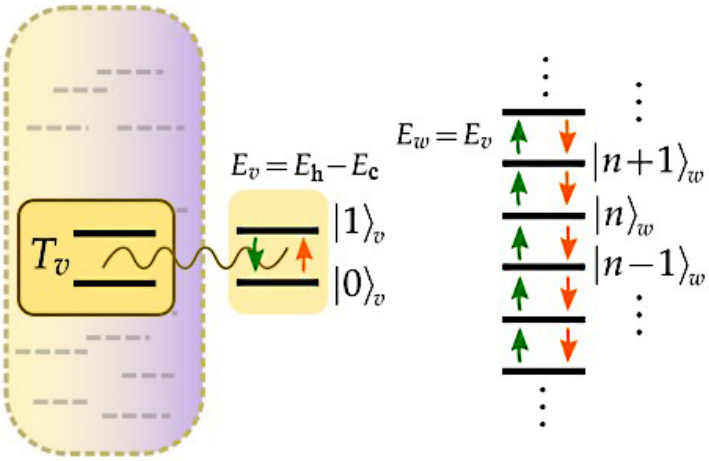

Figure 4.7: Schematic representation of the smallest heat engine. The virtual qubit machine is coupled resonantly to a quantum weight represented by a ladder system with energy spacing $E_w = E_v = E_h - E_c$, the quantum weight is lifted when the transition $|0\rangle_c|1\rangle_h|n\rangle_w \rightarrow |1\rangle_c|0\rangle_h|1+n\rangle_w$ occurs. Figure taken from [161].

As we have mentioned before, producing work is equivalent to inducing population inversion. This can be done only by lifting a quantum weight which can be, for instance, an infinite dimensional system consisting of equally spaced discrete levels of energy $\{|n\rangle_w\}$ and it is unbounded from below and above fig. 4.7. The free and interaction Hamiltonians are given by

$$H_0 = E_c|1\rangle_c\langle 1| + E_h|1\rangle_h\langle 1| + \sum_{n=-\infty}^{\infty} E_n|n\rangle_w\langle n| \tag{4.44}$$

$$H_{int} = g\sum_{n=-\infty}^{\infty} |0\rangle_v|n\rangle_w\langle 1|_v\langle n+1|_w + |1\rangle_v|n+1\rangle_w\langle 0|_v\langle n|_w, \tag{4.45}$$

where $H_w = \sum_{n=-\infty}^{\infty} E_n|n\rangle_w\langle n|$ $E_n = nE_w$ and $E_w = E_h - E_c$. The dynamics of the open quantum system considered in [161] are governed by the explicit master equation in 4.33. In the absence of the interaction term, the qubit of the machine thermalizes to its respective equilibrium state while generating an exponential decay Γ. Now if we want to analyze the heat engine regime, we need to look at the work and the heat currents that define the raising or lifting of the quantum weight, they can be obtained by calculating the rate change weight energy [161],

$$\dot{W} = \frac{d}{dt}\langle H_w\rangle = \frac{d}{dt}\,\mathrm{tr}(H_w\rho) \tag{4.46}$$

$$= -\frac{g^2\Gamma}{2g^2+\Gamma}E_w\langle M_v\rangle_{eq}, \tag{4.47}$$

$\langle M_v\rangle_{eq}$ is the expectation value at thermal equilibrium of the operator on the virtual qubit which depends on

its own population. It is expressed as

$$\begin{aligned} \langle M_v \rangle_{eq} &= \mathrm{tr}(|1\rangle_c|0\rangle_h\langle 1|_c\langle 0|_h - |0\rangle_c|1\rangle_h\langle 0|_c\langle 1|_h)\tau_c \otimes \tau_h) \quad (4.48) \\ &= p_{10} - p_{01}. \end{aligned}$$

The change of energy of each qubit as a result of the contact with the thermal baths determines the rate at which heat is transferred between the qubits and their surrounding environments

$$\begin{aligned} \frac{d}{dt}Q_c &= \mathrm{tr}(H_c D_c(\rho)) \quad ; \quad \frac{d}{dt}Q_h = -\frac{g^2\Gamma}{2g^2+\Gamma^2}E_h(p_{10}-p_{01}) \quad (4.49) \\ &= \frac{g^2\Gamma}{2g^2+\Gamma^2}E_c(p_{10}-p_{01}). \quad (4.50) \end{aligned}$$

By using Eq.4.46 and Eq.4.49, we can effortlessly verify the first law

$$\dot{W} = \dot{Q}_c + \dot{Q}_h. \quad (4.51)$$

In the case of the heat engine regime, the stored work in the quantum weight is extracted by absorbing heat $\dot{Q}_h$ from the hot bath and dumping it to the cold one. The corresponding efficiency can be obtained in terms of the virtual temperature and the Carnot efficiency

$$\begin{aligned} \eta &= \frac{\dot{W}}{\dot{Q}_h} = 1 + \frac{\dot{Q}_c}{\dot{Q}_h} \quad (4.52) \\ &= 1 - \frac{E_c}{E_h} = \eta_{Carnot}(1 - \underbrace{\frac{T_c}{T_c - T_v}}_{\alpha}). \quad (4.53) \end{aligned}$$

As we can notice, we can achieve the Carnot efficiency when $T_v \to -\infty$. It means that the correction term α must disappear and results in a vanishing population inversion. Therefore, the machine's properties such as the energy level spacing must be appropriately tuned to couple the precise virtual temperature that eliminates α.

Chapter 5

The Impact of Quantum Coherence on The performance of Coherent Thermal Machines

"I am firmly convinced that the automobile engine will come, and then I consider my life's work complete."

Rudolf Diesel.

The question of whether new thermodynamic characteristics may emerge from quantum features and aid thermodynamic tasks has long been debated. Answering this challenge might lead to obtain quantum advantages in thermodynamics, which could bring immense progress in the field. This outlook fueled a flurry of research papers on the use of quantum properties: correlations and quantum coherence.

Coherence as a resource was established in Sec.2.3, and its impact in thermal machines [129,175,187,245,246, 248, 249] has been investigated alongside work extraction [131]. It was also shown to be an essential ingredient for optimal charging of quantum batteries [250,251], helping in the transfer of energy in photosynthetic complexes [86, 252] as well as influencing quantum transport [253, 254] in nanoscale devices. However, coherence can exhibit detrimental effects in some cases. For instance, due to the incomplete isochores, coherence generated in the working substance by non-adiabatic driving in reciprocating machines can be harmful to power and efficiency [224, 255]. Similar results were found when taking into account system-reservoir correlations even when quantum

friction [256] doesn't play any role. Hence, the presence of quantum coherence is not always enough to claim quantum advantage, this is because it depends on the model of interest. Throughout this chapter, we simply analyze the operation of engines with and without coherence, this method represents the most genuine way to explore the nature of quantum coherence and its impact on thermal machine's performance.

As a matter of fact, all coherent machine models treated in this chapter use a collisional framework. This repeated interaction scheme has demonstrated to be a useful tool for studying Markovian and also non-Markovian dynamics [179–182, 241]. In the conventional Markovian case, Collision models depict the environment as a big ensemble of elementary components, often dubbed "ancillas". The system-ancilla joint dynamics are described by collisions that may or may not preserve energy, the conditions for a memoryless Markovian behavior of the open quantum system evolution entails that the ancillas state is initially prepared in a product state (uncorrelated), they never interact with each other and every ancilla collides only once with the system.

In the following sections, we discuss two different scenarios where energetic coherence appears. Section 5.1 presents the first coherent collision model in which we study the transport and performance a thermal machine that is composed of a single qubit interacting with environmental ancillas at different temperatures that are prepared with some initial coherence and we explore the role of dephasing between the system and the ancillas. Autonomous thermal machines [150] avoid time-dependent Hamiltonians and do not require exta sources of coherence not explicitly accounted for [157, 158]. They are the ideal platform to measure the role of coherence. In section 5.2, we quantify and optimize the impact of coherence on the operation of an autonomous thermal machine. By energetic coherence we refer to the coherence between non-degenerate energy levels, also called asymmetry under time-translations [56, 73]. Energetic coherence is a resource of particular relevance in quantum thermodynamics [168–171]. It constitutes an extra (independent) source of free energy [172, 173], allowing state transformations that would be otherwise impossible [69, 76, 174, 175], and has direct consequences on the entropy balance leading to the second law [176, 177].

The model considered in Sec.5.2 has been recently introduced in [178], although employed for different purposes. It represents one of the most prototypical quantum thermal machines, namely, a pair of two-level systems (or qubits) coupled to thermal baths at different temperatures [152, 161]. The machine works through the interaction with a stream of qubits (represented in a tape). In both models used in Sec.5.1 and Sec.5.2, we provide a detailed description of the different modes of operation of the machine by highlighting the role of the initial coherence as well as discussing the power optimization procedure, especially for the free energy engine and refrigerator regimes.

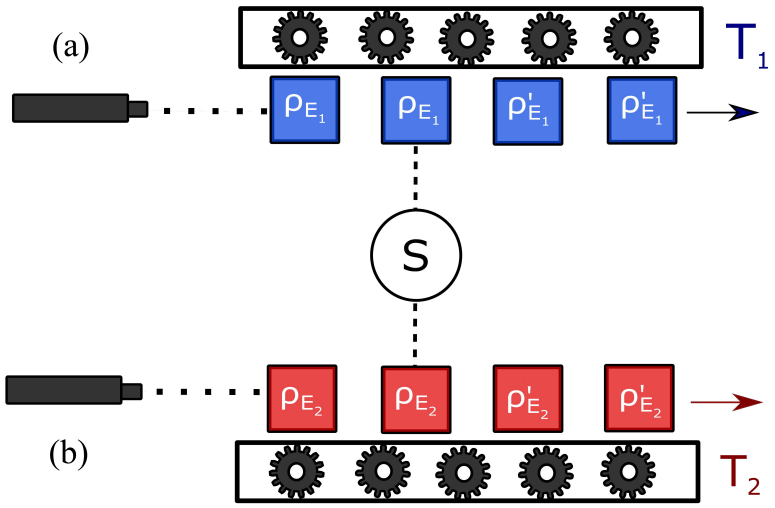

Figure 5.1: Schematic representation of a weakly coherent collisional machine. The single qubit system "S" interacts sequentially with subunits (dubbed "ancillas") of two baths at different temperatures, T_1 and T_2 respectively. Before they hit the system, a laser pulse is acting on them, thus preparing these ancillas with coherence in one of the baths: (a) cold bath or (b) hot bath.

5.1 Exploiting Coherence for Quantum Thermodynamic Advantage

5.1.1 Single Qubit Coherent Collision Machine Model

We consider a system described by the Hamiltonian H_S interacting with an environment [247] modelled with the collision model [182, 241]. The environment consists of N_B baths each containing an infinite ensemble of identically prepared ancillas which interact sequentially with the system for a time τ and then are discarded, see Figure.5.1 The reduced dynamics of the system after one collision can be written as ($\hbar = 1$)

$$\rho'_S = \mathrm{tr}_E \left\{ e^{-i\tau H_{\mathrm{tot}}} \rho_S \otimes \rho_E e^{i\tau H_{\mathrm{tot}}} \right\}, \tag{5.1}$$

where ρ_S $[\rho'_S]$ is the state of the system before [after] the collision. We do not assume any initial correlations between the system and the environment which is described by the following state

$$\rho_E = \bigotimes_{i=1}^{N_B} \rho_{E,i} \tag{5.2}$$

Now, we can define the total Hamiltonian of the entire system+environment (ancillas) by

$$H_{\rm tot} = H_S + H_E + H_{SE}. \tag{5.3}$$

The ancillas from different baths are independent and described by the Hamiltonian

$$H_E = \sum_{i=1}^{N_B} H_{E,i} \tag{5.4}$$

The system-environment interaction has the general form

$$H_{SE} = \sum_{i=1}^{N_B} \sum_k \frac{g_{i,k}}{\sqrt{\tau}} \left(S^\dagger_{i,k} A_{i,k} + S_{i,k} A^\dagger_{i,k} \right), \tag{5.5}$$

where $g_{i,k}$ are the coupling constants between the system and the ancilla from bath i. The index k lists the different system's operators interacting with a corresponding ancilla. The operators $S_{i,k}$ and $A_{i,k}$ pertain to the system and ancilla's Hilbert space, respectively. We assume that the operators $A_{i,k}$ are also eigenoperators of the ancilla's Hamiltonian, such that

$$H_{E,i} = \sum_k \omega_{i,k} A^\dagger_{i,k} A_{i,k}. \tag{5.6}$$

As we will see, the factor $\sqrt{\tau}$, though not necessary, ensures consistency when taking the continuous limit $\tau \to 0$.

We now consider that the ancillas are prepared in a thermal state at temperature T_i ($\beta_i = T_i^{-1}$) with a small coherence term ($k_B = 1$)

$$\rho_{E,i} = \rho^{\rm th}_{E,i} + \sqrt{\tau}\epsilon_i \chi_{E,i}, \tag{5.7}$$

where $\rho^{\rm th}_{E,i} = e^{-\beta_i H_{E,i}} / \left[e^{-\beta_i H_{E,i}} \right]$ and ϵ_i quantifies the ancilla's quantum coherence.

In the continuous limit, following [110, 182], the evolution of the system's reduced density matrix is ruled by the following Markovian master equation

$$\dot{\rho}_S = -i[H_S + G, \rho_S] + \sum_{i=1}^{N_B} D_i(\rho_S), \tag{5.8}$$

where the effective Hamiltonian correction is given by

$$G = \sum_{i=1}^{N_B} \epsilon_i \sum_k \left\{ S_{i,k}^\dagger \, \mathrm{tr}\left[\chi_{E,i} A_{i,k}\right] + \mathrm{h.c.} \right\}. \tag{5.9}$$

The dissipators are defined by

$$D_i(\rho_S) = \sum_k \gamma_{i,k}^- \mathcal{L}[S_{i,k}, \rho_S] + \gamma_{i,k}^+ \mathcal{L}[S_{i,k}^\dagger, \rho_S] \tag{5.10}$$

where the Lindblad operator is defined as:

$$\mathcal{L}[S, \rho] = 2S\rho S^\dagger - \{S^\dagger S, \rho\}. \tag{5.11}$$

The dissipation rates $\gamma_{i,k}^- = g_{i,k}^2 \langle A_{i,k} A_{i,k}^\dagger \rangle$ and $\gamma_{i,k}^+ = g_{i,k}^2 \langle A_{i,k}^\dagger A_{i,k} \rangle$ fullfil the local detailed balance condition $\gamma_{i,k}^+ / \gamma_{i,k}^- = \exp(-\beta_i \omega_{i,k})$.

Thermodynamic quantities can be calculated following [110, 182, 242]. The heat current flowing from bath i is obtained from the energy change of the ancilla before and after the collision

$$\dot{Q}_i = -\lim_{\tau \to 0} \frac{1}{\tau} \mathrm{tr}\left[H_{E,i} \Delta\rho\right], \tag{5.12}$$

where we have defined the change in the total density matrix of the system plus environment

$$\Delta\rho = e^{-i\tau H_{\mathrm{tot}}} \rho_S \otimes \rho_E e^{i\tau H_{\mathrm{tot}}} - \rho_S \otimes \rho_E. \tag{5.13}$$

Similarly, the work power that needs to be injected or extracted from the system due to the on and off switching of the system-ancilla interaction is

$$\dot{W} = \lim_{\tau \to 0} \frac{1}{\tau} \mathrm{tr}\left[\left(H_S + H_E\right) \Delta\rho\right]. \tag{5.14}$$

Notice that if we define the rate of change of the internal energy

$$\dot{U}_S = \lim_{\tau \to 0} \frac{1}{\tau} \mathrm{tr}\left[H_S \Delta\rho\right], \tag{5.15}$$

then the first law of thermodynamics is automatically satisfied

$$\dot{U}_S = \dot{W} + \sum_{i=1}^{N_B} \dot{Q}_i. \tag{5.16}$$

We are assuming the sign convention such that work or heat currents are positive when energy flows into the system. Depending on the signs of these quantities the device exhibits different functionings as discussed next.

We remark that we have followed a different although physically equivalent splitting of heat and work compared to [242]. In our case, we have included all work contributions, coherent or incoherent ones, in $\dot{W}$.

5.1.2 Steady-State Operation

We now specialise our problem to that of a single qubit in contact with two baths ($N_B = 2$). We assume the qubit's Hamiltonian to be

$$H_S = B\sigma_S^z. \tag{5.17}$$

The ancillas are represented by qubits such that their Hamiltonians read

$$H_{E,i} = B_i\sigma_{E,i}^z, \quad i = 1, 2$$

Notice that the ancillas are *not* resonant with the qubit. This causes extra terms to appear in the work and heat expressions proportional to the non vanishing gap [243]. The system-environment interaction Hamiltonian is assumed of the rotating-wave type with $S_i = \sigma_S^-$ and $A_i = \sigma_{E,i}^-$ (where we have therefore dropped the index k as there is only one value). For the state of the ancilla before the collision we choose

$$\chi_{E,i} = \cos\phi_i\sigma_{E,i}^x + \sin\phi_i\sigma_{E,i}^y, \tag{5.18}$$

where the angle ϕ_i can be interpreted as the azimuth of the ancilla's Bloch vector.

Under these assumptions, the master equation for the system's qubit becomes

$$\begin{aligned} \dot{\rho}_S &= -i[H_{\text{eff}}, \rho_S] + \gamma(n_1 + n_2 + 2)\mathcal{L}[\sigma_S^-, \rho_S] && (5.19)\\ &+ \gamma(n_1 + n_2)\mathcal{L}[\sigma_S^+, \rho_S], && (5.20) \end{aligned}$$

where we have defined the effective Hamiltonian as

$$H_{\text{eff}} = B\sigma_S^z + 2\sqrt{2\gamma}\sum_{i=1,2}\epsilon_i\sqrt{2n_i + 1}\left(\cos\phi_i\sigma_S^x + \sin\phi_i\sigma_S^y\right), \tag{5.21}$$

and we have assumed equal rates γ for the two baths such that: $g_{E,i}^2 = \gamma(2n_i + 1)/8$. Notice that in the absence

of environmental coherence ($\epsilon_i = 0$), the master equation would simply correspond to that of a qubit in contact with a single effective bath with an average thermal occupation $n = (n_1 + n_2)/2$ and in the long-time limit will equilibrate with this average thermal occupation.

The steady state of the system's qubit can be found by solving the equation $\dot{\rho}_S = 0$. We write the density matrix ρ_S in the basis of eigenstates of σ_S^z as:

$$\rho_S = \begin{pmatrix} \rho_{11} & \rho_{12} \\ \rho_{21} & \rho_{22} \end{pmatrix}. \tag{5.22}$$

In this representation, the analytical steady state reads

$$\rho_{11} = \frac{1}{R}\left\{4B^2 n + \gamma_{\text{eff}}(1+2n)^2(8\epsilon_{\text{eff}}^2 + n\gamma_{\text{eff}})\right\} \tag{5.23}$$

$$\rho_{22} = 1 - \rho_{11} \tag{5.24}$$

$$\rho_{21} = \frac{2\sqrt{2}i\epsilon_{\text{eff}}e^{i\phi}\sqrt{\gamma_{\text{eff}}}\sqrt{2n+1}}{R}\left\{2iB + (2n+1)\gamma_{\text{eff}}\right\} \tag{5.25}$$

$$R = (2n+1)\left[4B^2 + \gamma_{\text{eff}}(2n+1)(16\epsilon_{\text{eff}}^2 + (2n+1)\gamma_{\text{eff}})\right], \tag{5.26}$$

where we have introduced the effective decay rate $\gamma_{\text{eff}} = 2\gamma$ and an effective coherence strength, expressed in complex polar form

$$\sqrt{2}\sqrt{1+2n}\epsilon_{\text{eff}}e^{i\phi} = \epsilon_1 e^{i\phi_1}\sqrt{1+2n_1} + \epsilon_2 e^{i\phi_2}\sqrt{1+2n_2} \tag{5.27}$$

with ϵ_{eff} and ϕ, real parameters, denoting the magnitude and phase, respectively.

We now pass to the thermodynamic quantities, heat currents and work power in the steady state. To this end, for the results to be simplified, coherence is presumed to be only in one bath and set $\epsilon_2 = 0$.

Substituting the expressions for the steady state, in Eqs. 5.12-5.14, we obtain:

$$\dot{Q}_1 = B_1 N(\epsilon_1) \tag{5.28}$$

$$\dot{Q}_2 = -B_2 N(\epsilon_1) \tag{5.29}$$

$$\dot{W} = (B_2 - B_1)N(\epsilon_1), \tag{5.30}$$

where the common factor is given by

$$N(\epsilon_1) = 2\gamma \frac{B^2(n_1 - n_2) + \gamma(1 + n_1 + n_2)\left[(n_1 - n_2)(1 + n_1 + n_2)\gamma + (2n_1 + 1)\epsilon_1^2\right]}{(1 + n_1 + n_2)\left[B^2 + (1 + n_1 + n_2)^2\gamma^2 + (2n_1 + 1)\gamma\epsilon_1^2\right]}. \tag{5.31}$$

The fact that the thermodynamic quantities contain a common factor is a consequence of the system-environment exchange interaction Hamiltonian, even if not resonant in this case, that we have assumed and it has been found before in related models. An immediate consequence is that the ratios of these quantities linked to the efficiency and coefficient of performance (COP) only depend on the ratios of the ancillas magnetic fields yielding Otto-like expressions. For instance, for the efficiency we obtain

$$\eta = -\frac{\dot{W}}{\dot{Q}_{\rm in}} = 1 - \frac{\min\{B_1, B_2\}}{\max\{B_1, B_2\}}, \tag{5.32}$$

where the input heat $\dot{Q}_{\rm in}$ is the sum of all positive heat contributions. Notice that the factor $A(\epsilon_1)$ contains explicitly the strength of coherence ϵ_1 but not its phase. In the case of two baths with coherence, only their relative phase would appear in the expression, which for simplicity we do not report. The factor $N(\epsilon_1)$ also contains the system's magnetic field B and would appear also in the absence of bath coherence [243]. In this case this field plays the role of an effective detuning which increases the magnitude of the heat currents and work power but does not alter their signs and the operating machine.

In the next two subsections, we showcase our numerical results distinguishing the case in which the coherence is in the cold bath $T_1 < T_2$ from the case in which the coherence is in the hot bath $T_2 < T_1$.

5.1.3 Coherence in The Cold Bath

We start by assuming that the coldest bath has some small coherence; therefore we assume that $T_1 < T_2$. In this case, depending on the choice of the coherence strength ϵ_1 and the magnetic fields B_1 and B_2, the system behaves in different operating regimes, summarised in Table 5.1.

$\dot{W} < 0, \dot{Q}_1 < 0, \dot{Q}_2 > 0$	engine
$\dot{W} < 0, \dot{Q}_1 > 0, \dot{Q}_2 < 0$	hybrid refrigerator
$\dot{W} > 0, \dot{Q}_1 < 0, \dot{Q}_2 > 0$	accelerator
$\dot{W} > 0, \dot{Q}_1 > 0, \dot{Q}_2 < 0$	refrigerator

Table 5.1: Functionings for $T_1 < T_2$.

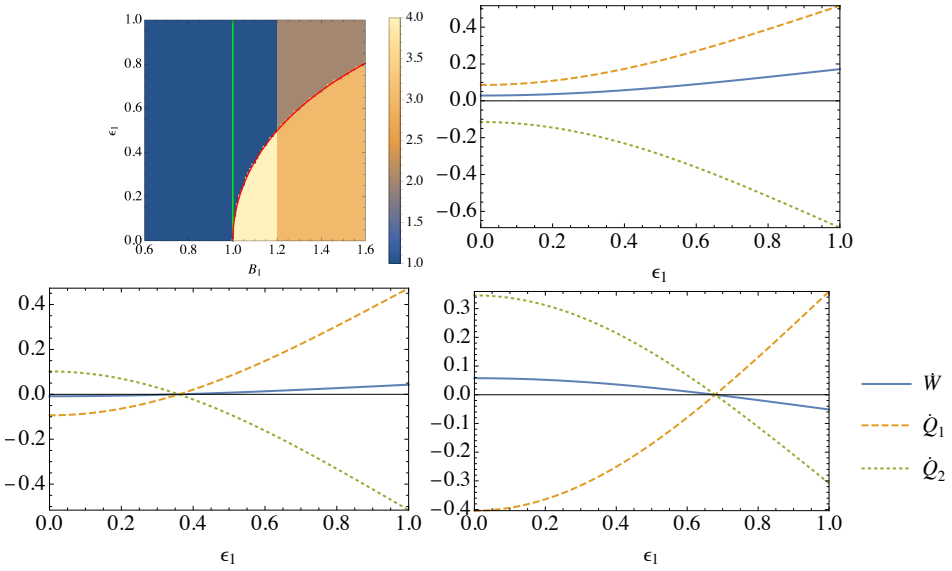

Figure 5.2: Coherence in the cold bath: (a) modes of operation for the different functionings of the thermal machine. Color coding is as follows: 1≡refrigerator, 2≡hybrid refrigerator, 3≡accelerator, 4≡engine. The vertical solid line indicates the condition $n_1 = n_2$. Heat currents and work power for (b) $B_1 = 0.9$, (c) $B_1 = 1.1$, (d) $B_1 = 1.4$. Other parameters: $B = 1, B_2 = 1.2, T_1 = 2.5, T_2 = 3, \gamma = 1$.

Looking at Eqs. 5.28-5.31 we see that $\dot{W}$ changes sign when

$$B_1 = B_2, \tag{5.33}$$

while all quantities, $\dot{W}, \dot{Q}_1, \dot{Q}_2$, become zero when $A(\epsilon_1)$ is zero. This occurs, in the presence of coherence, when

$$\epsilon_1^* = \frac{\sqrt{n_2 - n_1}\sqrt{B^2 + (1 + n_1 + n_2)^2\gamma^2}}{2\sqrt{(1 + 2n_1)(1 + n_1 + n_2)\gamma}}. \tag{5.34}$$

The two conditions Eqs.5.33-5.34 determine the functioning diagram reported in Fig. 5.2(a). There, we see that all four regimes illustrated in Table 5.1 appear for certain values of the parameters. In the panels (b,c,d) of Fig. 5.2 we plot the thermodynamic quantities $\dot{W}, \dot{Q}_1, \dot{Q}_2$ along three cuts of the functioning diagram. The crossing points that appear in panels (c) and (d) of Fig. 5.2 correspond to effective Carnot points where all thermodynamic quantities go to zero and change sign.

We now focus on investigating the efficiency and coefficient of performance of the thermal devices. As discussed in the previous section, these quantities are given by the Otto values

$$\eta = 1 - \frac{B_1}{B_2}, \tag{5.35}$$

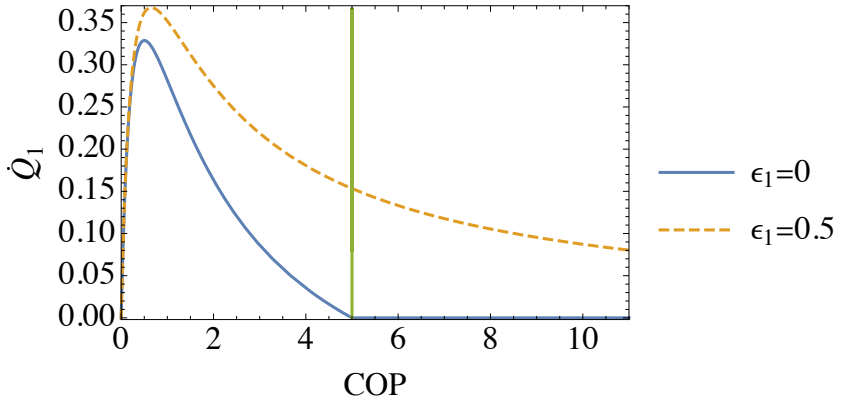

Figure 5.3: Cooling power $\dot{Q}_1$ against the COP for the device operating as a refrigerator. We compare the cases with no coherence (solid, $\epsilon_1 = 0$) and with coherence (dashed, $\epsilon_1 = 0.3$). Parameters as in Fig. 5.2 with $0 < B_1 < 1$.

when operating as an engine and

$$COP = \frac{B_1}{B_2 - B_1}, \tag{5.36}$$

when operating as a refrigerator.

In absence of coherence and for thermal baths, these quantities are less or equal than the corresponding Carnot values:

$$\eta_C = 1 - \frac{T_1}{T_2} \tag{5.37}$$

$$COP_C = \frac{T_1}{T_2 - T_1}, \tag{5.38}$$

with equality obtained only when rates drop to zero. This is because, in absence of coherence ($\epsilon_1 = 0$), the condition $COP < COP_C$ is equivalent to the condition $n_1 < n_2$ that corresponds to the functioning of the device as an engine. However, in the presence of coherence in Fig. 5.2, we see that the refrigerator regime survives in a classically “forbidden" area for which $n_1 > n_2$. In this area, labelled 1’ in the diagram, the coefficient of performance COP is indeed larger than the Carnot value COP_C as evidenced in Fig. 5.3.

In Fig. 5.3 we plot the cooling power $\dot{Q}_1$ against the COP. We find that in the region 1’ where $COP > COP_C$, the cooling power is nonzero, in contrast to the Carnot point where power is strictly null. Moreover, Fig. 5.3 shows that the COP at maximum cooling power is larger in the presence of coherence.

Regarding the efficiency of the system as an engine, applying the same considerations as before, we find that the condition $\eta > \eta_C$ would correspond to $n_2 < n_1$. In the diagram Fig. 5.2(a), we observe, however, that the

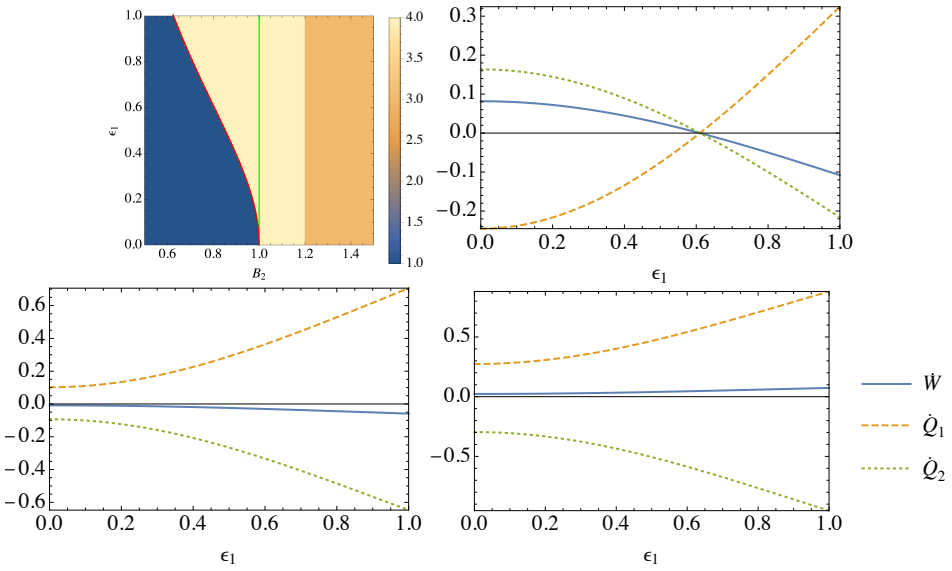

Figure 5.4: Coherence in the hot bath: (a) Phase diagram for the different functionings of the thermal machine. Color coding is as in Fig. 5.2. The vertical solid line indicates the condition $n_1 = n_2$. Heat currents and work power for (b) $B_2 = 0.8$, (c) $B_2 = 1.1$, (d) $B_2 = 1.3$. Other parameters: $B = 1, B_1 = 1.2, T_1 = 3, T_2 = 2.5, \gamma = 1$.

system never operates as an engine for $n_2 < n_1$, even in the presence of coherence.

Summarising, when coherence is present in the cold bath, there is a region of parameters for which the system operating as a refrigerator has a larger COP than the Carnot value. However, if the system operates as an engine, its efficiency is always smaller than the Carnot efficiency. As we will see in the next subsection, this situation will be reversed when the coherence is in the hot bath.

5.1.4 Coherence in The Hot Bath

We now consider the case where the coherence is in the hot bath. We thus assume $T_1 > T_2$. The conditions for the different operating regimes can be found by looking again at the signs of Eqs. 5.28-5.30 as we did in the previous section. Equations 5.33-5.34 are still valid and give us the conditions at which the work is zero. Using these equations we find the functioning diagram shown in Fig. 5.4. In contrast to the case where the coherence was in the cold bath, we see that the device never operates as a hybrid refrigerator. Moreover, a coherence $\epsilon_1 > \epsilon_1^*$ allows the system to operate as an engine even when $B_2 < B_1$, where in absence of coherence a refrigerator would be expected. In this classically forbidden zone, the efficiency of the corresponding engine is larger than the Carnot value as shown in Fig. 5.5.

In Fig. 5.5, we show the power output $\dot{W}$ against the efficiency when the system behaves as an engine. In

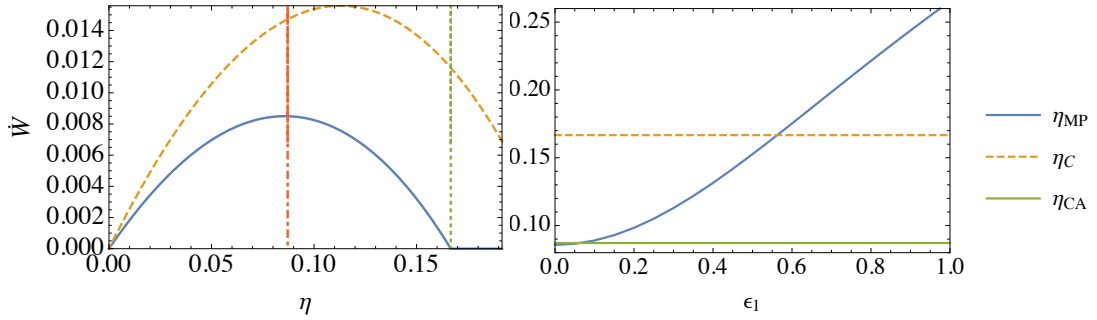

Figure 5.5: Top: Power versus efficiency when the system in operating as an engine with the magnetic field $0.98 < B_2 < 1.2$. The solid (dashed) line is the case with $\epsilon_1 = 0$ ($\epsilon_1 = 0.1$). The vertical dotted line corresponds to the Carnot value η_C (see Eq.) and the dot-dashed line corresponds to the Curzon-Ahlborn value η_{CA} (see Eq.). Bottom: Efficiency at maximum power as a function of the coherence in the hot bath. The two horizontal lines correspond to η_{CA} (solid) and η_C (dashed). Other parameters as in Fig. 5.4.

absence of coherence, $\epsilon_1 = 0$, the maximum achievable efficiency is the Carnot value η_C (Eq. 5.37) where however the power is zero. The value of the efficiency at maximum power is obtained at the Curzon-Ahlborn value

$$\eta_{CA} = 1 - \sqrt{\frac{T_1}{T_2}}. \tag{5.39}$$

On the other hand, in the presence of coherence $\epsilon_1 \neq 0$, the efficiency is much larger and surpasses both the Carnot value (at non zero power) and the Curzon-Ahlborn value. The bottom panel of Fig. 5.5, shows that the efficiency at maximum power η_{MP} grows quadratically for very small ϵ_1 and linearly for larger values.

5.2 Optimal Performance of a Two-Qubits Autonomous Machine Powered by Energetic Coherence

5.2.1 Autonomous Coherent Machine Model

The setup we employ along this study follows the configuration introduced in Ref. [178] and is sketched in Figs. 5.6 and 5.7. We consider a quantum thermal machine that consist of two qubits with energy spacing, E_c and E_h respectively, and Hamiltonian $H_\mathrm{m} = E_\mathrm{c} \left|1\right\rangle \left\langle 1\right|_\mathrm{c} \otimes 1_\mathrm{h} + E_\mathrm{h}\ 1_\mathrm{c} \otimes \left|1\right\rangle \left\langle 1\right|_\mathrm{h}$, where we assume for concreteness $E_\mathrm{h} \geq E_\mathrm{c}$. The two machine qubits are weakly coupled to thermal reservoirs (or baths) with different inverse temperatures ($\beta_\mathrm{c} \geq \beta_\mathrm{h}$) acting only locally on each qubit. We refer to the machine qubits and baths as the "cold" and "hot" qubits or baths, respectively.

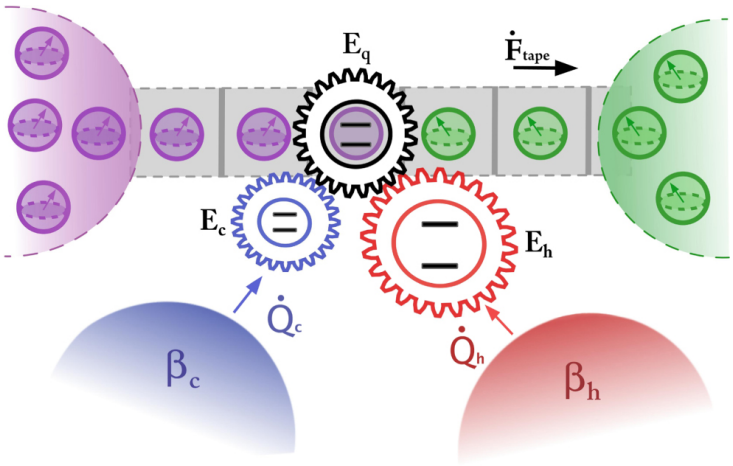

Figure 5.6: Coherent thermal machine model. An ensemble of qubits prepared in an arbitrary state ρ_{q} (left purple area) is put on a tape moving from left to right to interact, once at a time, with the two machine qubits (center gears), after which they are collected (green right area). The setup allows either free energy extraction on the output qubits in the tape, powered by a heat current from hot to cold local baths (bottom red and blue areas), or refrigeration of the cold bath by consuming free energy of the incoming tape qubits.

In addition, the machine sequentially interacts with a stream of qubits in a tape with fixed energy spacing

$$E_{\mathrm{q}} = E_{\mathrm{h}} - E_{\mathrm{c}}, \tag{5.40}$$

and Hamiltonian $H_{\mathrm{q}} = E_{\mathrm{q}} \left|1\right\rangle \left\langle 1\right|_{\mathrm{q}}$, where the subscript q stands for "qubits". All the qubits in the tape are assumed to start in the same generic initial state ρ_{q}, and interact with the machine, one by one, trough a sequence of energy-preserving unitary maps of the form $U = e^{-iH_{\mathrm{int}}\tau}$ (in interaction picture), where H_{int} is the following three-body Hamiltonian

$$H_{\mathrm{int}} = g\,(\sigma_{\mathrm{c}}^{+}\sigma_{\mathrm{h}}^{-}\sigma_{\mathrm{q}}^{+} + \sigma_{\mathrm{c}}^{-}\sigma_{\mathrm{h}}^{+}\sigma_{\mathrm{q}}^{-}), \tag{5.41}$$

where $\sigma_i^{-} \equiv \left|0\right\rangle \left\langle 1\right|_i$ denote the lowering operator of qubit $i = \mathrm{c}, \mathrm{h}, \mathrm{q}$ and $\sigma_i^{+} = (\sigma_i^{-})^{\dagger}$. We remark that strict energy conservation is enforced by the resonance condition 5.40, which implies $[H_{\mathrm{int}}, H_{\mathrm{m}} + H_{\mathrm{q}}] = 0$ and hence $[U, H_{\mathrm{m}} + H_{\mathrm{q}}] = 0$. Here it is also useful to define $\phi = g\tau$ as the effective strength of the collision, where τ denotes the interaction time. We are interested in the regime $\phi \ll 1$, corresponding to weak and fast collisions.

In the absence of the qubit tape, the two qubits of the machine do not interact between them at all. In that case the contact with local thermal baths would produce the independent thermalization of each machine qubit to the cold and hot temperatures, β_{c} and β_{h}, respectively. Even if in a product of thermal states, it is nonetheless interesting to look at the machine as composed of four levels (see Fig 5.7). Indeed the independent thermalization, would result in an effective population of the two inner levels $\{\left|10\right\rangle_{\mathrm{m}}, \left|01\right\rangle_{\mathrm{m}}\}$ [183] (also called *virtual qubit*),

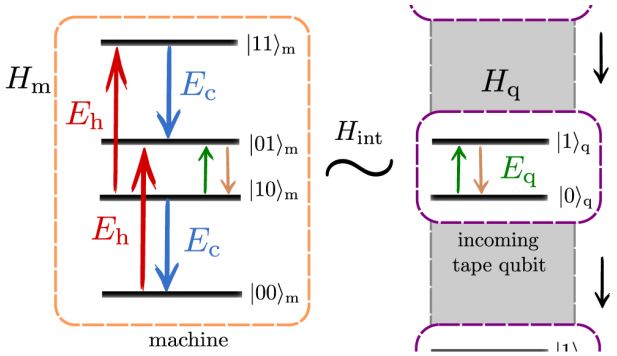

Figure 5.7: Representation of the machine as a 4-level system interacting with an incoming qubit of the tape. The interaction $H_{\rm int}$ with the resonance condition in Eq.5.40, allows the coherent exchange of excitations between the two inner machine levels and the tape qubit (green and orange arrows). The local reservoirs induce incoherent transitions on the machine levels with energy spacing $E_{\rm c}$ and $E_{\rm h}$ as represented, respectively, by the blue and red arrows.

which we denote as $p_{10}^{\rm eq}$ and $p_{01}^{\rm eq}$, showing a virtual inverse temperature $\beta_{\rm v}$ 4.42 defined by the Gibbs ratio $\beta_{\rm v}E_{\rm q} \equiv \ln(p_{10}^{\rm eq}/p_{01}^{\rm eq})$ [161]. It reads

$$\beta_{\rm v} = \frac{\beta_{\rm h}E_{\rm h} - \beta_{\rm c}E_{\rm c}}{E_{\rm h} - E_{\rm c}}. \tag{5.42}$$

Depending on the values of $E_{\rm c}$ and $E_{\rm h}$, the virtual temperature can be tuned to take different values, making the machine suitable for the performance of thermodynamic tasks, such as power generation or refrigeration, by connecting a external system to the inner transition $|10\rangle_{\rm m} \leftrightarrow |01\rangle_{\rm m}$ [184, 185]. In particular, for the choice $E_{\rm h} \geq E_{\rm c}$ and $\beta_{\rm c} \geq \beta_{\rm h}$, we always have $\beta_{\rm v} \leq \beta_{\rm c}$, and obtain population inversion, $\beta_{\rm v} \leq 0$, if and only if $E_{\rm h}/E_{\rm c} \leq \beta_{\rm c}/\beta_{\rm h}$. As we will see in the following sections, the virtual temperature $\beta_{\rm v}$ plays an important role in the characterization of the operational regimes of the autonomous thermal machine considered here.

When introducing the interactions with the tape, the two qubits of the machine are allowed to exchange heat between them and with the qubits in the tape, evolving through a nonequilibrium stationary state. We assume that collisions occur at random times following Poissonian statistics with rate r. A monotonic evolution towards stationarity is enforced by the Markovian character of the collisional model employed here, where every collision uses a "fresh" qubit in the tape in the same state

$$\rho_{\rm q} = \begin{pmatrix} p_0 & c \\ c^* & p_1 \end{pmatrix}, \tag{5.43}$$

with $p_0 + p_1 = 1$ and $|c| \leq \sqrt{p_0 p_1}$ ensuring a positive semi-definite density operator.

From the collisional model introduced here, we build a master equation in the GKLS form describing the open evolution of the machine density operator, $\rho_{\rm m}$, subjected to both the effects of the two thermal reservoirs and the

qubit's tape (see Appendix B). In the interaction picture, it reads

$$\dot{\rho}_{\rm m} = -i\,[V,\rho_{\rm m}] + \gamma^{\rm q}_{\downarrow}\mathcal{D}[\sigma^{+}_{\rm c}\sigma^{-}_{\rm h}]\rho_{\rm m} + \gamma^{\rm q}_{\uparrow}\mathcal{D}[\sigma^{-}_{\rm c}\sigma^{+}_{\rm h}]\rho_{\rm m} + \mathcal{L}_{\rm c}(\rho_{\rm m}) + \mathcal{L}_{\rm h}(\rho_{\rm m}) \equiv \mathcal{L}_{\rm tot}(\rho_{\rm m}), \tag{5.44}$$

where the first line describes the effects of the collisions with the tape, and the second line the interaction with cold and hot reservoirs, with

$$\mathcal{L}_i(\rho_{\rm m}) = \gamma^i_{\downarrow}\mathcal{D}[\sigma^{-}_i]\rho_{\rm m} + \gamma^i_{\uparrow}\mathcal{D}[\sigma^{+}_i]\rho_{\rm m}, \tag{5.45}$$

the local thermal Lindbladian acting on qubit $i = {\rm c},{\rm h}$ of the machine, and $\mathcal{D}[L]\cdot \equiv L\cdot L^{\dagger} - \frac{1}{2}\{L^{\dagger}L,\cdot\}$ denoting the usual Lindblad dissipators [97, 186] with rates fulfilling local detailed balance $\gamma^i_{\downarrow} = \gamma^i_{\uparrow}e^{\beta_i E_i}$.

As can be appreciated in the first line of Eq.5.44, the collisions with the tape qubits generate both coherent (driving-like) contributions, as given by the operator $V = r\phi(\sigma^{+}_{\rm c}\sigma^{-}_{\rm h}c^{*} + \sigma^{-}_{\rm c}\sigma^{+}_{\rm h}c)$, and dissipative terms analogous to the ones induced by the baths in Eq.5.45, with rates $\gamma^{\rm q}_{\uparrow} = r\phi^2 p_1$ and $\gamma^{\rm q}_{\downarrow} = r\phi^2 p_0$. These two contributions correspond, respectively, to coherent and incoherent transitions between the inner levels $|10\rangle_{\rm m} \leftrightarrow |01\rangle_{\rm m}$ of the machine (see Fig. 5.7), and depend explicitly on the initial state of the qubits in the tape, $\rho_{\rm q}$. As also noticed in Refs. [178, 182], the coherent contribution appears only when the tape qubits are initialized with non-zero coherence in the energy basis, $|c| \neq 0$ in Eq.5.43.

On the other hand, the local transitions induced by the baths on the machine qubits, can be written for the case of bosonic reservoirs as $\gamma^i_{\downarrow} = \Gamma^i_0(N^i_{\rm th}+1)$ and $\gamma^i_{\uparrow} = \Gamma^i_0 N^i_{\rm th}$, with Γ^i_0 the spontaneous emission rate and $N^i_{\rm th} = (e^{\beta_i E_i}-1)^{-1}$ the average number of excitations in the bath at temperature β_i with energy E_i [97, 186]. For the ease of simplicity, we assume in the following equal spontaneous emission rates, $\Gamma_0 \equiv \Gamma^{\rm c}_0 = \Gamma^{\rm h}_0$.

The relative weights of local thermal dissipation and collisional dynamics are then determined by the interplay of the parameters r, ϕ and Γ_0. More precisely, for $r\phi^2 \gg \Gamma_0$ the collisional tape qubits becomes the dominant contribution ot the dynamics, spoiling thermal effects induced by the baths. On the other hand, the regime $r\phi^2 \ll \Gamma_0$, corresponds to a weak impact of the tape qubits on the machine, where the incoherent terms in the first line of Eq.5.44 become negligible (but not necessarily first coherent term proportional to $r\phi$). In the following sections we consider both cases where $r\phi^2 \sim \Gamma_0$ and $r\phi^2 \ll \Gamma_0$ with still $\Gamma_0 < r\phi$.

The validity of the master equation 5.44 is warranted in the case of weak coupling to the local reservoirs, $\Gamma_0 \ll E_i$, as well as weak collisions $\phi \ll 1$ occurring on a fast time-scale with respect to the relaxation time-scales induced by the baths, $\Gamma_0 \ll 1/\tau$. It is indeed this later assumption that allows us to safely split the machine dynamics into pieces coming from the collisions with the tape in one side, and from the local thermal reservoirs in

the other side (see App. B).

5.2.2 Steady-State Dynamics and Thermodynamics

We focus on the operation of the machine in the stationary regime, namely, after which a sufficient number of collisions with the tape have already taken place. The steady state of the machine in the long time run, $\pi_{\rm m} = \lim_{t\to\infty}\rho_m$, can be obtained from Eq.5.44 by imposing $\mathcal{L}(\pi_{\rm m}) = 0$ (see Appendix C) and is of the form

$$\pi_{\rm m} = \begin{pmatrix} \pi_{00} & 0 & 0 & 0 \\ 0 & \pi_{10} & \pi_c & 0 \\ 0 & \pi_c^* & \pi_{01} & 0 \\ 0 & 0 & 0 & \pi_{11} \end{pmatrix}. \tag{5.46}$$

Crucially, the initial coherence in the tape qubits is partially transferred to the machine in the steady state, that acquires coherence in the non-degenerate subspace $\{|10\rangle_{\rm m}, |01\rangle_{\rm m}\}$ of $H_{\rm m}$. This is contrast to other models that acquire steady-state coherence only in a degenerate, or nearly-degenerate subspace [160, 187].

Under steady-state conditions, the effect of the coherent machine on every incoming qubit of the tape is equivalent and can be described through the following completely positive and trace preserving (CPTP) map $\rho_{\rm q} \to \mathcal{E}(\rho_{\rm q})$, with

$$\begin{aligned}\mathcal{E}(\rho_{\rm q}) = \rho_{\rm q} - i\phi[\sigma_{\rm q}^-\pi_c^* + \sigma_{\rm q}^+\pi_c, \rho_{\rm q}] \\ + \phi^2\pi_{01}\mathcal{D}[\sigma_{\rm q}^-]\rho_{\rm q} + \phi^2\pi_{10}\mathcal{D}[\sigma_{\rm q}^+]\rho_{\rm q},\end{aligned} \tag{5.47}$$

where again coherent and incoherent contributions can be identified, in analogy to Eq. 5.44. Notice that here, contrary to other models of collisional reservoirs [182, 188], we distinguish between the initial and final states of the qubits in the tape, which are collected after interaction with the machine (see Fig. 5.6).

The map $\mathcal{E}$ in Eq. 5.47 depends on the machine steady-state density operator elements π_{10}, π_{01} and π_c, which are linked, at the same time, to the initial state $\rho_{\rm q}$ through the coefficients in Eq. 5.44. Although this intricate dependence, we observe that this map turns out to be contractive, and shows a single fixed point, $\mathcal{E}(\tau_{\rm v}) = \tau_{\rm v}$, with thermal Gibbs form at the virtual temperature

$$\tau_{\rm v} = \frac{e^{-\beta_{\rm v}H_{\rm q}}}{Z_{\rm q}}, \tag{5.48}$$

where $Z_{\rm q} = {\rm tr}[e^{-\beta_{\rm v} H_{\rm q}}]$, and $\beta_{\rm v}$ is the virtual temperature in Eq. 5.42. Whenever the qubits in the tape are prepared in the state 5.48 the machine is unable to perform any change on it. Later on we will see that this state indeed corresponds to an equilibrium point.

With the help of Eq. 5.47, the master equation 5.44, and the expressions for the steady-state density operator in Eq. 5.46, we can directly compute the steady-state energy and heat currents into the qubit's tape and from the baths to obtain

$$\begin{aligned}
\dot{E}_{\rm tape} &= r\,{\rm tr}[H_{\rm q}\big(\mathcal{E}(\rho_{\rm q}) - \rho_{\rm q}\big)] = E_{\rm q}(\Delta + \zeta),\\
\dot{Q}_{\rm c} &= {\rm tr}[H_{\rm m}\mathcal{L}_1(\pi)] = -E_{\rm c}(\Delta + \zeta),\\
\dot{Q}_{\rm h} &= {\rm tr}[H_{\rm m}\mathcal{L}_2(\pi)] = E_{\rm h}(\Delta + \zeta),
\end{aligned} \tag{5.49}$$

[Δ and ζ are given below in Eq. 5.51] which verify $\dot{E}_{\rm tape} = \dot{Q}_{\rm c} + \dot{Q}_{\rm h}$ owing to Eq. 5.40, that is, any increase of energy in the tape qubits is due to input heat from hot and cold baths. Moreover, the currents verify the relation

$$\frac{\dot{E}_{\rm tape}}{E_{\rm q}} = -\frac{\dot{Q}_{\rm c}}{E_{\rm c}} = \frac{\dot{Q}_{\rm h}}{E_{\rm h}}, \tag{5.50}$$

implying that the proportionality of the steady-state currents flowing through the machine only depends on the energy spacings $E_{\rm q}$, $E_{\rm c}$, and $E_{\rm h}$.

In the above expressions Eq.5.49 we conveniently introduced the two following key quantities

$$\Delta \equiv r\phi^2\big(\pi_{01}p_0 - \pi_{10}p_1\big),\;\; \zeta \equiv ir\phi\big(\pi_c^* c - \pi_c c^*\big), \tag{5.51}$$

which capture the incoherent (Δ) and coherent components (ζ) of the energy currents. The quantity $\zeta \geq 0$ is real and positive, and becomes zero whenever the initial state of the qubits in the tape is diagonal in the energy basis, $c = 0$ in Eq. 5.43. Instead Δ can be either positive or negative, and both quantities vanish $\Delta = \zeta = 0$ when $\rho_{\rm q} = \tau_{\rm v}$, implying zero currents in Eq. 5.49.

The change in the entropy of the tape due to the interaction with the machine in the steady state can be calculated from Eq. 5.47 using perturbation theory (see Appendix C for details) and is given by

$$\begin{aligned}
\dot{S}_{\rm tape} &= -r\big({\rm tr}[\mathcal{E}(\rho_{\rm q})\ln\mathcal{E}(\rho_{\rm q})] - {\rm tr}[\rho_{\rm q}\ln\rho_{\rm q}]\big)\\
&= (\lambda_+ - \lambda_-)\ln\left(\frac{\lambda_-}{\lambda_+}\right)\Big(r\phi^2|\pi_c|^2 + \frac{\Delta(p_1 - p_0) - N|c|^2}{(p_1 - p_0)^2 + 4|c|^2}\Big),
\end{aligned} \tag{5.52}$$

where $N \equiv r\phi^2(\pi_{01}+\pi_{10})$ and we denoted the eigenvalues of $\rho_{\rm q}$ by $\lambda_\pm \equiv (1 \pm \sqrt{(p_1-p_0)^2+4|c|^2})/2$. Using the energy and entropy currents, we can now define the nonequilibrium free energy current of the qubits in the tape with respect to temperature $T_{\rm c}$,

$$\dot{F}_{\rm tape} \equiv \dot{E}_{\rm tape} - k_B T_{\rm c} \dot{S}_{\rm tape}. \tag{5.53}$$

The nonequilibrium free energy characterizes the maximum extractable work from nonequilibrium states by using local unitary operations and contact with a thermal bath (see e.g. Refs. [130, 189, 190]) at $T_{\rm c}$, we employ the cold temperature T_c since it maximizes the extractable work. Here it plays a prominent role for quantifying the tape qubits as a resource. Importantly, the free energy in Eq. 5.53 takes into account both thermal populations and coherence in the qubits, and can be split into two components by using the relative entropy of coherence [76, 172, 182] (see App. C for details). In Ref. [178], it has been shown that this model is able to amplify the relative entropy of coherence of the incoming qubits for an adequate choice of the parameters. Here we instead focus on the ability of this machine to perform thermodynamic tasks that may be enhanced or assisted by coherence.

From Eqs. 5.49 and 5.52, we are now in a position to state the second law of thermodynamics in steady-state conditions as the positivity of the total entropy production rate [191, 192]

$$\dot{S}_{\rm tot} = \dot{S}_{\rm tape} - \beta_{\rm c}\dot{Q}_{\rm c} - \beta_{\rm h}\dot{Q}_{\rm h} \geq 0, \tag{5.54}$$

where $\beta_i \dot{Q}_i$ are the entropy fluxes associated to the heat currents from/to reservoir i and $\dot{S}_{\rm tape}$ is entropy flux associated to exchange of energy between the machine and the qubits in the tape, $\dot{E}_{\rm tape}$. Reversibility conditions associated to a zero entropy production rate in Eq. 5.54 are verified when the tape qubits are initialized in the thermal state at the virtual temperature Eq. 5.48.

Making use of energy conservation to eliminate one of the two heat currents in Eq. 5.54, and identifying the nonequilibrium free energy in Eq. 5.53, we can rewrite Eq. 5.54 in the two following equivalent forms

$$\eta \equiv \frac{\dot{F}_{\rm tape}}{\dot{Q}_{\rm h}} \leq 1 - \frac{\beta_{\rm h}}{\beta_{\rm c}}, \tag{5.55}$$

$$\epsilon \equiv \frac{\dot{Q}_{\rm c}}{-\dot{F}_{\rm tape}} \leq \frac{\beta_{\rm c}}{\beta_{\rm c}-\beta_{\rm h}}, \tag{5.56}$$

where η stands for the efficiency of a heat engine increasing the free energy of the tape qubits $\dot{F}_{\rm tape}$ using the heat current from the hot bath $\dot{Q}_{\rm h}$ as a resource, and ϵ is the so-called coefficient of performance (COP) of a refrigerator extracting heat from the cold reservoir $\dot{Q}_{\rm c}$ by consuming free-energy of the input qubits on the tape. Remarkably, the second-law inequality 5.54 bounds both quantities, respectively, by Carnot efficiency $\eta_C \equiv 1 - \beta_{\rm h}/\beta_{\rm c}$ [1] and

reversible COP, $\epsilon_C \equiv \beta_{\rm c}/(\beta_{\rm c}-\beta_{\rm h})$ [149]. The bounds are reached, similarly to other models of (incoherent) autonomous thermal machines, at the equilibrium point ($\rho_{\rm q} = \tau_{\rm v}$), where every energy and entropy currents become zero. Similar notions of nonequilibrium free-energy efficiencies have been also proposed in the context of squeezed thermal reservoirs [193], molecular machines [194], dissipative chemistry [195] and multiterminal mesoscopic conductors [196].

5.2.3 Regimes of Operation

Equations 5.55 and 5.56 suggest that the thermal machine introduced here may act either as a heat engine or as a power-driven refrigerator, where the the free energy current to (from) the qubit tape plays the role of the output (input) work. This idea can be made more precise by exploring the joint behavior of the heat currents from the thermal reservoirs $\dot{Q}_{\rm c}$ and $\dot{Q}_{\rm h}$ and the free energy changes of the qubits in the tape, $\dot{F}_{\rm tape}$. We use different parameters of the thermal machine and initial states of the tape qubits, $\rho_{\rm q}$. The following three regimes of operation are found:

I **Free-energy heat engine (HE):** The thermal machine performs a continuous increase in the free energy of the qubits of the tape, $\dot{F}_{\rm tape} \geq 0$, using the natural heat current from the hot bath, $\dot{Q}_{\rm h} \geq 0$, which is partially dumped into the cold bath, $\dot{Q}_{\rm c} \leq 0$.

II **Refrigerator (R):** A heat current from the cold bath is extracted $\dot{Q}_{\rm c} \geq 0$ by consuming free energy of the tape qubits, $\dot{F}_{\rm tape} < 0$, while heat in transferred into the hot bath $\dot{Q}_{\rm h} < 0$. This configuration can be also seen as a free-energy driven heat pump.

III **Dissipator (D):** An input free-energy current from the tape qubits $\dot{F}_{\rm tape} < 0$ is, together with a heat current from the hot bath, $\dot{Q}_{\rm h} > 0$ dumped into the cold bath, $\dot{Q}_{\rm c} < 0$. In this regime no particularly useful thermodynamic tasks is performed.

The simplicity of the model allows us to obtain analytically the boundaries among steady-state regimes of operation in the absence of initial coherence in the tape. In the incoherent case, taking $c = 0$ in Eq. 5.43 immediately yields $\zeta = 0$ in Eqs. 5.49. Moreover we obtain a purely classical free energy

$$\dot{F}_{\rm tot} = E_{\rm q}\Delta(1-\beta_{\rm q}/\beta_{\rm c}), \tag{5.57}$$

where $\beta_{\rm q} \equiv \log(p_0/p_1)/E_{\rm q}$ represents the temperature of the incoming qubits in the tape. As a consequence, the regimes of operation in this case are solely determined by the interplay between $\beta_{\rm q}$, the virtual temperature $\beta_{\rm v}$,

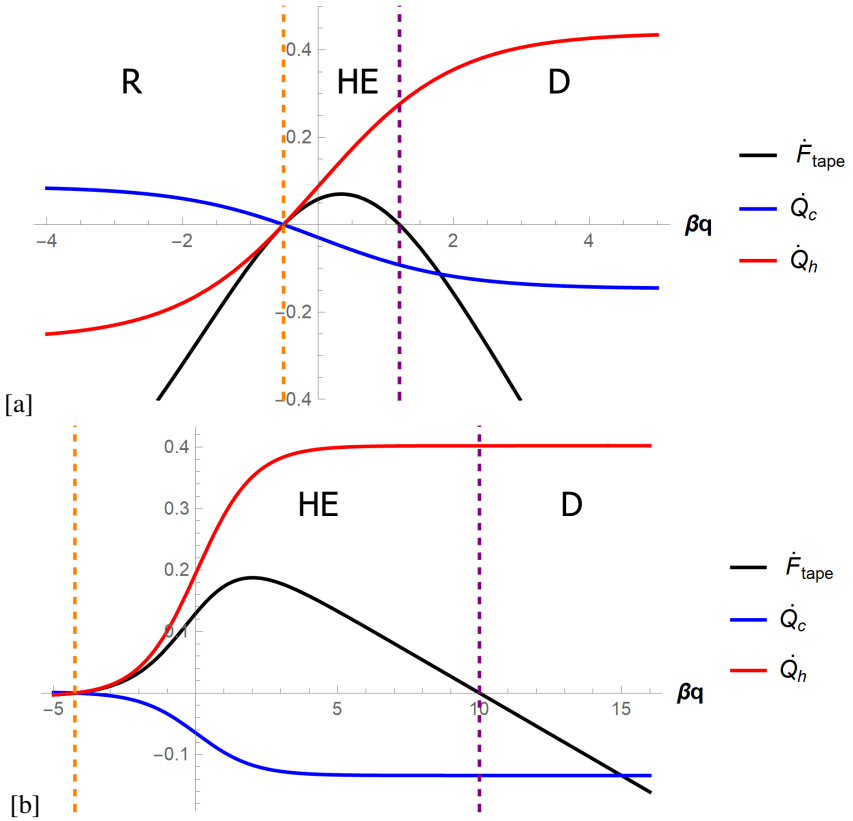

Figure 5.8: The thermodynamic quantities $\dot{F}_{tape}$,$\dot{Q}_c$ and $\dot{Q}_h$ as a function of the inverse temperature of the tape qubits β_q, for the case of a relatively large temperature gradient, $\beta_{\rm h} = 0.05\beta_{\rm c}$ when $c = 0$. For (a) moderate $\beta_c = 1.2/E_q$ and (b) extremely low $\beta_c = 10./E_q$ temperatures of the cold bath. The orange and purple dashed lines represent the inverse temperatures of the virtual qubit β_v and cold reservoir β_c respectively. Parameters: $E_{\rm c} = 0.5E_{\rm q}$, $E_{\rm h} = 1.5E_{\rm q}$, $r = 2/E_{\rm q}$, $\phi = 0.02$ and $\Gamma_0 = 0.0025/E_{\rm q}$.

and the temperature of the cold bath $\beta_{\rm c}$. We recall that here $\beta_{\rm v} \leq \beta_{\rm c}$ by construction. The refrigerator regime R is obtained when the qubits in the tape have initial temperatures higher than the virtual one (absorption refrigerator), or equivalently, when they show a higher population inversion (power-driven refrigerator), $\beta_{\rm q} \leq \beta_{\rm v} \leq \beta_{\rm c}$. This implies $\Delta \leq 0$ in Eq. 5.49, leading to $\dot{Q}_{\rm c} \geq 0$, $\dot{Q}_{\rm h} \leq 0$ and $\dot{E}_{\rm tape} \leq 0$. On the other hand, when the largest temperature (or largest negative temperature) is the virtual temperature, $\beta_{\rm v} \leq \beta_{\rm q} \leq \beta_{\rm c}$, the energetic currents change sign, $\Delta \geq 0$, and the machine is able to pump free energy into the tape, $\dot{F}_{\rm tape} \geq 0$, hence obtaining the heat engine regime HE. Finally, for temperatures of the tape qubits lower than the cold bath, $\beta_{\rm v} \leq \beta_{\rm c} \leq \beta_{\rm q}$, while we still have energy pumping into the tape (since $\Delta > 0$), the entropy flux associated to that energy current, $\dot{S}_{\rm tape}$ in Eq. 5.52 becomes so high that produces a loss of free energy in the tape, $\dot{F}_{\rm tape} \leq 0$, spoiling work extraction and leading to the (useless) dissipator regime D.

As an illustration, in fig. 5.8, we can see the different regimes of operation of the machine by plotting the free energy changes of the tape qubits $\dot{F}_{tape}$ and the heat currents $\dot{Q}_c$ and $\dot{Q}_h$ with respect to the inverse temperature

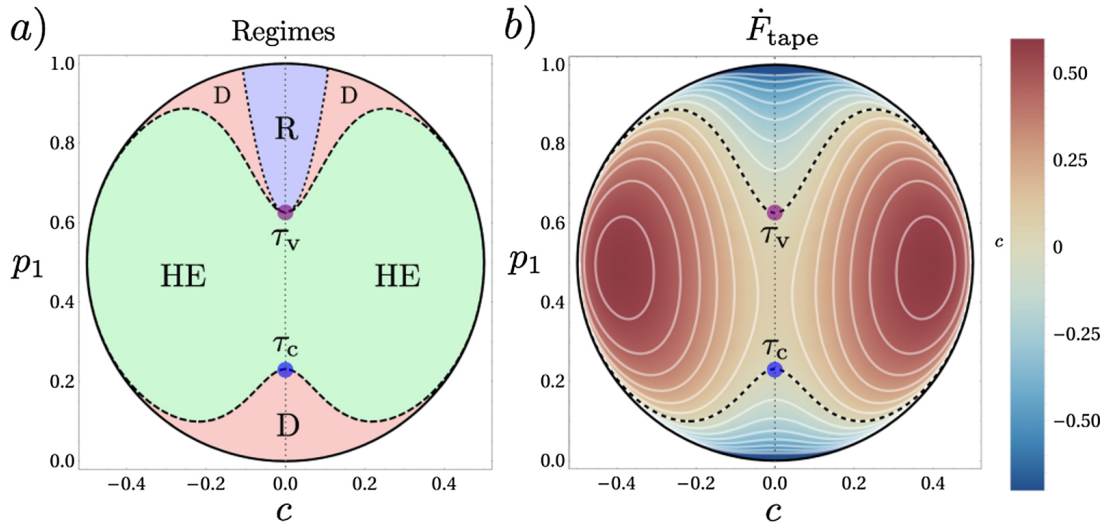

Figure 5.9: (a) Achievable regimes of operation as a function on the initial tape qubits excited population p_1 and off-diagonal element c, for the case of a relatively large temperature gradient, $\beta_{\rm h} = 0.05\beta_{\rm c}$. (b) Corresponding free energy changes in the tape qubits, in units of $r\phi^2 E_{\rm q}$. The dashed line represent $\dot{F}_{\rm tape} = 0$ and the purple and blue dots in both plots indicate the thermal states $\tau_{\rm v}$ and $\tau_{\rm c}$, respectively. Parameters: $E_{\rm c} = 0.5E_{\rm q}$, $E_{\rm h} = 1.5E_{\rm q}$, $\beta_{\rm c} = 1.2/E_{\rm q}$, $r = 2/E_{\rm q}$, $\phi = 0.02$ and $\Gamma_0 = 0.0025/E_{\rm q}$.

of the qubits in the tape β_q in the case of relatively large temperature gradient $\beta_h = 0.05\beta_c$. In Fig. 5.8(b), for extremely low temperatures of the cold bath $\beta_c = 10$ we can observe a more broad heat engine regime $\beta_{\rm v} \leq \beta_{\rm q} \leq \beta_{\rm c}$ than the case of moderate T_c 5.8(a).

A more complex situation arises when the input atoms have a non-zero initial coherence, $c \neq 0$ in Eq. 5.43. In that case an explicit analytical solution for the regimes boundaries is not available and we need to rely on numerical evaluation of the currents. In Figs. 5.9 and 5.10 we show, for different representative sets of parameters, the regimes of operation achieved by the machine as a function of the tape qubits initial state, $\rho_{\rm q}$. There we represent a cross section of the incoming qubit's Bloch sphere (in interaction picture) and, since the results only depend on $|c|$, we took c to be a real number without loss of generality.

The inclusion of coherence in the tape can greatly modify the regimes of operation with respect to the incoherent case (vertical dotted line at $c = 0$). The parameters in Fig. 5.9(a) corresponds to a relatively big temperature gradient in the baths, $\beta_{\rm h} = 0.05\beta_{\rm c}$, which favours a broad heat engine regime (green area) with respect to refrigeration (blue area) and the dissipator (red area). We also take a small value of the effective coupling of the tape qubits $\phi = 0.02$ ($r\phi^2 < \Gamma_0$). In Fig. 5.9(b) we show the corresponding free energy changes in the tape qubits, $\dot{F}_{\rm tape}$, in units of $E_{\rm q} r\phi^2$. Remarkably, we observe that the output free energy current can be enhanced up to 6 times with respect to its maximum incoherent value ($\dot{F}_{\rm tape} \simeq 0.1 E_{\rm q} r\phi^2$) for values of the initial coherence in the tape qubits $|c| \simeq 0.4$ and $p_1 \simeq 0.5$.

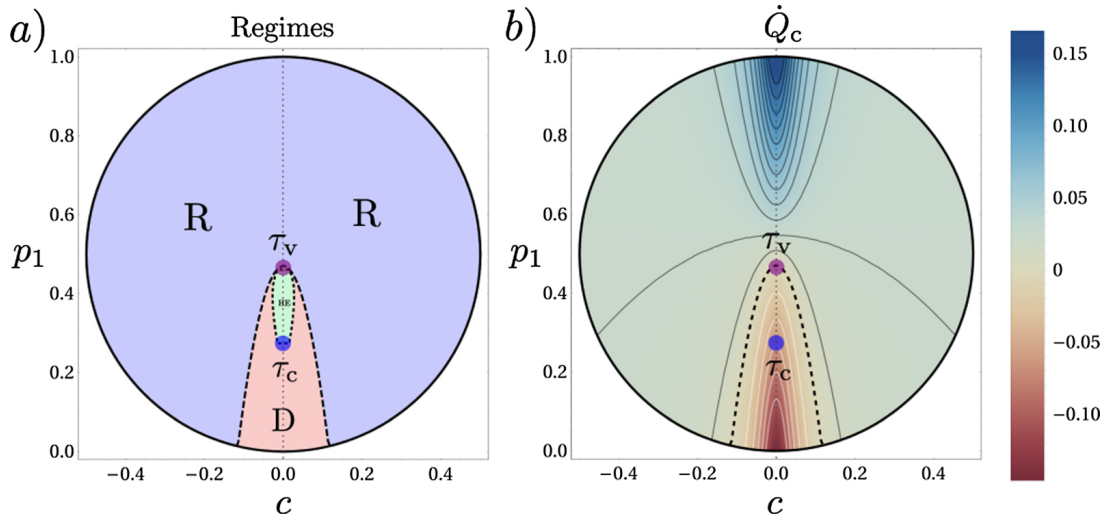

Figure 5.10: (a) Regimes of operation as a function of the initial tape qubits excited population p_1 and off-diagonal element c, for the case of a relatively small temperature gradient, $\beta_h = 0.5\beta_c$. (b) Cooling power associated to the regimes in (a) in units of $\Gamma_0 E_c$. The dashed line represent $\dot{Q}_c = 0$. Again purple and blue dots mark thermal states τ_v and τ_c, respectively. Parameters: $E_c = 0.8E_q$, $E_h = 1.5E_q$, $\beta_c = 1.2/E_q$, $r = 2/E_q$, $\phi = 0.04$ and $\Gamma_0 = 0.0025/E_q$.

On the other hand, Fig. 5.10(a) corresponds to a smaller temperature gradient between the baths, $\beta_h = 0.5\beta_c$ leading to a wider R regime (blue area), at expenses of the dissipator D (red area) and heat engine HE regimes (tiny green area). We also consider a higher effective coupling, $\phi = 0.04$, leading to a stronger impact of the tape qubits on the machine dynamics than the thermal reservoirs. Since the fuel used for cooling is provided by the free energy from the tape, a higher impact of the later ($r\phi^2 > \Gamma_0$) helps to improve the cooling power. The heat current from the cold reservoir $\dot{Q}_c$ (or cooling power) is plotted in Fig. 5.10(b) in units of $E_c\Gamma_0$. In this case we observe no enhancement in the cooling power by using initial coherence in the tape qubits. However, enhancements can be found for other sets of parameters (see e.g. Fig. 5.13). In any case, we observe a large region of parameters (south hemisphere of the Bloch sphere) where refrigeration becomes possible owing to the input coherence. In this region we therefore find a coherence-powered refrigerator. In all plots the blue and purple dots represent respectively the thermal states of the qubits with respect to β_c, that is, $\tau_c \equiv e^{-\beta_c H_q}/Z_c$, and β_v, that is, τ_v in Eq. 5.48.

We notice that since the coherent component of the currents in Eq. 5.49 is non-negative, $\zeta \geq 0$, an enhancement in the heat and energy currents with respect to the incoherent case may be expected. However, we remark that Figs. 5.9 and 5.10 show not only the possibility of coherence-induced enhancements in some regimes, but also that, due to the non-monotonic behavior of the currents with c, some thermodynamic operations become enabled by means of coherence in otherwise impossible situations and, for other cases, coherence maybe detrimental.

An important observation at this point is that, by employing initial coherence in the tape qubits, the distance

of $\rho_{\rm q}$ from the equilibrium state $\tau_{\rm v}$ increases in general, forcing the machine to work in further from equilibrium conditions. In other words, increasing the heat and energy currents comes at the price of increasing dissipation, which may eventually spoil the efficiency in the enhanced regimes. It is hence of primary interest to take into account the level of irreversibility of the machine operation, and, ultimately, compare the enhancements in power with respect to the efficiency achieved in each regime. While we will explore in detail the trade-off between power and efficiency in the next section, here we concentrate on the impact of coherence in dissipation as measured by the entropy production rate in Eq. 5.54. In Fig. 5.11 we show, for a particular choice of parameters, $\dot{S}_{\rm tot}$ as a function of p_1 for different values of $|c|$. We find a moderate increase in dissipation when increasing $|c|$ in the region close to the equilibrium point, at $p_1 \simeq 0.65$. However, as $|c|$ gets close to its maximum value $c_{\max} \equiv \sqrt{p_0 p_1}$, the entropy production starts growing exponentially. This is more apparent when we get closer to the maximum and minimum values of p_1, corresponding to small values of $c_{\max}$.

Finally, it is also worth pointing out that here we used the free energy in Eq. 5.53 to provide a notion of useful work performed by the thermal machine, since it naturally follows from the formulation of the second law in Eqs. 5.54 and 5.55. However, this interpretation is not the only one possible. For example one may be interested in alternative notions of work, applicable when assuming extra restrictions in the setup, see e.g. Refs. [76, 126]. One interesting alternative is given by the so-called *ergotropy*, defined in 3.2.2 as the maximum extractable work from a quantum state by only using unitary operations performing a cyclical variation of Hamiltonian parameters [123]. The ergotropy is strictly upper-bounded by the free energy for any temperature [197], and, like the nonequilibrium free energy, can be split into coherent and thermal components [128]. In appendix D we show that similar results as those reported here are obtained when replacing the free energy changes in the tape qubits [Eq. 5.53] by the change in their ergotropy, as induced by the machine operation.

5.2.4 Optimizing The Performance

The results presented in the previous section raise the question of up to what extent coherence can be employed to improve the two more useful regimes in our configuration, namely, free energy generation in the qubits of the tape or cooling the cold reservoir. More precisely, given fixed thermal resources as determined by the temperatures of the baths $\beta_{\rm c}$ and $\beta_{\rm h}$, and fixing also the coupling-dependent parameters Γ_0, r and ϕ, we ask ourselves: What is the optimal design of the machine ($E_{\rm c}$ and $E_{\rm h}$) and the optimal initial states of the qubits in the tape ($\rho_{\rm q}$) maximizing the free energy production (cooling power)? Is it possible to reach such maximum power regime at a reasonable efficiency (coefficient of performance)? May energetic coherence lead to an absolute enhancement for fixed resources?

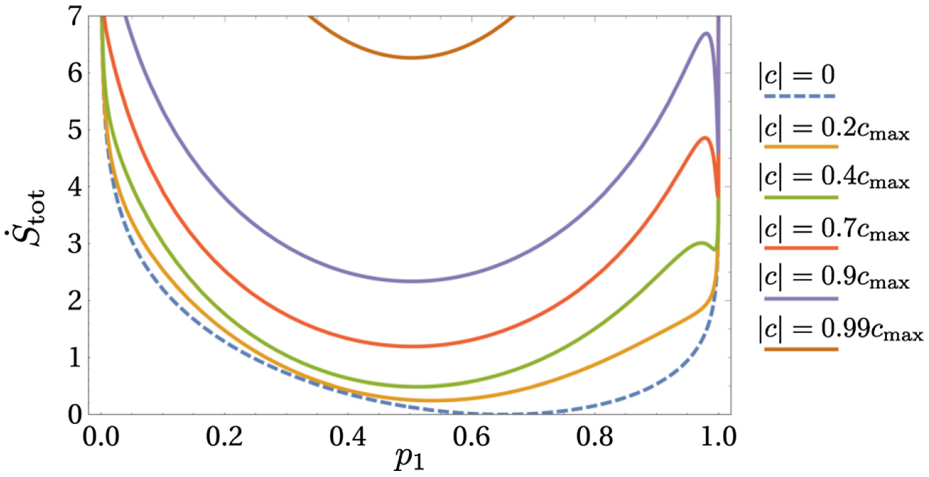

Figure 5.11: Entropy production rate as a function of the tape qubits population p_1 for different values of the off-diagonal element absolute vale $|c|$ (see legend). The dashed line corresponds to the incoherent case. Parameters: $E_{\rm c} = 0.6E_{\rm q}$, $E_{\rm h} = 1.6E_{\rm q}$, $\beta_{\rm c} = 1.2/E_{\rm q}$, $\beta_{\rm h} = 0.05\beta_{\rm c}$, $r = 2.5/E_{\rm q}$, $\phi = 0.08$ and $\Gamma_0 = 0.0025/E_{\rm q}$.

In order to address these questions we set the temperature scale of the setup by enforcing different values of the cold bath temperature $k_B T_{\rm c} = \{1.0\ E_{\rm q}, 0.5\ E_{\rm q}, 0.1\ E_{\rm q}\}$ and use as a free parameter in the optimization the largest energy spacing in the machine Hilbert space, $E_{\rm m} \equiv E_{\rm c} + E_{\rm h}$. We also fix the bath relaxation rates as $\Gamma_0 = 0.0025/E_{\rm q}$, and the parameters $r = 2/E_{\rm q}$ and $\phi = 0.02$, such that the action of the tape qubits in the machine is weak compared to the thermal reservoirs, $r\phi^2 \ll \Gamma_0$. This implies a weak back-reaction of the tape qubits on the machine, favoring the coherent exchange of energy between machine and tape. Hence we expect a higher impact of coherence in this regime of parameters.

Maximization of the free energy

We numerically maximize the free energy current in the tape qubits by varying the the largest energy gap in the machine, $E_{\rm m} \equiv E_{\rm c} + E_{\rm h}$ in the interval $[E_{\rm q}, 20E_{\rm q}]$, for fixed $E_{\rm q}$. We denote the optimal value of the free energy current by $\dot{F}^{\rm max}_{\rm tape}$. Since here we are interested in the performance of the machine as a heat engine, we consider a relatively big temperature gradient $\beta_{\rm c} = 0.05\beta_{\rm h}$, leading to a value for Carnot efficiency $\eta_C = 0.95$.

We show the results for the optimized free energy production $\dot{F}^{\rm max}_{\rm tot}$ as a function of the initial state of the tape qubits in Fig. 5.12(a)-(c). Since all results are symmetric with respect to the axis $c = 0$, we only show half of the Bloch sphere section. The three plots correspond to the three choices of $\beta_{\rm c}$ as stated above, i.e. moderate, low, and extremely-low temperatures, respectively. In all three cases, we obtain a clear maximum at values of p_1 around 0.5 and initial coherence $|c|$ between 0.3 and 0.37 (see red dots). This is an important feature, which indicates that the heat engine achieves maximum power when it is assisted by energetic coherence in the tape qubits. The free energy

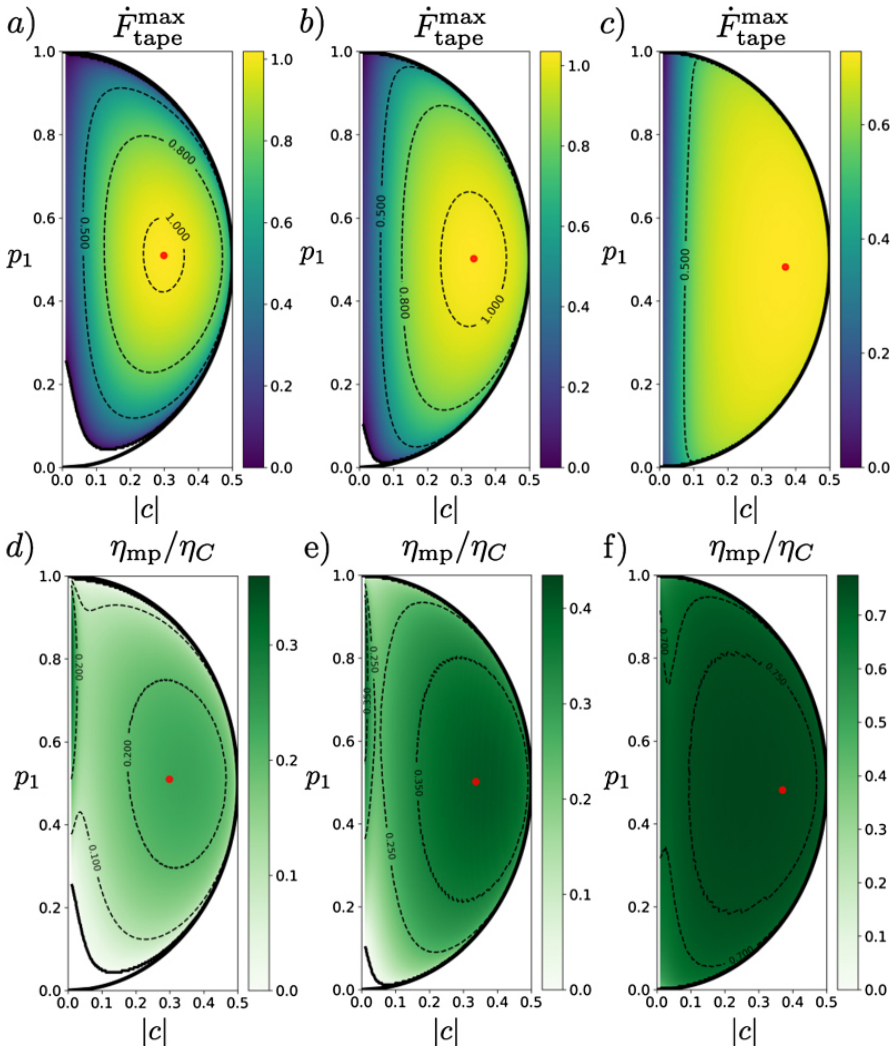

Figure 5.12: (a)-(c) Maximum free energy production $\dot{F}^{\max}_{\text{tape}}$ in $r\phi^2 E_{\text{q}}$ units for temperature scales $\beta_{\text{c}} E_{\text{q}} = \{1, 2, 10\}$ respectively and (d)-(f) efficiency at maximum power divided by Carnot efficiency, η_{mp}/η_C, for the same temperatures, as a function of the tape qubits initial state parameters p_1 and $|c|$. The red dots indicate the absolute maximum of $\dot{F}^{\max}_{\text{tape}}$. In the white region inside the semi-circumference the HE regime is not achievable within the range of values used for the optimization, $E_{\text{m}} \in [E_{\text{q}}, 20E_{\text{q}}]$. Parameters: $\beta_{\text{h}} = 0.05\beta_{\text{c}}$, $r = 2/E_{\text{q}}$, $\phi = 0.02$ and $\Gamma_0 = 0.0025/E_{\text{q}}$.

generation $\dot{F}_{\rm tape}^{\rm max}$ is enhanced with respect to its maximum value without coherence ($|c| = 0$) about 4.76 times in Fig. 5.12(a), 6.1 times in Fig. 5.12(b) and 3.34 times in Fig. 5.12(c). The corresponding values of $E_{\rm m}$ optimizing free energy generation are, respectively, $7.3E_{\rm q}$, $3.9E_{\rm q}$, and $1.7E_{\rm q}$, and vary only very slightly wihin the yellowish areas in Fig. 5.12. We also notice that optimization over $E_{\rm m}$ allows broadening the set of initial states $\rho_{\rm q}$ for which the HE regime is obtained. More precisely, the regions close to the north and south poles of the Bloch sphere for which operations R and D are achieved [see Fig. 5.9] eventually become HE by allowing larger values of $E_{\rm m}$. The white areas close to the south pole in Figs. 5.12(a) and (b) correspond to parameters for which the HE regime can only be achieved by increasing $E_{\rm m}$ over the maximum value $20E_{\rm q}$ considered in the optimization procedure. On the other hand, for very low temperatures [Fig. 5.12(c)] the HE regime is achieved for values $E_{\rm m} < 2.7E_{\rm q}$ within the whole Bloch sphere.

In Figs. 5.12(d)-(f) we show the efficiency at maximum free energy power divided by Carnot's efficiency η_C for the three values of the cold bath temperature, $\beta_{\rm c}$. For moderate temperatures [Fig. 5.12(d)] we observe a general detrimental role of coherence. The efficiency peaks at $p_1 = 0.9$ and $|c| = 0$, for which $\eta \simeq 0.47\eta_C$ and quickly drops to values around $\eta = 0.2\eta_C$ in the region where maximum free energy power is obtained [see Fig. 5.12(a)]. The situation radically changes for smaller temperatures of the cold bath [Figs.5.12 (e) and (f)], where a second peak in the efficiency emerges at $p_1 \sim 0.5$ and $|c| \sim 0.3$ leading to efficiencies around $0.35\eta_C - 0.42\eta_C$ in the region of maximum free energy generation in Figs. 5.12(b) and (c). These efficiencies are comparable to the ones reached for the first peak ($\eta \simeq 0.44\eta_C$ at $p_1 \simeq 0.88$ and $|c| = 0$). This second peak broadens when further decreasing the temperature (increasing $\beta_{\rm c}$) [see Fig. 5.12(f)] reaching high values for the efficiency around $\eta \simeq 0.78\eta_C$ at maximum free energy output, to be compared to $\eta \simeq 0.75\eta_C$, the maximum available efficiency at maximum power without using coherence in the tape (reached for $p_1 \simeq 0.73$). This is a remarkable feature, showing that the use and control of coherence at low temperatures plays a crucial role in developing power, and can be used to enhance the performance (both power and efficiency at maximum power) of thermal machines.

Maximization of cooling power

As a second case of interest, we consider the maximization of the cooling power, $\dot{Q}_{\rm c}$, that is, the heat current extracted from the cold reservoir by the machine. As before, optimization is performed by varying the largest energy gap in the machine, $E_{\rm m} \in [E_{\rm q}, 20E_{\rm q}]$ for fixed $E_{\rm q}$, and the three temperatures scales $\beta_{\rm c}E_{\rm q} = \{1, 2, 10\}$. On the contrary, in this case we consider a relatively small temperature gradient $\beta_{\rm c} = 0.5\beta_{\rm h}$, favoring cooling regimes R with respect to HE ones [see e.g. Fig. 5.10]. The reversible (maximum) COP value associated to this temperature ratio is $\epsilon_C = 1$ in all three cases.

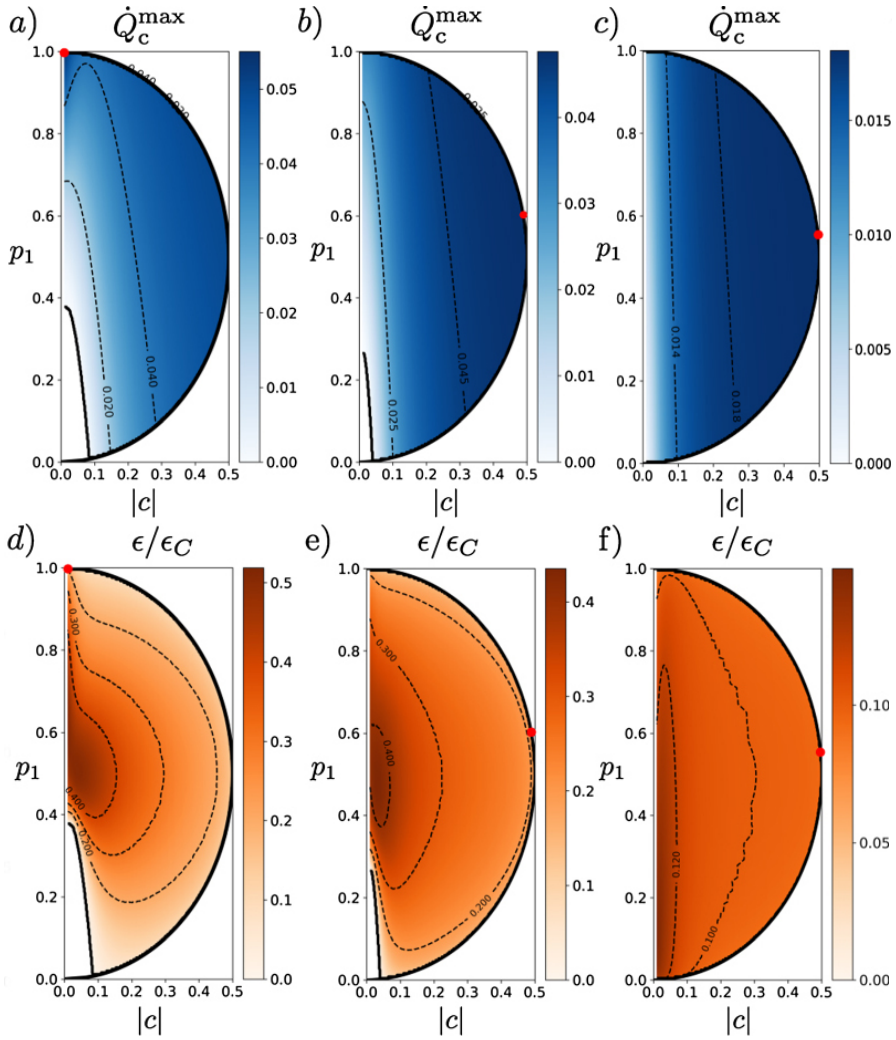

Figure 5.13: (a)-(c) Maximum cooling power $\dot{Q}_{\rm c}^{\rm max}$ in $\Gamma_0 E_{\rm q}$ units and (d)-(f) COP at maximum power divided by the reversible COP, η/η_C, for temperature scales $\beta_{\rm c}E_{\rm q} = \{1, 2, 10\}$, as a function of the tape qubits initial state parameters p_1 and $|c|$. The red dots indicate the absolute maximum of $\dot{Q}_{\rm c}^{\rm max}$. White areas inside the semi-circumference denote parameters regions for which the refrigerator regime R cannot be achieved. Parameters: $\beta_{\rm h} = 0.5\beta_{\rm c}$, $r = 2.5/E_{\rm q}$, $\phi = 0.08$ and $\Gamma_0 = 0.0025/E_{\rm q}$.

In Figs. 5.13(a)-(c) we show the maximum cooling power $\dot{Q}_{\rm c}^{\rm max}$ in units of $\Gamma_0 E_{\rm q}$ as a function of the initial state $\rho_{\rm q}$ for the three different values of $\beta_{\rm c}$. White areas in the bottom represent regions of parameters where cooling cannot be achieved, no matter the value of $E_{\rm m}$. The optimal values of $E_{\rm m}$ lie in between $E_{\rm q}$ and $4.5E_{\rm q}$ in any case, being smaller for lower temperatures of the cold bath. Similarly to the previous case, our results indicate that cooling can be optimized by allowing the initial states of the tape qubits to have non-zero coherence. This can be indeed appreciated in Figs. 5.13(b) and (c), where the maximum cooling power is achieved in the right part of the semi-cross sections of the tape qubits Bloch sphere. In particular the maximum of $\dot{Q}_{\rm c}^{\rm max}$ is achieved at points $(p_1 \simeq 0.6, |c| \simeq 0.49)$ for $\beta_{\rm c} = 2$ and at $(p_1 \simeq 0.55, |c| \simeq 0.50)$ for $\beta_{\rm c} = 10$, enhancing optimal incoherent cooling by 1.5 and 2.4 times, respectively. On the other hand, we confirm that allowing a non-zero coherence in the tape, allows reaching refrigeration in situations where it would be otherwise impossible, that is, for $p_1 \leq 0.38$ in Fig. 5.13(a), and for $p_1 \leq 0.26$ in Fig. 5.13(b).

Figs. 5.13(d)-(f) show the COP of the fridge ϵ at maximum cooling power, divided by the reversible (Carnot) value ϵ_C, corresponding to Figs. 5.13(a)-(c). In this case maximum values of the COP are obtained for $|c| = 0$ in all cases of moderate, low and very low temperatures. The overall maxima are located respectively at $p_1 \simeq 0.54$, $p_1 \simeq 0.51$ and $p_1 \simeq 0.27$, generating a high-COP area around them. As temperature decreases the values the COP become lower and more homogeneous over the whole Bloch sphere semi-cross section. Here we observe that the areas corresponding to maximum values of the cooling power $\dot{Q}_{\rm c}^{\rm max}$ and maximum COP do not overlap between them. This means that, contrary to the free energy generation case, coherence-enhanced cooling is not accompanied by an improved efficiency. Therefore, in this case the customary trade-off between power and efficiency extends to the initial state $\rho_{\rm q}$ optimization.

Chapter 6

Conclusion and Outlook

6.1 Summary

The focus of this dissertation is upon the study of the role of quantum coherence on the performance of quantum thermal machines operating in the weak-coupling regime and under steady-state conditions. The first part of the thesis sets preliminary concepts and basic quantum mechanics tools and notations needed to understand the rest of the thesis. We provide a characterization of quantum states, correlations and entropy which is a key ingredient in defining the second law of thermodynamics. Then we adopt a resource theoretic outlook to define quantum coherence and display ways to quantify it.

Since a dynamical approach is primordial to describe quantum thermal machines, we devote the second part of the thesis to the introduction of the theoretical foundations for open quantum systems [97]. The memoryless Markovian dynamics are obtained from tackling the dynamical semigroups and performing the Born-Markov and secular approximations. We distinguish between two forms of the Lindblad (GKLS) master equations, namely the local and global master equations. Before we introduce quantum thermodynamic as the essence of this thesis work, we end the first section of Chapt.3 with a basic example of the thermalization procedure of an open quantum system embedded in an environment at a temperature T. The rest of the chapter is an overview on quantum thermodynamics, we discuss mainly the laws that it is built upon in the classical and quantum regimes with a particular focus on the first and the second laws. The exchange of energy between a quantum system and a thermal bath can be divided into two contributions : heat and work. The latter can be quantified by the non-equilibrium free energy or the ergotropy that are used to address work extraction from quantum systems [130]. Although fluctuation rela-

tions are not the center of our thesis work, we introduce them as another intriguing subject of research to consider when dealing with the fluctuations of heat and work in coherent collisional models presented in the last chapter as a future perspective.

Quantum thermal machines are the core study of this dissertation. In Chapter 4, we discuss the quantum features of thermal machines working at the nanoscale. We outline the working principle of a very simple yet intuitive model of the earliest proposal of a quantum heat engine [187]. Thermal machines can operate in cycles with discrete strokes and through continuous coupling with the thermal baths, we give fundamental examples of the Otto and Carnot cycles that illustrate cyclic and reciprocating machines as well as a simple continuous refrigeration protocol where we apply a unitary transformation to perform cooling on a qubit system. Using external driving to achieve thermodynamic operations can be avoided by relying on autonomous settings. The last section deals with the definition of autonomous quatum thermal machines as machines that function exclusively via incoherent interactions with thermal baths at different temperatures and they cannot be described with time-dependent Hamiltonians. We present the three-qubit absorption refrigerator [160] as the prime illustration of the simplicity of the implementation of autonomous thermal machines. It can be analyzed in a different way by employing the concept of virtual qubits [161] which is a simplifying approach to predict the machine's behavior. It constitutes the primary element in the design of the autonomous model analyzed in the last chapter.

Finally, chapter 5 presents an extensive theoretical work where we derived the thermodynamic behavior of two collisional models undergoing steady-state conditions and explored the impact of quantum coherence on their performance. The first model, which is still under ongoing investigation, consists of a single qubit interacting sequentially with ancillas of two reservoirs at different temperatures. Coherence was shown to be a tuning parameter alongside the magnetic field of the baths for characterizing the different regimes defined as the accelerator, heat engine and refrigerator regimes. We found that injecting some amount of coherence into the cold bath allows the refrigerator to survive the classically forbidden regime, and its coefficient of performance (COP) was shown to surpass the Carnot limit for some regions of parameters, its value at maximum power is larger comparing to the incoherent regime. In addition, coherence can result in the appearance of a hybrid refrigerator that produces work. However, the machine never operates as a hybrid refrigerator when considering coherent contributions from the hot ancillas, in the case of the heat engine regime, the efficiency goes beyond the Carnot and the Curzon-Ahlborn value. In the second part, we have shown that, using energetic coherence, thermodynamic tasks can be enabled and/or enhanced by autonomous thermal machines. In particular we considered a setup where both thermal and coherent resources mix up in a beneficial way, namely, a virtual qubit machine that works through the interaction with a stream of qubits (represented in a tape) via a sequence of energy-preserving collisions [129]. We explored

both situations where the tape of qubits is operated by the machine to obtain a useful output (free energy), as well as cases in which the qubits in the tape are used as a fuel to power standard thermodynamic tasks, like refrigeration of a cold reservoir. The relative simplicity of the model allowed us to quantitatively assess the impact of the initial state of the qubits in the tape, ρ_q, and in particular its initial coherence c, in these two main situations. Our results indicate that coherence can notably enhance the power of the machine in some regimes of operation and that it can be used to enable the machine's operation in otherwise impossible situations. These enhancements are not obtained for every value of the initial coherence c in general, and coherence can be detrimental : enhanced cooling doesn't coincide with improved efficiency in the case of the cooling power. Selecting properly the initial value of coherence allows the optimization over the machine's design resulting in broader regions of parameters where coherence plays a beneficial role. We have shown that these improvements are the result of a nonequilibrium effect, with a non-zero associated entropy production. Our results go beyond weakly-coherent models [182], linear-response regime [245] or weak-dissipation engines [257], paving the way for understanding energetic-coherence-enhanced performance in autonomous thermal machines.

6.2 Outlook and Perspectives

In quantum thermodynamics, theory is ahead of experimental implementations, and there is a lack of genuine quantum thermal machines that live up to certain desiderata [258]. Since coherence is proven to play a decisive role in the optimization of the performance of the collisional thermal machines in this thesis, the promising results that it entails can be further explored in experimental one-atom maser configurations [259–261] or NMR settings [262] for instance. In fact, collisional models have seen in the last few years a rapid spread in open quantum systems dynamics and non-equilibrium thermodynamics. For example, they have proven to be successful approaches to efficiently simulate any Markovian dynamics [263]. They can be also used to analyze Non-Markovian effects and investigate quantum batteries. Although these repeated interaction schemes have advantages, they are still rather abstract. Extending to other autonomous configurations beyond the case of qubits considered here would point at probable directions towards practical and tractable realisations of quantum coherence-enhanced thermal machines. For example, it would be interesting to consider situations where the single qubit system or the tape qubits are replaced by other physical systems, like e.g. harmonic oscillators, also in view of possible implementations in trapped ion setups [156] or circuit QED architectures [264]. Another avenue for further exploration of this thesis research would be instead of considering average quantities of work and heat one can look at their fluctuations and their probability distributions. In fact, measuring work distribution in coherent systems would affect their

thermodynamic processes, to avoid such conundrum one can introduce the concept of predictor of work [265] which gives the optimal and best guess about work given information about stochastic heat currents. This procedure can be done by using Quantum Bayesian Networks [266,267] which preserve quantum coherences and correlations. This formalism can be extended to our models, we can build a work predictor as long as we have access to incoherent baths and there are correlations between the system and the ancillas. For instance, this might be done by replacing the thermal baths by other tapes where the input qubits states are always thermal in the case of our virtual qubit machine model.

References

[1] L. N. S. Carnot. "Réflexions sur la puissance motrice du feu et sur les machines propres à développer cette puissance", [Reflections on the Motive Power of Fire and on Machines Fitted to Develop that Power], Bachelier, Paris, France, (1824).

[2] M.K.E.L. Planck. "Zur theorie des gesetzes der energieverteilung im normalspectrum", Verhandl. Dtsc. Phys. Ges. 2, 237,(1900).

[3] A. Einstein. "Über einen die erzeugung und verwandlung des lichtes betreffenden heuristischen gesichtspunkt", Annalen der physik 322(6), 132–148, (1905).

[4] C. Cohen-Tannoudji, B. Diu, and F. Laloë, Quantum Mechanics, Vol. I. John Wiley and Sons, (1977).

[5] J. Baugh, O. Moussa, C. A. Ryan, A. Nayak and R. Laflamme. "Experimental implementation of heat-bath algorithmic cooling using solid-state nuclear magnetic resonance", Nature 438, 470-473, (2005).

[6] J. P. Pekola. "Towards quantum thermodynamics in electronic circuits", Nature Phys 11, 118, (2015).

[7] Quantum Mechanics, Vol. II. John Wiley and Sons, (1977).

[8] M. Bellac, A short introduction to quantum information and quantum computation. Cambridge University Press, (2006).

[9] P. A. M. Dirac. A new notation for quantum mechanics. Mathematical Proceedings of the Cambridge Philosophical Society, 35:416, (1939).

[10] W. Gerlach and O. Stern, Z. Physik. 8, 110 (1921); Z. Physik. 9, 349, 353 (1922).

[11] Schrodinger. E. Die gegenw ¨ artige situation in der quantenmechanik. ¨ Naturwissenschaften, 23, (1935).

[12] Monroe, C. and Meekhof, D. M. and King, B. E. and Wineland, D. J. A. Schrödinger Cat Superposition State of an Atom. American Association for the Advancement of Science. (1996).

[13] P.A.M. Dirac. The Principles of Quantum Mechanics (2nd ed.). Clarendon Press. p. 12 (1947).

[14] J. V. Neumann, Mathematische Grundlagen der Quantenmechanik./ Mathematical Foundations of Quantum Mechanics,. Berlin: Springer, (1932).

[15] B. Schumacher, “Quantum coding,” Phys. Rev. A, vol. 51, pp. 2738–2747, (1995).

[16] W. K. Wootters and W. H. Zurek, “A single quantum cannot be cloned,” Nature, vol. 299, no. 5886, pp. 802–803,(1982).

[17] J. S. Bell, “On the einstein-podolsky-rosen paradox.” Physics (Long Island City, N.Y.), p. 195–200, (1964).

[18] E. Schrödinger, “Die gegenwärtige situation in der quantenmechanik,” Naturwissenschaften, vol. 23, pp.807–812, (1935).

[19] A. Einstein, B. Podolsky, and N. Rosen, “Can quantum-mechanical description of physical reality be considered complete?” Phys. Rev., vol. 47, pp. 777–780, (1935).

[20] A. K. Ekert, “Quantum cryptography based on bell’s theorem,” Phys. Rev. Lett., vol. 67, pp. 661–663, (1991).

[21] C. H. Bennett, G. Brassard, C. Crépeau, R. Jozsa, A. Peres, and W. K. Wootters, “Teleporting an unknown quantum state via dual classical and einstein-podolsky-rosen channels,” Phys. Rev. Lett., vol. 70,pp. 1895–1899, (1993).

[22] G. Adesso et al. "TOPICAL REVIEW: Measures and applications of quantum correlations" J. Phys. A: Math. Theor. 49 473001 (2016).

[23] C. E. Shannon, “A mathematical theory of communication,” Bell System Technical Journal, vol. 27, no. 3,pp. 379–423, (1948).

[24] H. Umegaki, “Conditional expectation in an operator algebra. iv. entropy and information,” Kodai Math. Sem. Rep., vol. 14, no. 2, pp. 59–85, (1962).

[25] S. Kullback; R.A. Leibler, . "On information and sufficiency". Annals of Mathematical Statistics. 22 (1): 79–86. (1951)

[26] A. Ekert and R. Jozsa, “Quantum computation and shor’s factoring algorithm,” Rev. Mod. Phys., vol. 68, pp. 733–753, (1996).

[27] R. Horodecki, P. Horodecki, M. Horodecki and K. Horodecki, Rev. Mod. Phys.81, 865 (2009).

[28] E. Knill and R. Laflamme, “Power of one bit of quantum information,” Phys. Rev. Lett., vol. 81, pp. 5672–5675, (1998).

[29] H. Ollivier and W. H. Zurek, “Quantum discord: A measure of the quantumness of correlations,” Phys. Rev. Lett., vol. 88, p. 017901, Dec (2001).

[30] L. Henderson and V. Vedral, “Classical, quantum and total correlations,” J. Phys. A: Math. Gen, vol. 34, p. 6899, (2001).

[31] C. H. Bennett, H. J. Bernstein, S. Popescu, and B. Schumacher,"Concentrating partial entanglement by local operations",Phys. Rev. A 53, 2046 – (1996).

[32] C. H. Bennett, D. P. DiVincenzo, J. A. Smolin, and W. K. Wootters, “Mixed-state entanglement and quantum error correction,” Phys. Rev. A, vol. 54, pp. 3824–3851, (1996).

[33] V. Vedral, M. B. Plenio, M. A. Rippin, and P. L. Knight, “Quantifying entanglement,” Phys. Rev. Lett.,vol. 78, pp. 2275–2279, (1997).

[34] M. B. Plenio and S. Virmani, “An introduction to entanglement measures,” Quantum Info. Comput., vol. 7, no. 1, pp. 1–51,(2007).

[35] S. Hill and W. K. Wootters, “Entanglement of a pair of quantum bits,” Phys. Rev. Lett., vol. 78, pp. 5022–5025, (1997).

[36] L. Henderson and V. Vedral, “Classical correlations and entanglement,” J. Phys.A - Math Gen, vol.34,35, pp. 6899 – 6905, (2001).

[37] V. Vedral, "Classical Correlations and Entanglement in Quantum Measurements" Phys. Rev. Lett. 90, 050401, (2003).

[38] K. Modi, A. Brodutch, H. Cable, T. Paterek, and V. Vedral, “The classical-quantum boundary for correlations: Discord and related measures,” Rev. Mod. Phys., vol. 84, pp. 1655–1707, (2012).

[39] A. Ferraro, L. Aolita, D. Cavalcanti, F. M. Cucchietti, and A. Acín, “Almost all quantum states have nonclassical correlations,” Phys. Rev. A, vol. 81, p. 052318,(2010).

[40] D. F. Walls and G. J. Milburn, "Quantum Optics", Springer– Verlag, Berlin, (1995).

[41] R. J. Glauber, "Coherent and Incoherent States of the Radiation Field", Phys. Rev. 131, 2766, (1963).

[42] M. O. Scully,"Enhancement of the index of refraction via quantum coherence" Phys. Rev. Lett. 67, 1855 (1991).

[43] V. Giovannetti, S. Lloyd, and L. Maccone,"Quantum-Enhanced Measurements: Beating the Standard Quantum Limit", Science 306, 1330,(2004).

[44] L. H. Ford, "Quantum coherence effects and the second law of thermodynamics", Proc. R. Soc. Lond. A 364, 227, (1978).

[45] C.L Latune, I. Sinayskiy and F. Petruccione, "Roles of quantum coherences in thermal machines", Eur. Phys. J. Spec. Top. (2021).

[46] S. Lloyd, "Quantum coherence in biological systems",J. Phys.: Conf. Ser. 302, 012037, (2011).

[47] I. Khmelinskii, V. I. Makarov, "Analysis of quantum coherence in biology" ,Chemical Physics,Volume 532,110671,(2020).

[48] J. Cao *et al.*,"Quantum biology revisited", Science Advances, Vol. 6, no. 14, eaaz4888, (2020).

[49] Brandao, F.G.S.L., Gour, G.: Reversible framework for quantum resource theories. Phys. Rev. Lett. 115, 070503 (2015).

[50] E. Chitambar and G. Gour, "Quantum resource theories", Reviews of Modern Physics 91 2, 025001 (2019).

[51] C. Sparaciari, L. del Rio, C. M. Scandolo, P. Faist, and J. Oppenheim. "The first law of general quantum resource theories", Quantum 4, 259 (2020).

[52] C. H. Bennett, H. J. Bernstein, S. Popescu, and B. Schumacher, "Concentrating partial entanglement by local operations" Phys. Rev. A 53, 2046 (1996).

[53] J. Eisert, K. Jacobs, P. Papadopoulos, and M. B. Plenio, "Optimal local implementation of nonlocal quantum gates" Phys. Rev. A 62, 052317 (2000).

[54] V. Veitch, C. Ferrie, D. Gross, and J. Emerson,"Negative quasi-probability as a resource for quantum computation" New J. Phys. 14,113011 (2012).

[55]] M. Howard and E. Campbell,"Application of a Resource Theory for Magic States to Fault-Tolerant Quantum Computing" Phys. Rev. Lett. 118, 090501(2017).

[56] Streltsov, A., Adesso, G., Plenio, M.B.: "Colloquium: Quantum coherence as a resource." Rev. Mod.Phys. 89, 041003 (2017).

[57] Winter, A., Yang, D. "Operational resource theory of coherence." Phys. Rev. Lett. 116, 120404 (2016).

[58] J. Aberg, Quantifying Superposition, arXiv:quant-ph/0612146 (2006).

[59] E. Chitambar, and G.Gour, Critical Examination of Incoherent Operations and a Physically Consistent Resource Theory of Quantum Coherence, Phys. Rev. Lett. 117, 030401 (2016).

[60] T. Baumgratz, M. Cramer, and M. B. Plenio, Quantifying Coherence, Phys. Rev. Lett. 113, 140401 (2014).

[61] F. G. S. L. Brandão, M. Horodecki, J. Oppenheim, J. M. Renes, and R. W. Spekkens,"Resource Theory of Quantum States Out of Thermal Equilibrium" Phys. Rev. Lett. 111, 250404 (2013).

[62] J. Goold, M. Huber, A. Riera, L. del Rio, and P. Skrzypczyk,"The role of quantum information in thermodynamics—a topical review" J. Phys. A: Math. Theor. 49, 143001 (2016).

[63] N. H. Y. Ng and M. P. Woods, “Resource theory of quantum thermodynamics: Thermal operations and second laws,” in Thermodynamics in the Quantum Regime, pp. 625–650, Springer, (2018).

[64] M. Lostaglio, "An introductory review of the resource theory approach to thermodynamics" Rep. Prog. Phys. 82 114001, (2019).

[65] C. Sparaciari, J. Oppenheim, and T. Fritz, "Resource theory for work and heat", Phys. Rev. A 96, 052112 (2017).

[66] V. Giovannetti, S. Lloyd, and L. Maccone,"Advances in quantum metrology" Nat Photon 5, 222-229 (2011).

[67] A. Streltsov, U. Singh, H. S. Dhar, M. N. Bera, and G. Adesso, "Measuring Quantum Coherence with Entanglement ", Phys. Rev. Lett. 115, 020403(2015).

[68] T. R. Bromley, M. Cianciaruso, and G. Adesso, "Frozen Quantum Coherence ", Phys. Rev.Lett. 114, 210401 (2015).

[69] I. Marvian, and R. W. Spekkens,"Extending Noether’s theorem by quantifying the asymmetry of quantum states", Nat. Commun. 5, 3821 (2014).

[70] I. Marvian, R. W. Spekkens, and P. Zanardi,"Quantum speed limits, coherence, and asymmetry", Phys. Rev. A 93, 052331 (2016).

[71] I. Marvian and R. W. Spekkens,"How to quantify coherence: Distinguishing speakable and unspeakable notions", Phys. Rev. A 94, 052324 (2016).

[72] M. A. Nielsen, I. L. Chuang, "Quantum Computation and Quantum Information" (10th ed.)Cambridge University Press, (2010).

[73] S. D. Bartlett, T. Rudolph, and R. W. Spekkens,"Reference frames, superselection rules, and quantum information", Rev. Mod. Phys. 79, 555 (2007).

[74] I. Marvian and R. W. Spekkens,"Modes of asymmetry: The application of harmonic analysis to symmetric quantum dynamics and quantum reference frames", Phys. Rev. A 90, 062110 (2014).

[75] M. Lostaglio, D. Jennings, and T. Rudolph,"Description of quantum coherence in thermodynamic processes requires constraints beyond free energy", Nat. Commun. 66383 (2015).

[76] M. Lostaglio, K. Korzekwa, D. Jennings, and T. Rudolph, "Quantum Coherence, Time-Translation Symmetry, and Thermodynamics", Phys. Rev. X 5, 021001 (2015).

[77] G. Gour, I. Marvian, and R. W. Spekkens,"Measuring the quality of a quantum reference frame: The relative entropy of frameness", Phys. Rev. A 80, 012307 (2009).

[78] M. Zhao, T. Ma, Q. Quan, H. Fan and R. Pereira, "The l_1 Norm of Coherence of Assistance",Physical Review A 100, 012315 (2019).

[79] M. Liu, DM. Gao, and XQ. Cai, "Operational Interpretations of the l1 Norm Coherence in Pure Quantum Systems". Int J Theor Phys 58, 3627–3631 (2019).

[80] Y. Jing, CK. Li, E. Poon, and C. Zhang, "Coherence measures induced by norm functions",Journal of Mathematical Physics 62, 042202 (2021).

[81] C. Napoli, T.R. Bromley, M. Cianciaruso, M. Piani, N. Johnston, G. Adesso, "Robustness of coherence: An operational and observable measure of quantum coherence". Phys. Rev. Lett., 116, 150502,(2016).

[82] A. Streltsov, U. Singh, H.S Dhar, M.N. Bera, G. Adesso, "Measuring quantum coherence with entanglement", Phys. Rev. Lett., 115, 020403,(2015).

[83] S. Rana, P. Parashar, M. Lewenstein, "Trace-distance measure of coherence", Phys. Rev. A , 93, 012110, (2016).

[84] B. Chen, S.M Fei, "Notes on modified trace distance measure of coherence", Quantum Inf. Comput., 17, 107, (2018).

[85] X. Qi, T. Gao, F. Yan, "Measuring coherence with entanglement concurrence". J. Phys. A Math. Theor.50, 285301, (2017).

[86] F. Caruso, A. W. Chin, A. Datta, S. F. Huelga, and M. B. Plenio. “Entanglement and entangling power of the dynamics in light-harvesting complexes”, Phys. Rev. A, vol. 81, p. 062346,(2010).

[87] Morigi, G. et al. "Dissipative quantum control of a spin chain", Physical Review Letters 115, 200502,(2015).

[88] R.P Feynman and F.L Vernon. "The theory of a general quantum system interacting with a linear dissipative system",Annals of Physics, vol. 24, pp. 118-173, (1963).

[89] H. D. Zeh. “On the interpretation of measurement in quantum theory,” Foundations of Physics, vol. 1, pp. 69–76, (1970).

[90] W. H. Zurek, “Decoherence, einselection, and the quantum origins of the classical,” Rev. Mod. Phys., vol. 75, pp. 715–775, (2003).

[91] W. H.Zurek. “Decoherence and the transition from quantum to classical,” Physics Today, vol. 44, p. 36, (1991).

[92] E. Schrödinger. An undulatory theory of the mechanics of atoms and molecules. ¨ Phys. Rev., 28:1049, (1926).

[93] A. Rivas and S. F. Huelga, "Open Quantum Systems : An Introduction", (Springer, Berlin Heidelberg, Germany, 2012).

[94] K. Kraus, States, Effects, and Operations, J. D. D. A. Böhm and W. H. Wootters, Eds. Springer-Verlag Berlin Heidelberg, vol. 190. (1983)

[95] U. Weiss, "Quantum Dissipative Systems", 3rd ed. Singapore: World Scientific, vol. 13, (2008).

[96] C. Gardiner and P. Zoller, "Quantum Noise". Springer-Verlag Berlin Heidelberg, (2004).

[97] H.-P. Breuer and F. Petruccione, "The theory of open quantum systems". Wotton-under-Edge: Clarendon press Oxford, (2006).

[98] D. Manzano, "A short introduction to the Lindblad master equation",AIP Advances 10(2):025106, (2020).

[99] V. Gorini, A. Kossakowski, and E. C. G. Sudarshan, “Completely positive dynamical semigroups of n-level systems,” Journal of Mathematical Physics, vol. 17, no. 5, pp. 821–825, (1976).

[100] G. Lindblad, “On the generators of quantum dynamical semigroups,” Comm. Math. Phys., vol. 48, no. 2, pp. 119–130, (1976).

[101] A. Galindo and P. Pascual. "Quantum Mechanics I". Springer, Berlin, (1990).

[102] H. J. Carmichael and D. F. Walls. "Master equation for strongly interacting systems". Journal of Physics A: Mathematical, Nuclear and General, 6:1552, (1973).

[103] J. O. González, L. A. Correa, G. Nocerino, J. P. Palao, D. Alonso and G. Adesso, "Testing the Validity of the ‘Local’ and ‘Global’ GKLS Master Equations on an Exactly Solvable Model",Open Systems Information DynamicsVol. 24, No. 04, 1740010, (2017).

[104] Marco Cattaneo et al. "Local versus global master equation with common and separate baths: superiority of the global approach in partial secular approximation", New J. Phys. 21 113045, (2019).

[105] J. Kołodyński, J. B. Brask, M. Perarnau-Llobet, and B. Bylicka. "Adding dynamical generators in quantum master equations", Phys. Rev. A, 97:062124,(2018).

[106] J. T. Stockburger and T. Motz. "Thermodynamic deficiencies of some simple lindblad operators", Fortschritte der Physik, 65(6-8):1600067, (2016).

[107] P. P Hofer et al. "Markovian master equations for quantum thermal machines: local versus global approach ", New J. Phys. 19 123037, (2017).

[108] S. Scali, J. Anders, and L. A. Correa. "Local master equations bypass the secular approximation",Quantum 5, 451 (2021).

[109] P. D. Manrique, F. Rodríguez, L. Quiroga, and N. F. Johnson, "Nonequilibrium quantum systems: Divergence between global and local descriptions", Advances in Condensed Matter Physics, 2015:1–7, (2015).

[110] G. De Chiara, G. Landi, A. Hewgill, B. Reid, A. Ferraro, A. J. Roncaglia, and M. Antezza, "Reconciliation of quantum local master equations with thermodynamics", New J. Phys. 20 113024, (2018).

[111] P. P. Hofer, M. Perarnaut-Llobet, J. B. Brask, R. Silva, M. Huber, and N. Brunner. "Autonomous quantum refrigerator in a circuit qed architecture based on a josephson junction". Phys. Rev. B, 94:235420, (2016).

[112] A. Rivas, S. F. Huelga, and M. B. Plenio. "Quantum non-markovianity: characterization, quantification and detection", Reports on Progress in Physics, 77:094001, (2014).

[113] D. Kondepudi and I. Prigogine. "Modern Thermodynamics, From Heat Engines to Dissipative Structures".(John Wiley Sons, Chichester, England, 1998).

[114] M. Flanders and D. Swann, “First and Second Law,” in At the Drop of Another Hat (Parlophone Ltd. 2nd ed),(1964).

[115] R. Clausius, “Ueber verschiedene f¨ur die Anwendung bequeme Formen der Hauptgleichungen der mechanischen W¨armetheorie”, Ann. Phys. 201, 353–400, (1865).

[116] H. B. Callen, "Thermodynamics and an introduction to thermostatistics". Second ed. (John Wiley Sons, Singapore, 1985).

[117] S. Vinjanampathy and J. Anders, "Quantum thermodynamics", Contemp. Phys. 57, 1–35, (2016).

[118] P. Talkner, E. Lutz, and P. Hänggi. "Fluctuation theorems: Work is not an observable", Physical Review E 75 , p. 050102, (2007).

[119] R. Clausius. "Mechanical Theory of Heat", (John van Voorst, London, UK, 1867).

[120] R. Alicki and M. Fannes. "Entanglement boost for extractable work from ensembles of quantum batteries", Phys. Rev. E, 87:042123, (2013).

[121] A. Lenard. "Thermodynamical proof of the Gibbs formula for elementary quantum systems", Journal of Statistical Physics, 19(6):575-586, (1978).

[122] A. E. Allahverdyan." Nonequilibrium quantum fluctuations of work", Physical Review E, 90(3):032137, (2014).

[123] A. E. Allahverdyan, R. Balian, and T. M. Nieuwenhuizen. "Maximal work extraction from finite quantum systems", Europhysics Letters (EPL) 67, 565-571 (2004).

[124] D. von Lindenfels, O. Grab, C. T. Schmiegelow, V. Kaushal, J. Schulz, M. T. Mitchison, J. Goold, F. Schmidt-Kaler, and U. G. Poschinger. "Spin Heat Engine Coupled to a Harmonic Oscillator Flywheel", Phys. Rev. Lett. 123, 080602, (2019).

[125] N. V. Horne, D. Yum, T. Dutta, P. Hanggi, J. Gong, D. Poletti, and M. Mukherjee. "Single-atom energy conversion device with a quantum load", npj Quantum Information 6, 37,(2020).

[126] W. Niedenzu, M. Huber, and E. Boukobza. "Concepts of work in autonomous quantum heat engines", Quantum 3, 195, (2019).

[127] F. Binder, S. Vinjanampathy, K. Modi, Kavan, and J. Goold. "Quantum thermodynamics of general quantum processes", Phys. Rev. E 91, 032119, (2015).

[128] G. Francica, F.C. Binder, G. Guarnieri, M.T. Mitchison, J. Goold, and F. Plastina. "Quantum Coherence and Ergotropy", Phys. Rev. Lett. 125, 180603, (2020).

[129] K. Hammam, Y. Hassouni, R. Fazio, G. Manzano. "Optimizing autonomous thermal machines powered by energetic coherence", New J. Phys. 23 043024, (2021).

[130] P. Skrzypczyk, A. J. Short, and S. Popescu. "Work extraction and thermodynamics for individual quantum systems", Nat. Commun. 5, 4185,10.1038/ncomms5185, (2014).

[131] K. Korzekwa, M. Lostaglio, J. Oppenheim and D. Jennings. "The extraction of work from quantum coherence", New J. Phys. 18 023045, (2016).

[132] M. Horodecki and J. Oppenheim. "Fundamental limitations for quantum and nanoscale thermodynamics ", Nature Communications 4, 2059, (2013).

[133] J. Aberg. "Truly work-like work extraction via a singleshot analysis", Nat. Comm. 4, 1925, (2013).

[134] O. C. O. Dahlsten, R. Renner, E. Rieper, and V. Vedral. "Inadequacy of von Neumann entropy for characterizing extractable work", New J. Phys. 13, 053015, (2011).

[135] G. Gallavotti and E. G. D. Cohen. "Dynamical ensembles in nonequilibrium statistical mechanics", Phys. Rev. Lett., 74:2694,(1995).

[136] J. Lebowitz and H. Spohn. "A Gallavotti-Cohen-type symmetry in the large deviation functional for stochastic dynamics". J. Stat. Phys, 95:333, (1999).

[137] J. Kurchan. "Fluctuation theorem for stochastic dynamics", J. Phys. A: Math. Gen., 31:3719, (1998).

[138] C. Jarzynski. "Equalities and inequalities: Irreversibility and the second law of thermodynamics at the nanoscale", Ann. Rev. Cond. Matt. Phys., 2:329, (2011).

[139] G. E. Crooks. "Nonequilibrium measurements of free energy differences for microscopically reversible Markovian systems", J. Stat. Phys., 90:1481, (1998).

[140] G. E. Crooks. "Entropy production fluctuation theorems and the nonequilibrium work relation for free energy differences", Phys. Rev. E , 60:2721, (1999).

[141] G. E. Crooks. "Path-ensemble averages in systems driven far from equilibrium", Physical Review E 61, 2361–2366, (2000).

[142] B. Cleuren, C. Van den Broeck R. Kawai. "Fluctuation and dissipation of work in a Joule experiment". Physical Review Letters 96, 050601, (2006).

[143] G. Gradenigo, A. Puglisi, A. Sarracino, U. M. B. Marconi. "Nonequilibrium fluctuations in a driven stochastic lorentz gas", Physical Review E 85, 031112, (2012).

[144] O.-P Saira, Y. Yoon, T. Tanttu, M. Möttönen, D.V. Averin J.P. Pekola, "Test of the Jarzynski and Crooks fluctuation relations in an electronic system", Physical Review Letters 109, 180601, (2012).

[145] K. Hayashi, H. Ueno, R. Iino H. Noji. "Fluctuation theorem applied to F1- ATPase", Physical Review Letters 104, 218103, (2010).

[146] F. Ritort. "Single-molecule experiments in biological physics: methods and applications", Journal of Physics: Condensed Matter 18, R531, (2006).

[147] M. Campisi, P. Hänggi, and P. Talkner. "Colloquium: Quantum fluctuation relations: Foundations and applications", Rev. Mod. Phys. 83, 771, (2011).

[148] H. E. D. Scovil and E. O. Schulz-DuBois. "Three-level masers as heat engines", Phys. Rev. Lett. 2, 262-263 (1959).

[149] R. Kosloff and A. Levy. "Quantum Heat Engines and Refrigerators: Continuous Devices", Annu. Rev. Phys. Chem. 65, 365-393 (2014).

[150] F. Binder, L. A. Correa, C. Gogolin, J. Anders, and G. E. Adesso. "Thermodynamics in the Quantum Regime. Fundamental Aspects and New Directions" (Springer, Switzerland, 2018).

[151] H. T. Quan, Y.-x. Liu, C. P. Sun, and F. Nori. "Quantum thermodynamic cycles and quantum heat engines",Phys. Rev. E 76, 031105 (2007).

[152] R. Kosloff and Y. Rezek. "The quantum harmonic otto cycle", Entropy 19, 136 (2017).

[153] J. Roßnagel, S. T. Dawkins, K. N. Tolazzi, O. Abah, E. Lutz, F. Schmidt-Kaler, and K. Singer. "A single-atom heat engine", Science 352, 325-329 (2016).

[154] J. P. S. Peterson, T. B. Batalh ao, M. Herrera, A. M. Souza, R. S. Sarthour, I. S. Oliveira, and R. M. Serra. "Experimental characterization of a spin quantum heat engine", Phys. Rev. Lett. 123, 240601 (2019).

[155] J. Klatzow, J. N. Becker, P. M. Ledingham, C. Weinzetl, K. T. Kaczmarek, D. J. Saunders, J. Nunn, I. A. Walmsley, R. Uzdin, and E. Poem. "Experimental demonstration of quantum effects in the operation of microscopic heat engines", Phys. Rev. Lett. 122, 110601 (2019).

[156] D. von Lindenfels, O. Gräb, C. T. Schmiegelow, V. Kaushal, J. Schulz, M. T. Mitchison, J. Goold, F. Schmidt-Kaler, and U. G. Poschinger. "Spin heat engine coupled to a harmonic-oscillator flywheel", Phys. Rev. Lett. 123, 080602 (2019).

[157] J. Aberg. "Catalytic coherence", Phys. Rev. Lett. , 150402, (2014).

[158] H. Tajima, N. Shiraishi, and K. Saito. "Coherence cost for violating conservation laws", Phys. Rev. Research 2, 043374 (2020).

[159] J. P. Palao, R. Kosloff, and J. M. Gordon. "Quantum thermodynamic cooling cycle", Phys. Rev. E 64, 056130 (2001).

[160] N. Linden, S. Popescu, and P. Skrzypczyk. "How small can thermal machines be? the smallest possible refrigerator", Phys. Rev. Lett. 105, 130401 (2010).

[161] N. Brunner, N. Linden, S. Popescu, and P. Skrzypczyk. "Virtual qubits, virtual temperatures, and the foundations of thermodynamics", Phys. Rev. E 85, 051117 (2012).

[162] A. Levy and R. Kosloff. "Quantum absorption refrigerator", Phys. Rev. Lett. 108, 070604 (2012).

[163] D. Venturelli, R. Fazio, and V. Giovannetti. "Minimal selfcontained quantum refrigeration machine based on four quantum dots", Phys. Rev. Lett. 110, 256801 (2013).

[164] P. A. Erdman, B. Bhandari, R. Fazio, J. P. Pekola, and F. Taddei. "Absorption refrigerators based on coulomb-coupled single-electron systems", Phys. Rev. B 98, 045433 (2018).

[165] P. P. Hofer, M. Perarnau-Llobet, J. B. Brask, R. Silva, M. Huber, and N. Brunner. "Autonomous quantum refrigerator in a circuit qed architecture based on a josephson junction", Phys. Rev. B 94, 235420 (2016).

[166] M. T. Mitchison, M. Huber, J. Prior, M. P. Woods, and M. B. Plenio. "Realising a quantum absorption refrigerator with an atom-cavity system", Quantum Science and Technology 1, 015001 (2016).

[167] G. Maslennikov, S. Ding, R. Habltzel, J. Gan, A. Roulet, S. Nimmrichter, J. Dai, V. Scarani, and D. Matsukevich. "Quantum absorption refrigerator with trapped ions", Nat. Commun. 10, 202 (2019).

[168] M. P. Woods, R. Silva, and J. Oppenheim. "Autonomous quantum machines and finite sized clocks", J. Ann. Henri Poincar´e (2018).

[169] M. Lostaglio and M. P. M üller, Coherence and asymmetry cannot be broadcast, Phys. Rev. Lett. 123, 020403 (2019).

[170] I. Marvian and R. W. Spekkens. "No-broadcasting theorem for quantum asymmetry and coherence and a trade-off relation for approximate broadcasting", Phys. Rev. Lett. 123, 020404 (2019).

[171] I. Marvian. "Coherence distillation machines are impossible in quantum thermodynamics", Nat. Commun. 11, 25 (2020).

[172] D. Janzing. "Quantum thermodynamics with missing reference frames: Decompositions of free energy into nonincreasing components", J. Stat. Phys. 125, 761 (2006).

[173] P. Kammerlander and J. Anders. "Coherence and measurement in quantum thermodynamics", Sci. Rep. 6, 22174 (2016).

[174] P. Cwiklinski, M. Studzinski, M. Horodecki, and J. Oppenheim. "Limitations on the evolution of quantum coherences: Towards fully quantum second laws of thermodynamics", Phys. Rev. Lett. 115, 210403 (2015).

[175] R. Uzdin. "Coherence-induced reversibility and collective operation of quantum heat machines via coherence recycling", Phys. Rev. Applied 6, 024004 (2016).

[176] J. P. Santos, L. C. Céleri, G. T. Landi, and M. Paternostro. "The role of quantum coherence in non-equilibrium entropy production", npj Quantum Information 5, 23 (2019).

[177] G. Francica, J. Goold, and F. Plastina. "Role of coherence in the nonequilibrium thermodynamics of quantum systems", Phys. Rev. E 99, 042105 (2019).

[178] G. Manzano, R. Silva, and J. M. R. Parrondo. "Autonomous thermal machine for amplification and control of energetic coherence", Phys. Rev. E 99, 042135 (2019).

[179] V. Scarani, M. Ziman, P. Stelmachovic, N. Gisin, and V. Buzek. "Thermalizing quantum machines: Dissipation and entanglement", Phys. Rev. Lett. 88, 097905 (2002).

[180] M. Ziman and V. Buzek. "All (qubit) decoherences: Complete characterization and physical implementation", Phys. Rev. A 72, 022110 (2005)

[181] S. Lorenzo, F. Ciccarello, and G. M. Palma "Composite quantum collision models", Phys. Rev. A 96, 032107 (2017).

[182] F. L. S. Rodrigues, G. De Chiara, M. Paternostro, and G. T. Landi. "Thermodynamics of weakly coherent collisional models", Phys. Rev. Lett. 123, 140601 (2019).

[183] (Here we denote $|ij\rangle_m|i\rangle_c \otimes |j\rangle_h$ for $i, j = 0, 1$ the energetic basis of the machine Hilbert space).

[184] R. Silva, G. Manzano, P. Skrzypczyk, and N. Brunner. "Performance of autonomous quantum thermal machines: Hilbert space dimension as a thermodynamical resource", Phys. Rev. E 94, 032120 (2016).

[185] P. Erker, M. T. Mitchison, R. Silva, M. P. Woods, N. Brunner, and M. Huber. "Autonomous quantum clocks: Does thermodynamics limit our ability to measure time?",Phys. Rev. X 7, 031022 (2017).

[186] H. M. Wiseman and G. J. Milburn. "Quantum measurement and control", (Cambridge University Press, Cambridge, UK, 2010).

[187] M. O. Scully, K. R. Chapin, K. E. Dorfman, M. B. Kim, and A. Svidzinsky. "Quantum heat engine power can be increased by noise-induced coherence", Proc. Natl. Acad. Sci. 108, 1509715100 (2011).

[188] P. Strasberg, G. Schaller, T. Brandes, and M. Esposito. "Quantum and information thermodynamics: A unifying framework based on repeated interactions", Phys. Rev. X 7, 021003 (2017).

[189] J. M. R. Parrondo, J. M. Horowitz, and T. Sagawa. "Thermodynamics of information", Nat. Phys. 11, 131-139 (2015).

[190] R. Gallego, J. Eisert, and H. Wilming." Thermodynamic work from operational principles", New Journal of Physics 18, 103017, (2016).

[191] G. Manzano, J. M. Horowitz, and J. M. R. Parrondo. "Quantum fluctuation theorems for arbitrary environments: Adiabatic and nonadiabatic entropy production", Phys. Rev. X 8, 031037, (2018).

[192] G. T. Landi and M. Paternostro. "Irreversible entropy production, from quantum to classical", arXiv:2009.07668 [quant-ph] (2020).

[193] G. Manzano. "Thermodynamics and Synchronization in Open Quantum Systems", Springer Theses (Springer,2018).

[194] A. I. Brown and D. A. Sivak. "Theory of nonequilibrium free energy transduction by molecular machines", Chemical Reviews 120, 434-459 (2020).

[195] E. Penocchio, R. Rao, and M. Esposito. "Thermodynamic efficiency in dissipative chemistry", Nat. Commun. 10, 3865 (2019).

[196] F. Hajiloo, R. Sanchez, R. S. Whitney, and J. Splettstoesser. "Quantifying nonequilibrium thermodynamic operations in a multiterminal mesoscopic system", Phys. Rev. B 102, 155405 (2020).

[197] G. Manzano, F. Plastina, and R. Zambrini. "Optimal work extraction and thermodynamics of quantum measurements and correlations", Phys. Rev. Lett. 121, 120602 (2018).

[198] D. Kondepudi and I. Prigogine. "Modern Thermodynamics: From Heat Engines to Dissipative Structures", 2nd ed. (Wiley).

[199] R. Uzdin, A. Levy, and R. Kosloff."Equivalence of Quantum Heat Machines, and Quantum-Thermodynamic Signatures", Phys. Rev. X 5, 031044 (2015).

[200] D. Gelbwaser-Klimovsky, W. Niedenzu, and G. Kurizki. "Thermodynamics of quantum systems under dynamical control", Adv. At. Mol. Opt. Phys. 64, 329 (2015).

[201] F. Curzon and B. Ahlborn. "Efficiency of a Carnot engine at maximum power output", Am. J. Phys. 43, 22 (1975).

[202] P. Skrzypczyk, N. Brunner, N. Linden and S. Popescu. "The smallest refrigerators can reach maximal efficiency", J. Phys. A: Math. Theor. 44, 492002 (2011).

[203] G.A Barrios, F. Albarrán-Arriagada, F.J Peña, E. Solano, J.C Retamal. " Light-matter quantum Otto engine in finite time", arXiv:2102.10559, (2021).

[204] O. Abah, M. Paternostro. "Shortcut-to-adiabaticity Otto engine: A twist to finite-time thermodynamics", Phys. Rev. E, 99, 022110, (2019).

[205] B. Çakmak, O.E. Müstecaplıo˘glu. "Spin quantum heat engines with shortcuts to adiabaticity". Phys. Rev. E, 99, 032108, (2019).

[206] M. Beau, J. Jaramillo, A. del Campo. "Scaling-Up Quantum Heat Engines Efficiently via Shortcuts to Adiabaticity", Entropy, 18, 168,(2016).

[207] S. Deffner. "Efficiency of Harmonic Quantum Otto Engines at Maximal Power", Entropy, 20, 875, (2018).

[208] Z. Smith, P.S Pal, S. Deffner. "Endoreversible Otto Engines at Maximal Power", J. Non-Equilib. Thermodyn, 45, 305, (2020).

[209] E. Muñoz, F.J Peña. "Quantum heat engine in the relativistic limit: The case of a Dirac particle", Phys. Rev. E, 86, 061108, (2012).

[210] N. Papadatos. "The Quantum Otto Heat Engine with a relativistically moving thermal bath". arXiv:2104.06611, (2021).

[211] A. Friedenberger, E. Lutz. "When is a quantum heat engine quantum?", Europhys. Lett., 120, 10002, (2017).

[212] W. Niedenzu, I. Mazets, G. Kurizki, F. Jendrzejewski. "Quantized refrigerator for an atomic cloud", Quantum , 3, 155, (2019).

[213] O. Abah, J. Roßnagel, G. Jacob, S. Deffner, F. Schmidt-Kaler, K. Singer, E. Lutz. "Single-Ion Heat Engine at Maximum Power" Phys.Rev. Lett., 109, 203006, (2012).

[214] K. Zhang, F. Bariani, P. Meystre. "Quantum Optomechanical Heat Engine", Phys. Rev. Lett., 112, 150602, (2014).

[215] F.J Peña, E. Muñoz. "Magnetostrain-driven quantum engine on a graphene flake", Phys. Rev. E, 91, 052152, (2015).

[216] F.J Peña, D. Zambrano, O. Negrete, G. De Chiara,P.A Orellana, P. Vargas. "Quasistatic and quantum-adiabatic Otto engine for a two-dimensional material: The case of a graphene quantum dot", Phys. Rev. E, 101, 012116,(2020).

[217] J. Klaers, S. Faelt, A. Imamoglu and E. Togan. "Squeezed Thermal Reservoirs as a Resource for a Nanomechanical Engine beyond the Carnot Limit", Phys. Rev. X, 7, 031044,(2017).

[218] N. Van Horne, D. Yum, T. Dutta, P. Hänggi, J. Gong, D. Poletti, M. Mukherjee. "Single-atom energy-conversion device with a quantum load", Npj Quantum Inf., 6, 37,(2020).

[219] R. Alicki. "The quantum open system as a model of the heat engine", J. Phys A: Math.Gen., vol. 12, page L103, (1979).

[220] R. Kosloff. "A quantum mechanical open system as a model of a heat engine", The Journal of chemical physics, vol. 80, no. 4, pages 1625–1631, (1984).

[221] E. Geva and R. Kosloff. "A quantum-mechanical heat engine operating in finite time. A model consisting of spin-1/2 systems as the working fluid", J. Chem. Phys. 96, 3054, (1992).

[222] T. Feldmann and R. Kosloff. "Performance of discrete heat engines and heat pumps in finite time", Phys. Rev. E 61, 4774, (2000).

[223] T. Feldmann, E. Geva and P. Salamon. "Heat engines in finite time governed by master equations", Am. J. Phys. 64, 485, (1996).

[224] T. Feldmann and R. Kosloff. "Quantum four-stroke heat engine: Thermodynamic observables in a model with intrinsic friction", Phys. Rev. E 68, 016101, (2003).

[225] R. Dann and R. Kosloff. "Quantum signatures in the quantum Carnot cycle", New J. Phys. 22 013055, (2020).

[226] G. Manzano, F. Galve, R. Zambrini, and J. M. R. Parrondo. "Entropy production and thermodynamic power of the squeezed thermal reservoir ", Phys. Rev. E 93, 052120, (2016).

[227] H. J. Briegel and S. Popescu. "Entanglement and intra-molecular cooling in biological systems? - A quantum thermodynamic perspective", arXiv:0806.4552, (2008).

[228] S. K. Manikandan, F. Giazotto and A. N. Jordan. "Superconducting Quantum Refrigerator: Breaking and Rejoining Cooper Pairs with Magnetic Field Cycles", Physical Review Applied, (2019).

[229] C.M. Bender, D.C. Brody, and B.K. Meister. "Quantum mechanical carnot engine", Journal of Physics A: Mathematical and General 33, p. 4427, (2000).

[230] B. Lin and J. Chen. "Performance analysis of an irreversible quantum heat engine working with harmonic oscillators", Physical Review E 67, p. 046105, (2003).

[231] L. Schulman and U. Vazirani. "Scalable NMR Quantum Computation", Proc. 31st STOC (ACM Symp. Theory Comp.), ACM Press (1999).

[232] F. Clivaz, R. Silva, G. Haack, J.B. Brask, N. Brunner and M. Huber. "Unifying paradigms of quantum refrigeration: Fundamental limits of cooling and associated work costs", Physical Review E, 100, 042130 (2019).

[233] N. Brunner, M. Huber, N. Linden, S. Popescu, R. Silva, and P.Skrzypczyk. "Entanglement enhances cooling in microscopic quantum refrigerators", Phys. Rev. E 89, 032115, (2014).

[234] G. Manzano, G. Giorgi, R. Fazio and R. Zambrini. "Boosting the performance of small autonomous refrigerators via common environmental effects", New J. Phys. 21 123026 (2019).

[235] J. B. Brask, N. Brunner, G. Haack and M. Huber. "Autonomous quantum thermal machine for generating steady-state entanglement", New Journal of Physics 17, 113029, (2015).

[236] P. Erker, M. T. Mitchison, R. Silva, M. P. Woods, N. Brunner and M. Huber. "Autonomous quantum clocks: does thermodynamics limit our ability to measure time?", Phys. Rev. X 7, 031022, (2017).

[237] A. Rignon-Bret, G. Guarnieri, J. Goold and M. T. Mitchison. "Thermodynamics of precision in quantum nanomachines", Phys. Rev. E 103, 012133 , (2021).

[238] E. Schwarzhans, M. P.E. Lock, P. Erker, N. Friis and M. Huber. "Autonomous Temporal Probability Concentration: Clockworks and the Second Law of Thermodynamics", Phys. Rev. X 11, 011046, (2021).

[239] M. T. Mitchison. "Quantum thermal absorption machines: refrigerators, engines and clocks ", Contemp. Phys. 60, 164 (2019).

[240] A Usui, W Niedenzu and M Huber. "Simplifying multi-level thermal machines using virtual qubits", arXiv:2009.03832, (2021).

[241] F. Ciccarello, S. Lorenzo, V. Giovannetti and G. M. Palma. "Quantum collision models: open system dynamics from repeated interactions", arXiv:2106.11974.

[242] G. De Chiara and M. Antezza. "Quantum machines powered by correlated baths", Phys. Rev. Research 2, 033315, (2020).

[243] N. Piccione, G. De Chiara and B. Bellomo. "Power maximization of two-stroke quantum thermal machines", Phys. Rev. A 103, 032211, (2021).

[244] K. Brandner, M. Bauer, M. T. Schmid, and U. Seifert. "Coherence-enhanced efficiency of feedback-driven quantum engines", New J. Phys. 17, 065006, (2015).

[245] K. Brandner, M. Bauer, and U. Seifert. "Universal Coherence-Induced Power Losses of Quantum Heat Engines in Linear Response", Phys. Rev. Lett. 119, 170602, (2017).

[246] W. Niedenzu, V. Mukherjee, A. Ghosh, A. G. Kofman, and G. Kurizki. "Quantum engine efficiency bound beyond the second law of thermodynamics", Nat Commun 9, 165 (2018).

[247] K. Hammam, H. Leitch, Y. Hassouni and G. De Chiara. “Exploiting coherence for quantum thermodynamic advantage”. (Submitted).

[248] D. Newman, F. Mintert and A. Nazir. "Quantum limit to nonequilibrium heat-engine performance imposed by strong system-reservoir coupling", Phys. Rev. E 101, 052129, (2020).

[249] J. P. Pekola, B. Karimi, G. Thomas, and D. V. Averin. "Supremacy of incoherent sudden cycles", Phys. Rev. B 100, 085405, (2019).

[250] S. Seah, M. Perarnau-Llobet, G. Haack, N. Brunner, and S. Nimmrichter. "Quantum Speed-Up in Collisional Battery Charging ", Phys. Rev. Lett. 127, 100601 , (2021).

[251] F. H. Kamin, F. T. Tabesh, S. Salimi, and A. C. Santos. "Entanglement, coherence, and charging process of quantum batteries", Phys. Rev. E 102, 052109, (2020).

[252] M. Mohseni, P. Rebentrost, S. Lloyd and A. Aspuru-Guzik. "Environment-Assisted Quantum Walks in Photosynthetic Energy Transfer", Journal of Chemical Physics 129, 174106, (2008).

[253] P. Rebentrost, M. Mohseni, I. Kassal, S. Lloyd and A. Aspuru-Guzik. "Environment-assisted quantum transport", New J. Phys. 11 033003, (2009).

[254] J. Yoneda, W. Huang, M. Feng, C. H. Yang, K. W. Chan, T. Tanttu, W. Gilbert, R. C. C. Leon, F. E. Hudson, K. M. Itoh, A. Morello, S. D. Bartlett, A. Laucht, A. Saraiva and A. S. Dzurak. "Coherent spin qubit transport in silicon", Nature Communications volume 12, 4114 (2021).

[255] R. Kosloff and T. Feldmann. "Discrete four-stroke quantum heat engine exploring the origin of friction", Phys. Rev. E 65, 055102, (2002).

[256] F. Plastina, A. Alecce, T.J.G. Apollaro, G. Falcone, G. Francica, F. Galve, N. Lo Gullo, and R. Zambrini. "Irreversible Work and Inner Friction in Quantum Thermodynamic Processes", Phys. Rev. Lett. 113, 260601, (2014).

[257] P. Abiuso and M. Perarnau-Llobet. "Optimal cycles for low-dissipation heat engines", Phys. Rev. Lett. 124 110606, (2020).

[258] M. Gluza, J. Sabino, N. H. Y. Ng, G. Vitagliano, M. Pezzutto, Y. Omar, I. Mazets, M. Huber, J. Schmiedmayer and J. Eisert. "Quantum field thermal machines", PRX Quantum 2, 030310 (2021).

[259] D. Meschede, H. Walther and G. Müller. "One-atom maser", Phys. Rev. Lett. 54 551–4, (1985).

[260] G. Rempe, H. Walther and N. Klein. "Observation of quantum collapse and revival in a one-atom maser", Phys. Rev. Lett. 58 353–6, (1987).

[261] B-L. Najera-Santos, P. A. Camati, V. Métillon, M. Brune, J-M Raimond, A. Auffèves and I. Dotsenko. "Autonomous Maxwell's demon in a cavity QED system", Phys. Rev. Res. 2 032025, (2020).

[262] N. K. Bernardes, J. P. S. Peterson, R. S. Sarthour, A. M. Souza, C. H. Monken, I. Roditi, I. S. Oliveira, M. F. Santos. "High Resolution non-Markovianity in NMR", Scientific Reports 6 33945, (2016).

[263] M. Cattaneo, G. De Chiara, S. Maniscalco, R. Zambrini, and G. L. Giorgi. "Collision Models Can Efficiently Simulate Any Multipartite Markovian Quantum Dynamics", Phys. Rev. Lett. 126, 130403, (2021).

[264] J. P. Pekola and I. M. Khaymovich. "Thermodynamics in single-electron circuits and superconducting qubits", Annu. Rev. Condens. Matter Phys. 10 193–212, (2019).

[265] M. Janovitch and G. T. Landi. "Quantum mean-square predictors of work", arXiv:2104.07132, (2021).

[266] J. J. Park, S. W. Kim, and V. Vedral. "Fluctuation Theorem for Arbitrary Quantum Bipartite Systems: Presence of Quantumness in Information Fluctuation Theorem", arXiv:1705.01750, (2017).

[267] K. Micadei, G. T. Landi, and E. Lutz. "Quantum Fluctuation Theorems beyond Two-Point Measurements", Phys. Rev. Lett. 124, 90602, (2020).

Appendix A

The Secular Approximation

In contrast to the Lindblad master equation, the Redfield equation is not strictly Markovian and does not guarantee a positive time evolution of the density matrix of the system. Since 3.56 is not the generator of a dynamical semigroup, it is required to use another approximation called the *secular approximation* to ensure that Eq.3.56 can be written in the Lindblad form Eq.3.47. The secular approximation consists of a sort of *rotating wave approximation* (RWA) in which the fast oscillating terms in the master equation are averaged. Without loss of generality, we consider the interaction Hamiltonian in the interaction picture

$$\tilde{H}_I(t) = \sum_\alpha \tilde{A}_\alpha \otimes \tilde{R}_\alpha, \tag{A.1}$$

where $\tilde{A}_\alpha^\dagger = \tilde{A}_\alpha$ and $\tilde{R}_\alpha^\dagger = \tilde{R}_\alpha$ are Hermitian operators such that $\tilde{A}_\alpha$ acts on the system's subspace and $\tilde{R}_\alpha$ acts on the environment's subspace. The equation 3.56 becomes

$$\frac{d}{dt}\tilde{\rho_S}(t) = -\int_0^\infty ds\, \mathrm{tr}_E[\tilde{A}_\alpha(t) \otimes \tilde{R}_\alpha(t), [\tilde{A}_\beta(t-s) \otimes \tilde{R}_\beta, \tilde{\rho_S}(t) \otimes \rho_E]. \tag{A.2}$$

Then we decompose $\tilde{A}_\alpha$ in terms of the eigenvectors of the system Hamiltonian $\Pi(\varepsilon)$, with ε being the corresponding eigenenergy

$$\tilde{A}_\alpha(\omega) = \sum_{\omega=\varepsilon'-\varepsilon} \Pi(\varepsilon)\tilde{A}_\alpha\Pi(\varepsilon'). \tag{A.3}$$

These operators fulfill the following conditions

$$[\tilde{H}_S, \tilde{A}_\alpha(\omega)] = -\omega\tilde{A}_\alpha(\omega) \quad , \quad [\tilde{H}_S, \tilde{A}^\dagger_\alpha(\omega)] = \omega\tilde{A}^\dagger_\alpha(\omega) \tag{A.4}$$

$$\tilde{A}^\dagger_\alpha(\omega) = \tilde{A}_\alpha(-\omega) \quad , \quad [\tilde{H}_S, \tilde{A}^\dagger_\alpha(\omega)\tilde{A}_\beta] = 0 \tag{A.5}$$

$$\sum_\omega \tilde{A}_\alpha(\omega) = \sum_\omega \tilde{A}^\dagger_\alpha(\omega) = \tilde{A}_\alpha \quad \text{(Completeness relation).} \tag{A.6}$$

In the interaction picture, the interaction Hamiltonian becomes

$$\tilde{H_I}(t) = \sum_{\alpha,\omega} e^{-i\omega t}\tilde{A}_\alpha(\omega) \otimes \tilde{R}_\alpha(t), \tag{A.7}$$

such that $\tilde{R}_\alpha(t) = e^{i(H_S+H_E)t}\tilde{R}_\alpha e^{-i(H_S+H_E)t}$ is the environment's operator in the interaction picture. Substituting Eq.A.7 into Eq.A.2

$$\frac{d}{dt}\tilde{\rho_S}(t) = \sum_{\omega,\omega'}\sum_{\alpha,\beta} e^{i(\omega-\omega')t}\Gamma_{\alpha,\beta}(\omega)(\tilde{A}_\beta(\omega)\tilde{\rho_S}(t)\tilde{A}^\dagger_\alpha(\omega') - \tilde{A}^\dagger_\alpha(\omega')\tilde{A}_\beta(\omega)\tilde{\rho_S}(t)) + h.c, \tag{A.8}$$

where h.c is the Hermitian conjugate and $\Gamma_{\alpha,\beta}(\omega) = \int_0^\infty ds e^{i\omega s}\langle\tilde{R}^\dagger_\alpha(t)\tilde{R}_\beta(t-s)\rangle$. Introducing the environment correlation functions with

$$\langle\tilde{R}^\dagger_\alpha(t)\tilde{R}_\beta(t-s)\rangle \equiv tr_E(\tilde{R}^\dagger_\alpha(t)\tilde{R}_\beta(t-s)\tilde{\rho_E}). \tag{A.9}$$

We can clearly see that now all the terms are oscillating with the frequency $(\omega - \omega')$. To simplify, we apply the secular approximation by neglecting terms with $\omega \neq \omega'$ while assuming that the timescale of the system is small compared to the timescale of the interaction with the reservoir $\tau_S \sim 1/(\omega - \omega') \ll \tau_R$ [97]. Now Eq.A.8 becomes

$$\frac{d}{dt}\tilde{\rho_S}(t) = \sum_{\alpha,\beta}\sum_{\omega} \Gamma_{\alpha,\beta}(\omega)(\tilde{A}_\beta(\omega)\tilde{\rho_S}(t)\tilde{A}^\dagger_\alpha(\omega) - \tilde{A}^\dagger_\alpha(\omega)\tilde{A}_\beta(\omega)\tilde{\rho_S}(t)) + h.c, \tag{A.10}$$

where we decompose $\Gamma_{\alpha,\beta}(\omega)$ into:

$$\Gamma_{\alpha,\beta}(\omega) = \frac{1}{2}\gamma_{\alpha,\beta}(\omega) + iS_{\alpha,\beta}(\omega), \tag{A.11}$$

with

$$S_{\alpha,\beta}(\omega) \equiv \frac{1}{2i}(\Gamma_{\alpha,\beta}(\omega) - \Gamma^*_{\alpha,\beta}(\omega)) \tag{A.12}$$

$$\gamma_{\alpha,\beta}(\omega) \equiv \Gamma_{\alpha,\beta}(\omega) + \Gamma^*_{\alpha,\beta}(\omega) = \int_{-\infty}^{\infty} ds e^{i\omega s}\langle \tilde{R}^\dagger_\alpha(s)\tilde{R}_\beta(0)\rangle. \tag{A.13}$$

Eventually, the master equation in the interaction picture is as follows

$$\frac{d}{dt}\tilde{\rho_S}(t) = -i[\tilde{H}_{LS}, \tilde{\rho_S}(t)] + D(\tilde{\rho_S}(t)), \tag{A.14}$$

such that we define the *Lamb-Shift* Hamiltonian which is Hermitian

$$\tilde{H}_{LS} = \sum_{\omega}\sum_{\alpha,\beta} S_{\alpha,\beta}(\omega)\tilde{A}^\dagger_\alpha(\omega)\tilde{A}_\beta(\omega). \tag{A.15}$$

By obtaining the Lamb-Shift Hamiltonian, a renormalization on the unperturbed energy levels of the system is introduced and it is due to the presence of the bath. The second term of A.14 represents the dissipator

$$D(\tilde{\rho_S}(t)) = \sum_{\omega}\sum_{\alpha,\beta} \gamma_{\alpha,\beta}(\omega)(\tilde{A}_\beta(\omega)\tilde{\rho_S}(t)\tilde{A}^\dagger_\alpha(\omega) - \frac{1}{2}\{\tilde{A}^\dagger_\alpha(\omega)\tilde{A}_\beta(\omega), \tilde{\rho_S}(t)\} \tag{A.16}$$

$\gamma_{\alpha,\beta}$ describes the relaxation rates for different decay modes of the open systems and are dependent on the correlation functions of the environment. By rewriting A.14 in the Lindblad form, we can see that it portrays CPTP dynamics , this can be realized by diagonalizing the relaxation rates. In the Schrödinger picture, A.14 takes the following GKLS form

$$\frac{d}{dt}\tilde{\rho_S}(t) = -i[\tilde{H}_S + \tilde{H}_{LS}, \tilde{\rho_S}(t)] + D(\tilde{\rho_S}(t)). \tag{A.17}$$

Appendix B

Derivation of The Dynamics of The Autonomous Coherent Thermal Machine

We obtain the master equation 5.44 in Sec. 5.2.1 for the thermal machine by explicitly modelling its interaction with the thermal baths and with the qubits in the tape. In particular we consider bosonic baths with Hamiltonian $H_B^{(i)} = \sum_k \Omega_k^{(i)} a_k^{(i)\dagger} a_k^{(i)}$ for $i = \mathrm{c}, \mathrm{h}$ and where the index k labels the bath's field modes with frequencies $\Omega_k^{(i)}$, and $a_k^{(i)\dagger}(a_k)$ being their usual creation (annihilation) operators. We assume a weak coupling between the baths and the corresponding machine qubits, in the rotating wave approximation

$$H_{\mathrm{m}B} = \sum_{i=\mathrm{c},\mathrm{h}} \sum_k g_k^{(i)} (\sigma_i a_k^{(i)\dagger} + \sigma_i^\dagger a_k^{(i)}), \tag{B.1}$$

with $g_k^{(i)} \ll E_i$ the coupling strength of the i-th qubit to each of the k modes of the bath i, with spectral densities $J_i(\Omega) = \sum_k (g_k^{(i)})^2 \delta(\Omega - \Omega_k^{(i)})/\Omega_k^{(i)}$.

In the absence of interactions with the tape qubits, each machine qubit is independently coupled to a local thermal bath. The reduced dynamics of the machine can then be easily obtained using the Born-Markov and secular approximations [97, 186]

$$\dot{\rho}_{\mathrm{m}}(t) = \sum_{i=\mathrm{c},\mathrm{h}} \gamma_\downarrow^i \mathcal{D}[\sigma_i^-]\rho_{\mathrm{m}} + \gamma_\uparrow^i \mathcal{D}[\sigma_i^+]\rho_{\mathrm{m}} \equiv \mathcal{L}_0(\rho_{\mathrm{m}}), \tag{B.2}$$

where $\gamma_{\downarrow}^{i} = \Gamma_0^i(1+N_{\rm th}^i)$, $\gamma_{\uparrow}^{i} = \Gamma_0^i N_{\rm th}^i$ are the rates of emission and absorption processes induced by the thermal baths. Here we assumed an Ohmic behavior of the of the baths around the respective qubit frequencies and no modes at the frequency of the complementary qubit, leading to $J_i(E_j) \simeq (\Gamma_0^i/2\pi)\delta_{ij}$.

Then, we consider the successive interactions (or collisions) of the machine with a series of qubits in the tape, one at a time. Crucially we assume that the interactions last a very short time τ, which we assume to be smaller than the timescales of the machine's relaxation dynamics, $\tau \ll 1/\Gamma_0^i$ for $i = {\rm c}, {\rm h}$. In this way, the collisions occur almost instantaneously and can be described by a unitary (energy-preserving) operator acting over the machine and the tape qubits, while the presence of the baths during the collisions becomes negligible. For a collision occurring at time t we have $U(t+\tau,t) = e^{-iH_{int}\tau}$. Therefore, after the collision the joint state of machine and qubit tape (in interaction picture) is given by

$$\rho(t+\tau) = U(t+\tau,t)\;\rho(t)\;U^{\dagger}(t+\tau,t), \tag{B.3}$$

where $\rho(t) = \rho_{\rm m}(t)\otimes\rho_q$ is the joint state before interaction, corresponding to an (uncorrelated) product state of the machine at time t and a "fresh" qubit in the tape. Notice that we assume all tape qubits to have the same phase when they interact with the machine.

The reduced evolution of the machine is given by a completely positive and trace-preserving (CPTP) map, obtained after partial tracing of the qubit degrees of freedom in Eq. B.3. Using the expression of $H_{\rm int}$ in Eq. 5.41 and expanding up to second order in $\phi = g\tau \ll 1$, we obtain

$$\begin{aligned}\rho_{\rm m}(t+\tau) \equiv \Xi(\rho_{\rm m}) &= {\rm tr}_{\rm q}[\rho(t+\tau)] \\ &= \rho_{\rm m}(t) - i\phi[\sigma_{\rm c}^{-}\sigma_{\rm h}^{+}c^{*} + \sigma_{\rm c}^{+}\sigma_{\rm h}^{-}c, \rho_{\rm m}(t)] \\ &+ \phi^2 p_1 \mathcal{D}[\sigma_{\rm c}^{-}\sigma_{\rm h}^{+}]\rho_{\rm m}(t) + \phi^2 p_0 \mathcal{D}[\sigma_{\rm c}^{+}\sigma_{\rm h}^{+}]\rho_{\rm m}(t).\end{aligned} \tag{B.4}$$

Finally we need to combine the dynamics induced by the baths in Eq. B.2 with the instantaneous collisions as described by Eq. B.4. For this purpose, we assume that the collisions occur at random times following Poissonian statistics with rate r. The state of the machine at time t after n collisions can then be explicitly computed as

$$\rho_m^{(n)}(t) = \int_0^t ds\; w(t-s) e^{\mathcal{L}_0(t-s)}\;\Xi(\rho_m^{(n-1)}(s)), \tag{B.5}$$

where $\rho_m^{(n-1)}(s)$ is the state of the system after $n-1$ collisions at time s, and $w(\Delta t) = re^{-r\Delta t}$ is the

so-called waiting-time distribution corresponding to Poisson statistics, which captures the probability that a collision does not happen in the interval Δt. The last term inside the integral describes a collision at time s through the CPTP map Ξ, and the second exponential term describes the evolution of the machine up to the next collision, i.e. the interval of time when the tape is stopped and only the thermal baths act on the machine. Taking the time-derivative of Eq. B.5, summing over n, and replacing the expressions for the Liouvillian $\mathcal{L}_0$ in Eq. B.2 and the CPTP map Ξ in Eq. B.4, we recover the master equation 5.44 in Sec. 5.2.1.

Appendix C

Steady-State Operation

The collision of the machine with the tape results in driving the machine to a nonequilibrium steady state $\pi_{\rm m}$ in the long time run. To obtain it, we separate the master equation 5.44 into a set of coupled differential equations for the relevant populations and coherences of $\rho_{\rm m}$, which can be expressed in matrix form as $\dot{P} = M \cdot P$, with the vector $P^T \equiv (\varrho_{00}, \varrho_{01}, \varrho_{10}, \varrho_{11}, \varrho_{\rm v}, \varrho_{\rm v}^*)$ containing the elements $\varrho_{ij} = \langle ij|\rho_{\rm m}|ij\rangle_{\rm m}$ and $\varrho_{\rm v} = \langle 10|\rho_{\rm m}|01\rangle_{\rm m}$ of $\rho_{\rm m}$, and the dynamical matrix

$$M = \begin{bmatrix} -(\gamma_\uparrow^c + \gamma_\uparrow^h) & \gamma_\downarrow^c & \gamma_\downarrow^h & 0 & 0 & 0 \\ \gamma_\uparrow^c & -\gamma_\uparrow^q - (\gamma_\downarrow^c + \gamma_\uparrow^h) & -\gamma_\downarrow^q & \gamma_\downarrow^h & -ir\phi c^* & irc\phi \\ \gamma_\uparrow^h & \gamma_\uparrow^q & -\gamma_\downarrow^q - (\gamma_\downarrow^h + \gamma_\uparrow^c) & \gamma_\downarrow^c & ir\phi c^* & -irc\phi \\ 0 & \gamma_\uparrow^h & \gamma_\uparrow^c & -(\gamma_\downarrow^h + \gamma_\downarrow^c) & 0 & 0 \\ 0 & -irc\phi & irc\phi & 0 & D & 0 \\ 0 & irc^*\phi & -irc^*\phi & 0 & 0 & D \end{bmatrix}, \quad \text{(C.1)}$$

where $D = -(\gamma_\uparrow^q + \gamma_\downarrow^q) - \frac{1}{2}(\gamma_\downarrow^c + \gamma_\downarrow^h + \gamma_\uparrow^c + \gamma_\uparrow^h)$. The steady-state elements of the density operator in Eq. 5.46 are calculated by solving the kernel of the dynamical matrix M above, that is, imposing $M \cdot \Pi = 0$, and obtaining $\Pi^T = (\pi_{00}, \pi_{01}, \pi_{10}, \pi_{11}, \pi_{\rm v}, \pi_{\rm v}^*)$. Notice that in the vectors P and Π, we excluded all other non-diagonal elements of $\rho_{\rm m}$, since they are only subjected to exponential decay (decoherence), and are hence zero in the steady state regime. On the other hand, the CPTP map describing the operation of the machine on the tape qubits in the steady state, is obtained, similarly to Eq. B.4, by tracing out the machine degrees of freedom in Eq. B.3, that is, $\mathcal{E}(\rho_{\rm q}) \equiv {\rm tr}_{\rm m}[\rho(t+\tau)]$. Expanding up to second order in ϕ we recover straightforwardly Eq. 5.47.

The changes in energy and entropy of the tape qubits due to the collisions, as given in Eqs. 5.49 and 5.52 in Sec. 5.2.2, are calculated using the explicit expression of the map $\mathcal{E}(\rho_{\rm q})$ in Eq. 5.47. The only less straightforward point is the computation of the rate of entropy change in Eq. 5.52, for which we expand the eigenvalues and eigenstates of $\mathcal{E}(\rho_{\rm q})$, to second order in ϕ as $\lambda'_k = \lambda_k + \phi\lambda_k^{(1)} + \phi^2\lambda_k^{(2)}$, where λ_k and $|\lambda_k\rangle_{\rm q}$ denote the eigenvalues and eigenstates of $\rho_{\rm q}$. The first and second-order contributions to the eigenvalues (and eigenstates) are computed by using perturbation theory for the density operator [178]. The entropy changes in the tape are then approximated, up to second order in ϕ, by

$$\begin{aligned}\dot{S}_{\rm tape} &= -r\sum_k(\lambda'_k\ln\lambda'_k - \lambda_k\ln\lambda_k)\\ &\simeq -r\phi^2\sum_k\lambda_k^{(2)}\ln\lambda_k,\end{aligned} \tag{C.2}$$

where we used $\lambda_k^{(1)} = 0$ and for the second-order contribution we have

$$\begin{aligned}\lambda_k^{(2)} = {}&\pi_{01}\langle\lambda_k|\mathcal{D}[\sigma_{\rm q}^-]\rho_{\rm q}|\lambda_k\rangle + \pi_{10}\langle\lambda_k|\mathcal{D}[\sigma_{\rm q}^+]\rho_{\rm q}|\lambda_k\rangle\\ &-\sum_{l\neq k}(\lambda_l-\lambda_k)|\langle\lambda_l|\sigma_{\rm q}^-\pi_c^* + \sigma_{\rm q}^+\pi_c|\lambda_k\rangle|^2.\end{aligned} \tag{C.3}$$

By plugging C.3 into C.2, and operating we obtain the expression for the entropy changes in the tape given in Eq. 5.52 of Sec. 5.2.2.

Finally, we recall that the non-equilibrium free energy changes of the tape qubits $\dot{F}_{\rm tape}$ in Eq. 5.53 can be divided into thermal and coherent parts [178]. This split is performed by introducing the dephased states in the energy basis, $\bar{\rho}_{\rm q} = \sum_j \Pi_j\rho_{\rm q}\Pi_j$, with $\Pi_j = \{|0\rangle\langle 0|_{\rm q}, |1\rangle\langle 1|_{\rm q}\}$ the projectors of the spectral decomposition of $H_{\rm q}$.

By considering the dephased states of input and output tape qubits, we can calculate the part of the qubit entropy changes only due to the populations, obtaining $\dot{\bar{S}}_{\rm tape} = (\Delta+\zeta)\ln(p_0/p_1)$. The associated (classical) free energy changes are then defined as $\dot{\bar{F}}_{\rm tape} \equiv \dot{E}_{\rm tape} - \dot{\bar{S}}_{\rm tape}$. The free energy split then reads [172,176,178]

$$\dot{F}_{\rm tape} = \dot{\bar{F}}_{\rm tape} + \dot{C}_{\rm tape}, \tag{C.4}$$

where $\dot{C}_{\rm tape} = \dot{\bar{S}} - \dot{S}$ is the change in relative entropy of coherence, $C(\rho) = S(\rho||\bar{\rho}) = S(\bar{\rho}) - S(\rho) \geq 0$, which is non-negative, monotonic and constitutes a proper measure of coherence [56, 73]. We notice that whenever the initial state of the qubits in the tape is diagonal in the energy basis ($c = 0$), we have $\dot{C}_{\rm tape} = 0$,

and the free energy reduces to its classical contribution.

Appendix D

Ergotropy Generation

The results provided in Sec. 5.2.3 for the generation of free energy in the tape qubits, can be complemented by considering ergotropy as an alternative quantifier for the power of the machine. In this way, the operation of the machine would be to increase or decrease the ergotropy of the tape qubits. The name ergotropy was coined in Ref. [122] to quantify the maximum work extractable from a generic quantum state σ by using unitary transformations $\mathcal{U}$ describing the cyclic variation of a parameter controlling the system Hamiltonian H

$$\begin{aligned}\mathcal{W}(\sigma) &= \mathrm{tr}[H\sigma] - \min_{\mathcal{U}} \mathrm{tr}[H\,\mathcal{U}\sigma\mathcal{U}^{\dagger}] \\ &= \sum_{jk} \lambda_j E_k (|\langle\lambda_j|E_k\rangle|^2 - \delta_{jk}),\end{aligned} \tag{D.1}$$

where $\lambda_1 \geq \lambda_2 \geq ...$ denote the ordered eigenvalues of σ and $E_1 \leq E_2 \leq ...$ the eigenvalues of H. In the case of qubits, the optimal unitary $\mathcal{U}$ corresponds to a rotation in the Bloch sphere that transforms the initial state σ into a thermal Gibbs state $\tau_\beta \equiv e^{-\beta H}/Z$ with β determined by the entropy of the initial state σ.

Applying the definition Eq. D.1 to the input and output states of the tape qubits, and calculating their difference, we obtain

$$\dot{\mathcal{W}}_{\mathrm{tape}} = \dot{E}_{\mathrm{tape}} - r\phi^2 \lambda_-^{(2)} E_{\mathrm{q}}, \tag{D.2}$$

where we used that the optimal unitary transforms the eigenstate of ρ_{q} corresponding to highest (lowest) eigenvalue, $\lambda_+ \geq \lambda_-$, to the ground (excited) states [similarly for $\mathcal{E}(\rho_{\mathrm{q}})$], and used $\lambda'_- - \lambda_- = \phi^2 \lambda_-^{(2)}$.

Introducing into Eq. D.2 the expression for $\lambda_-^{(2)}$ as given by Eq. C.3, and operating we obtain

$$\dot{\mathcal{W}}_{\rm tape} = \dot{E}_{\rm tape} - E_{\rm q}(\lambda_+ - \lambda_-)\cdot \left(r\phi^2|\pi_c|^2 + \frac{\Delta(p_1-p_0) - N|c|^2}{(p_1-p_0)^2 + 4|c|^2}\right). \tag{D.3}$$

Using Eq. D.3, we can redefine the regimes of operation of the device reported in Sec. 5.2.3 by replacing free-energy changes in the tape qubits, $\dot{F}_{\rm tape}$, by the corresponding ergotropy changes, $\dot{\mathcal{W}}_{\rm tape}$. In Fig. D.1(a), we show the regions of the Bloch sphere corresponding to such new operational regimes for same parameters as in Fig. 5.9 of Sec. 5.2.3. By comparing the two figures, we notice that, as expected, the refrigerator regime (characterized by $\dot{Q}_{\rm c} > 0$) appears in the same region, while we observe differences for the shape of HE ($\dot{\mathcal{W}} > 0$) and D ($\dot{\mathcal{W}} < 0$) regions. In particular the HE regime broadens, including the whole south hemisphere. This indicates the existence of situations where the ergotropy of the tape qubits increases while their free energy decreases. While the opposite situation is not observed, there are, nevertheless, cases for which the free energy increases more than the ergotropy. For example, along the line $c = 0$, the ergotropy changes vanishes in the south hemisphere while $\dot{F}_{\rm tape}$ is still positive.

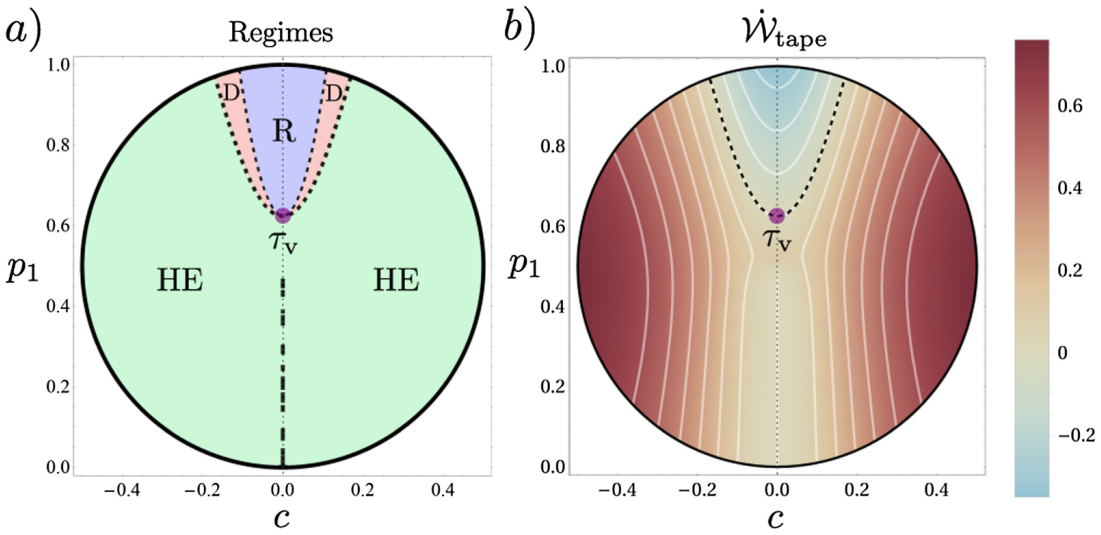

Figure D.1: (a) Regimes of operation using ergotropy to characterize work in a cross section of the tape qubits Bloch sphere. Ergotropy vanishes along the dashed line at $c = 0$ in the south hemisphere. (b) Ergotropy changes in the tape qubits, in units of $r\phi^2 E_{\rm q}$. The dashed line represent $\dot{W}_{\rm tape} = 0$ and the purple dot is the thermal state $\tau_{\rm v}$. Other parameters are as in Fig. 5.9: $\beta_{\rm h} = 0.05\beta_{\rm c}$, $E_{\rm c} = 0.5E_{\rm q}$, $E_{\rm h} = 1.5E_{\rm q}$, $\beta_{\rm c} = 1.2/E_{\rm q}$, $r = 2/E_{\rm q}$, $\phi = 0.02$ and $\Gamma_0 = 0.0025/E_{\rm q}$.

In Fig. D.1(b) we plot the values of $\dot{\mathcal{W}}_{\rm tape}$ in units of $r\phi^2 E_{\rm q}$. Similarly to the case of free energy changes, we observe that highest values are reached for non-zero initial coherence of the tape qubits. More precisely,

the maximum value of $\dot{\mathcal{W}}_{\rm tape}$ is reached for $|c| \sim 0.4$ and $p \simeq$, being 3 times greater than the best incoherent case (reached at $p_1 =$ and $c = 0$). Therefore, allowing initial coherence in the tape qubits enhances the output ergotropy current when maintaining all other resources constant. This confirms that input coherence plays a crucial role for the optimization of the performance of the machine, also from the point of view of ergotropy generation.

Résumé

La découverte des moteurs thermiques a eu un impact considérable sur notre société notamment à travers le déclenchement de la révolution industrielle et le développement de nouvelles technologies. De nos jours, la miniaturisation des appareils est davantage répandue, nécessitant des sources d'énergie microscopiques, bien précisément quantiques. Dans les faits, les systèmes quantiques ne peuvent pas être entièrement isolés dans la nature, ils sont toujours couplés à un environnement. Comprendre leur interaction dynamique et thermodynamique avec leurs environnements respectifs est le but ultime de la thermodynamique quantique. À travers le travail de cette thèse, nous étudions le rôle de la cohérence quantique sur la performance en régime stationnaire de deux machines thermiques. Ces dernières sont sujets du formalisme des modèles collisionnels qui repose sur des interactions répétées entre un système et les ancillas de l'environnement. Au sein du premier modèle, nos résultats montrent que la cohérence dans l'état des ancillas du réservoir froid génère un meilleur rendement que celle de Carnot dans le cas du moteur thermique et du réfrigérateur. Tant dis que pour le deuxième modèle, nous exprimons à la fois les avantages et les inconvénients de l'utilisation de la cohérence comme ressource dans une machine à qubits virtuels autonome.

Mots-clés (6) : La cohérence quantique, les machines thermiques quantiques, les modèles collisionnels, la thermodynamique hors équilibre, la dynamique des états stationnaires, les machines thermiques autonomes.

Abstract

The discovery of heat engines had a huge influence on our society. Their introduction opened the door for the industrial revolution and the development of ground-breaking new technologies. Currently, engineering smaller devices is becoming more popular before, thus requiring smaller sources of energy, particularly at the nanoscale. In reality, quantum systems can't be entirely isolated in nature, they are always coupled to an environment. Understanding their dynamical and thermodynamic interaction with their respective environments is the ultimate goal of quantum thermodynamics. In this thesis, we study the role of quantum coherence on the transport phenomena and steady-state operation of two thermal machines which can act either as a heat engine or as a refrigerator. Both settings employ a collisional model framework which relies on repeated interactions between a system and the environmental ancillas. In the first model, our findings show that coherence in the state of the ancillas of the cold reservoir results in an efficiency that goes beyond the Carnot limit. In the second model, we express and discuss both the advantages and drawbacks of using coherence as a resource in the case of an autonomous virtual qubit machine.

Keywords (6): Quantum coherence, quantum thermal machines, collisional models, non-equilibrium thermodynamics, steady-state dynamics, autonomous thermal machines.